CHRISTIAN-ALBRECHTS-UNIVERSITÄT ZU KIEL

Wissenschaftlicher Endbericht
zum Forschungsprojekt

Age and Geochemistry of the Hawaiian – Emperor and Musicians Seamounts

HULA: SONNE 141 – 142

03G0141A/3

O'Connor, J.M., Stoffers, P., Wijbrans, J.R.,
Worthington, T.J., Pan, Y., Batiza, R.

November 2001

Berichtsblatt

1. ISBN oder ISSN	2. Berichtsart Wissenschaftlicher Endbericht zum Forschungsprojekt

3a. Titel des Berichts

Age and Geochemistry of the Hawaiian–Emperor and Musicians Seamounts

3b. Titel der Publikation

4a. Autoren des Berichts (Name, Vorname(n))	5. Abschlußdatum des Vorhabens
O'Connor, J.M., Stoffers, P., Wijbrans, J.R., Worthington, T.J., Yucheng, P., Batiza, R.	28.2.2001
	6. Veröffentlichungsdatum
4b. Autoren der Publikation (Name, Vorname(n))	30.11.2001
	7. Form der Publikation

8. Durchführende Institution(en) (Name, Adresse)	9. Ber.Nr. Durchführende Insitution
Institut für Geowissenschaften Universität Kiel Olshausenstr. 40 D-24098 Kiel	10. Förderkennzeichen *) 03G0141A/3
	11a. Seitenzahl Bericht 61
	11b. Seitenzahl Publikation
13. Fördernde Institution (Name, Adresse)	12. Literaturangaben 36
Bundesministerium für Bildung und Forschung (BMBF)	14. Tabellen 8
53170 Bonn	15. Abbildungen 16

16. Zusätzliche Angaben

17. Vorgelegt bei (Titel, Ort, Datum)

18. Kurzfassung

Neue hochpräzise $^{40}Ar/^{39}Ar$ Altersdatierungen und geochemische Analysen der Dredgeproben von den Hawaii (SO 141) und Musician (SO 142) Seamount-Ketten stellen einen bedeutenden Fortschritt im Verständnis der Bewegung der Pazifischen Platte, der Wechselwirkung zwischen Pazifischer Lithosphäre und Mantelplumes sowie der Dynamik von Mantelplumes dar. Sowohl tholeiitische als auch alkalische Basalte wurden von den westlichen Hawaiianischen Seamounts beprobt. Die Tholeiite eruptierten während die Seamounts über dem Hawaii Plume lagen und ihre Alter bestimmen den Zeitpunkt des Abknickens der Hawaii–Emperor Kette und den Wechsel der Bewegungsrichtung der Pazifischen Platte vor 43 Ma eindeutig. Obwohl die Abstände zwischen den Vulkanen und das Volumen der Seamounts variieren, treten Tholeiite in den meisten Seamounts der westlichen Hawaii-Kette auf. Außerdem hat der Hawaiianische Plume seine geochemische und isotopische Charakteristik seit der Zeit des Knicks in der Hawaii–Emperor Kette beibehalten.

Neue geochemische Daten zeigen, daß die langgestreckten vulkanischen Rücken an der Musician Seamount Kette durch eine Wechselwirkung zwischen einem Musician Hotspot und einer ozeanischen Spreizungsachse entstanden sind. Allerdings liegen die neuen $^{40}Ar/^{39}Ar$ Altersdaten der SO 142 Ausfahrt im Bereich von 44–90 Ma und können nicht einfach mit dem Modell einer östlich gelegenen Plume-beeinflußten Spreizungsachse in Einklang gebracht werden. Unsere Daten erfordern eine signifikante Änderung dieses Modells der Entstehung der vulkanischen Rücken der Musician Seamounts sowie von anderen vulkanischen Rücken.

19. Schlagwörter

plumes; hot spots; Pacific Plate; $^{40}Ar/^{39}Ar$; geochemistry; plate motion

20. Verlag	21. Preis

*) Auf das Förderkennzeichen des BMBF soll auch in der Veröffentlichung hingewiesen werden.

Document Control Sheet

1. ISBN or ISSN	2. Type of Report Wissenschaftlicher Endbericht zum Forschungsprojekt
3a. Report Title Age and Geochemistry of the Hawaiian–Emperor and Musicians Seamounts	
3b. Title of Publication	
4a. Author(s) of the Report (Family Name, First Name(s)) O'Connor, J.M., Stoffers, P., Wijbrans, J.R., Worthington, T.J., Yucheng, P., Batiza, R.	5.End of Project 28.2.2001
4b. Author(s) of the Publication (Family Name, First Name(s))	6. Publication Date 30.11.2001
	7. Form of Publication
8. Performing Organization(s) (Name, Address) Institut für Geowissenschaften Universität Kiel Olshausenstr. 40 D-24098 Kiel	9. Originator's Report No.
	10. Reference No. 03G0141A/3
	11a. No. of Pages Report 61
	11b. No. of Pages Publication
13. Sponsoring Agency (Name, Address) Bundesministerium für Bildung und Forschung (BMBF) 53170 Bonn	12. No. of References 36
	14. No. of Tables 8
	15. No. of Figures 16
16. Supplementary Notes	
17. Presented at (Title, Place, Date)	

18. Abstract

New high precision $^{40}Ar/^{39}Ar$ age dating and geochemical analyses of dredge samples from the Hawaiian (SO 141) and Musician (SO 142) Seamount Chains provide a significant advance in the understanding of Pacific Plate motion, interaction between Pacific lithosphere and mantle plumes, and mantle plume geochemistry and dynamics. Both tholeiitic and alkali basalts were recovered from the western Hawaiian Seamounts. The tholeiites represent lavas erupted as these seamounts passed over the Hawaiian hotspot, and their ages unequivocally date the timing of the Hawaiian–Emperor bend and the ~43 Ma change in Pacific Plate motion. Despite changes in seamount spacing and volume, tholeiites have been erupted at most of the western Hawaiian volcanoes. Similarly, the Hawaiian hotspot has maintained its distinctive geochemical and isotopic characteristics from the time of the Hawaiian–Emperor bend until the present day.

New geochemical results suggest that the series of volcanic elongate ridges (VERs) associated with the Musicians Seamount Chain developed as a result of interaction between the Musicians hotspot and a mid-ocean ridge. However, the new SO 142 $^{40}Ar/^{39}Ar$ ages range from 44–90 Ma, and are not easily reconciled with the model of a plume-fed spreading center to the east of the hotspot. Our data will require a major change in the proposed model for the development of both the Musicians VERs and VERs in general.

19.Keywords

plumes; hot spots; Pacific Plate; $^{40}Ar/^{39}Ar$; geochemistry; plate motion

20. Publisher	21. Price

Table of Contents

List of Tables **Page**

List of Figures

Acknowledgements

We would like to express our deepest gratitude to Captain Hartmut Andresen, his officers and the crew of the FS *SONNE* for their expert help, advise and professionalism during cruises SO 141 and SO 142. No dredges or other equipment was lost during these cruises, and minor equipment problems were always resolved and repaired before the equipment was needed for further use. These are significant achievements given the difficulties of dredging old Fe-Mn oxide encrusted seamounts under variable sea conditions.

We also thank the United States Government for granting us permission to work within its territorial waters and recover important samples from Kure, Midway, and Pearl & Hermes Reef. A highlight of both cruises was the exchange of scientists and crew at Midway Atoll. We thank the officials and local inhabitants of Midway for their hospitality and the opportunity to see one of the main albatross sanctuaries and wildlife reserves of the Pacific.

Both SO 141 and SO 142 were funded by a Bundesministerium für Bildung und Forschung (BMBF) award to Prof. Dr. Peter Stoffers. We thank the funding agency for their support, without which neither cruise could have occurred.

1 Project Objectives

John O'Connor and Peter Stoffers

The goal of the HULA project (cruises SO 141 and SO 142; Fig. 1.1) was to use the opportunity of a FS *SONNE* transit from the western to the eastern Pacific for an interdisciplinary study of two important problems concerning hotspot volcanism. The first part of the study was to dredge two adjacent seamounts situated at the Hawaiian–Emperor bend and a series of other Hawaiian Ridge seamounts extending further SE during cruise SO 141 (Fig. 1.2). Previous drilling of these seamounts collected alkaline rocks from their summits. Those samples provide the key data constraining the assumed ~43 Ma age of the change in absolute motion of the Pacific Plate (e.g., Clague and Dalrymple, 1989). The problems with this age estimate are two-fold:

(1) If this age is actually the age of the change in plate motion, then there is no change in Pacific Plate motion associated with the major Pacific–Farallon change in plate motion at ~48–50 Ma. At that time there were also significant changes in spreading direction along the Mid-Atlantic Ridge (MAR) and the Southwest Indian Ridge (SWIR), suggesting that the ~49 Ma change in relative plate motions was a nearly synchronous global event.

(2) There are no apparent changes in Pacific–Farallon Plate motion at the presumed ~43 Ma age of the Hawaiian–Emperor bend. This would imply that even a large change in the absolute motion of the Pacific Plate had no effect on the relative motion between the Pacific Plate and the adjacent Farallon Plate.

Recent studies have revealed that volcanism at intraplate seamounts can persist for at least ~6 Ma (e.g., Kauai- Clague and Dalrymple, 1989), that there are 5–10 Ma differences in the apparent ages of adjacent seamounts along parts of the Hawaiian chain (e.g., Fig. 1 of Clague and Dalrymple, 1989), and that there is a well-documented ~4–7 Ma interval of volcanism at Vlinders Seamount (Koppers et al., 1998). Thus, it is now known that late-stage hotspot volcanism often persists for 5–10 Ma after the initial passage of a plate over a hotspot. The paradox of the apparent ~43 Ma age of the Hawaiian–Emperor bend would be resolved if the actual "age" of the Hawaiian–Emperor bend was ~49 Ma, but geoscientists have been misled by the dating of late-

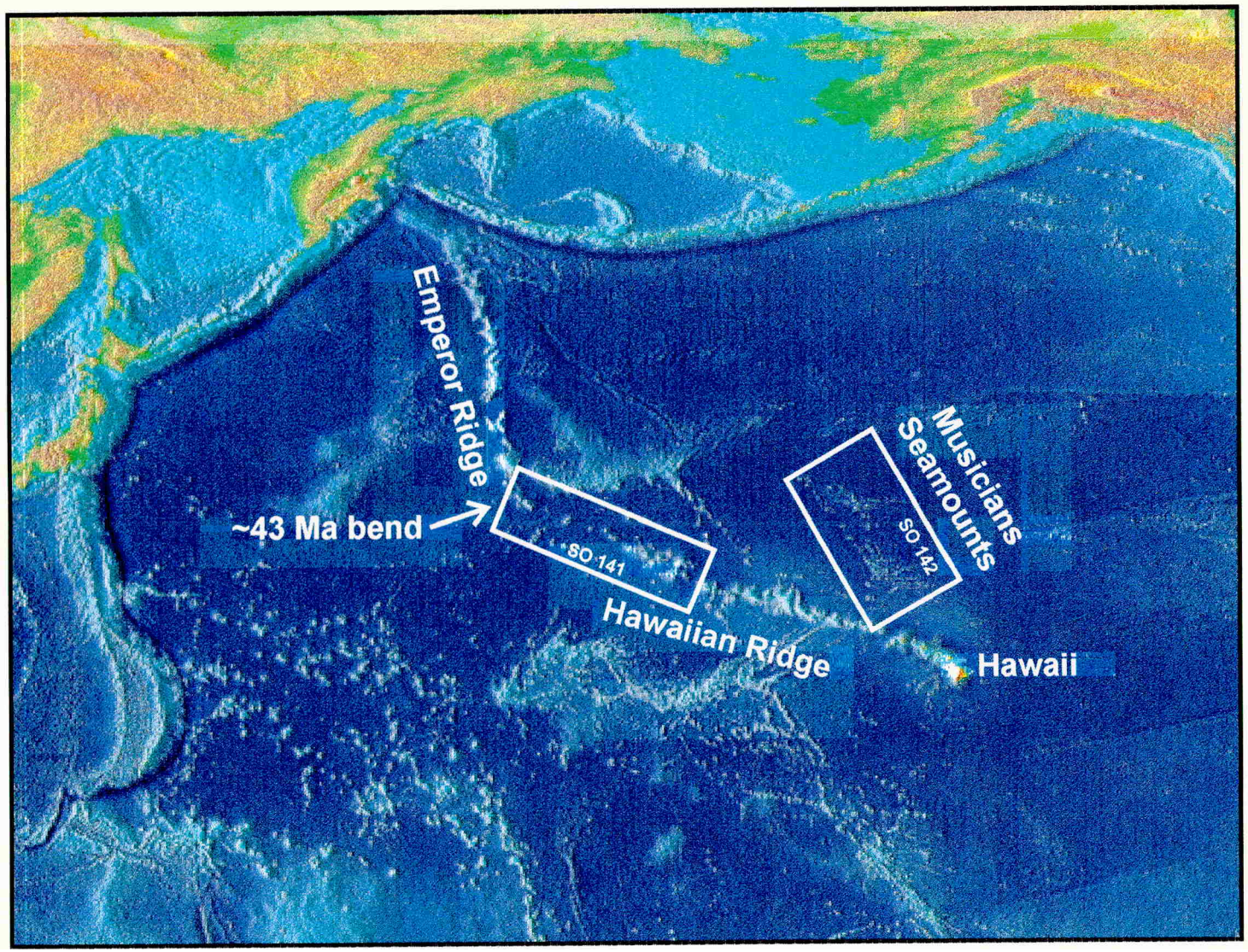

Fig. 1.1: Hawaiian-Emperor Ridge and Musicians Seamounts, NE Pacific

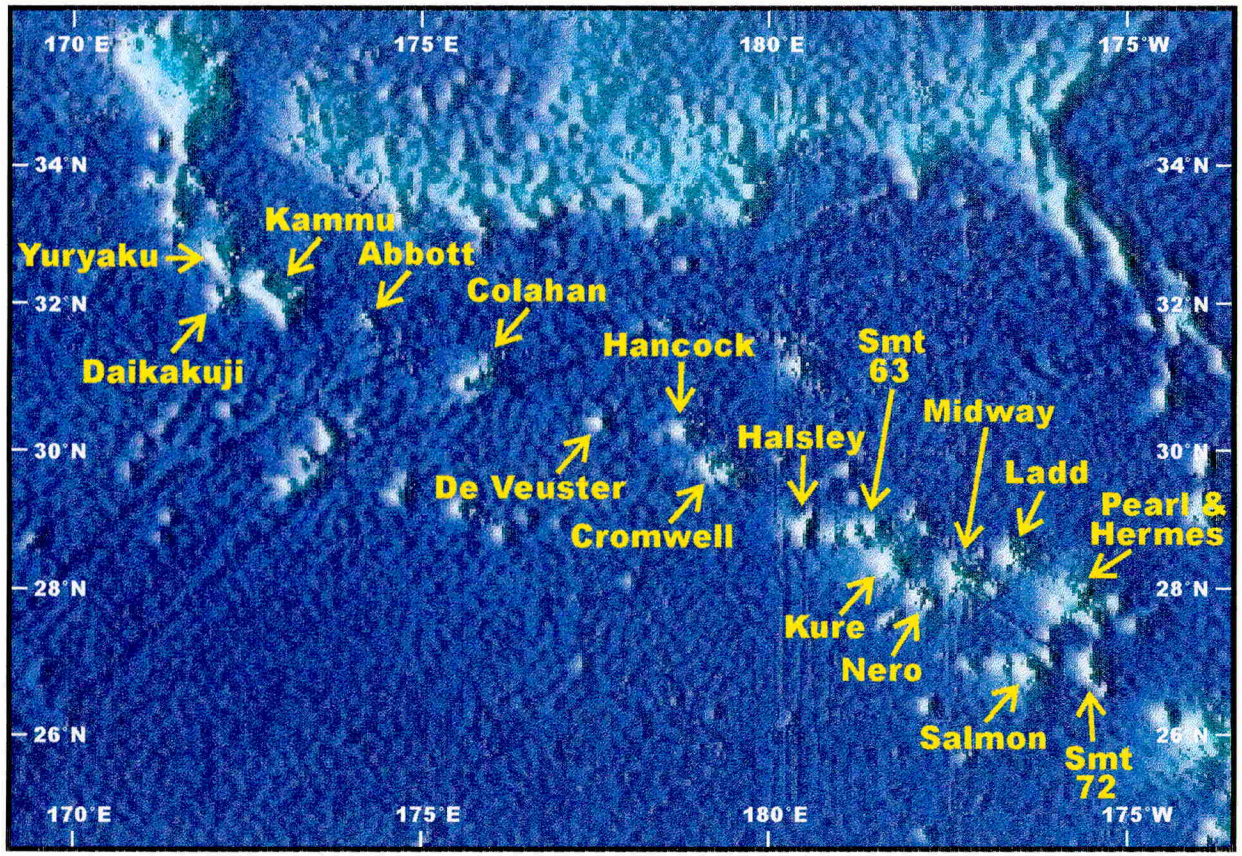

Fig. 1.2: Western Hawaiian Ridge- SO 141 Working Area

stage alkaline rocks erupted at ~43 Ma (long after these seamounts were created by the passage of the Pacific Plate over the Hawaiian hotspot).

At Daikakuji Seamount, HYDROSWEEP bathymetric surveys completed during a previous FS *SONNE* transit (SO 112) located a large landslide that was considered likely to expose the older core of the seamount. Our prime objective was to dredge this outcrop and undertake precise $^{40}Ar/^{39}Ar$ dating of recovered lavas. If the core of Daikakuji Seamount proved to be ~49 Ma in age, this would date the timing of the Hawaiian–Emperor bend and resolve the above paradoxes. The migration rate of volcanism along the Hawaiian Chain is well constrained by measured rock ages for the last ~15 Ma (e.g., Fig. 1 of Clague and Dalrymple, 1989). However, because of a major gap in sample recovery and age control, it is unclear what the migration rate was between ~15 Ma and the formation of the Hawaiian–Emperor bend (~43–49 Ma). Therefore, it is possible that further significant changes in Pacific Plate motion occurred sometime during this interval (e.g., Lonsdale, 1988).

Precise $^{40}Ar/^{39}Ar$ ages determined for lavas from ~21 Ma to zero age along the Foundation Chain (FS *SONNE* cruise SO 100) show that it is possible to calculate with high accuracy the rate at which volcanism has migrated along Pacific hotspot chains (O'Connor et al., 1998; 2001). A combination of fast plate motion and relatively low plume flux appears to be the optimum for producing a trail of discrete seamounts that best record plate motion. In the case of the Hawaiian plume, its magma flux is far greater than that of the Foundation plume. This has resulted in the formation of a trail consisting mostly of relatively large ridge segments, and in marked contrast to the isolated seamounts of the Foundation Chain. However, the Hawaiian Chain does include a ~1200 km-long line of isolated seamounts between the Hawaiian–Emperor bend and Pearl & Hermes Reef. In this respect, this is a unique section of the Hawaiian–Emperor Chain where relatively few high precision $^{40}Ar/^{39}Ar$ ages of rock samples can provide an important new constraint on Pacific Plate motion. A reliable estimate of the migration rate of volcanism along the Hawaiian Chain older than ~15 Ma would provide a second constraint (independent of the direct dating approach) on the age of the Hawaiian–Emperor bend.

Hawaiian–Emperor seamounts have long been known to evolve through an initial alkalic phase, a dominant shield-building tholeiitic phase, a late-stage alkalic phase,

and often a resurgent (or post-erosional) alkalic phase (Clague and Dalrymple, 1989). Only the dominant (>95%) tholeiitic phase directly marks the passage of the seamount over the hot spot. Consequently, a major second objective of the Hawaiian–Emperor project was to undertake geochemical analyses of the recovered lavas and determine which were tholeiitic (and thus of great importance for the age dating program) and which were alkalic. It was anticipated that dredging landslide scarps on the upper to mid-flanks of the seamounts would bias the sampling in favour of tholeiites from the upper part of the shield, and provide a window through the capping alkalic lavas that are mostly from the resurgent and late stages.

Additional sub-projects of the geochemistry program concern medium and long term variations in composition of the Hawaiian mantle plume. It is now recognised that some lavas from the oldest Emperor Seamounts (e.g., Meiji, Detroit) have geochemical and isotopic characteristics that are transitional between the standard composition of the plume (i.e., Mauna Loa and Kilauea) and mid-ocean ridge basalt (MORB). These changes may reflect plume–ridge interactions between the Hawaiian plume and a now subducted paleo-spreading centre in the northern Pacific (e.g., Keller et al., 2000; Regelous et al., 2001). However, it is also possible that they represent real compositional variations with time in the composition of the plume itself. We also seek to discover whether the change from large nearly continuous seamounts along the southern Emperors and at the Hawaiian–Emperor bend to small widely spaced seamounts between the Hawaiian–Emperor bend and Pearl & Hermes Reef is accompanied by any change in plume composition.

The second leg of the cruise (SO 142) involved a geophysical, geochronological, and geochemical investigation of a new type of hotspot volcanism whose large-scale impact only became evident with the recent "predicted topography" maps based on dense satellite altimetric coverage (e.g., Smith and Sandwell, 1997). The Musicians Seamount Chain is a classic example of this type of feature (Fig. 1.3). Here, the Pacific Plate was moving NNW (azimuth ~320°) between ~80–95 Ma when the north–south striking spreading axis was located less than 1000 km to the east of the Musicians hotspot. Several long (~500 km) east–west oriented ridges formed between the hotspot and paleo-spreading axis (Fig. 1.3). Many similar long volcanic(?) features appear to have been created in a similar style during other ridge–hotspot interactions. For

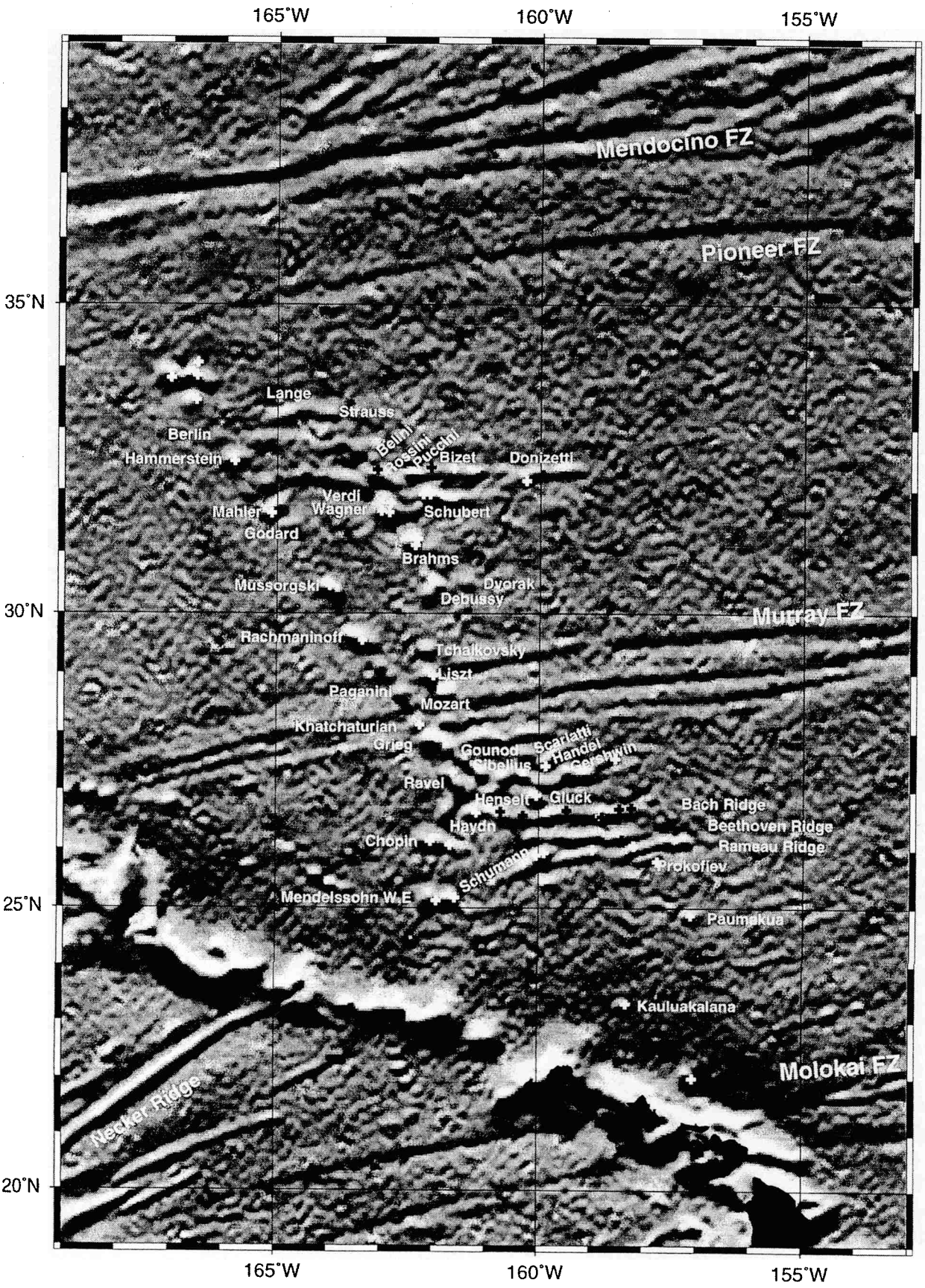

Fig. 1.3: Musicians Seamounts- SO 142 Working Area

example, smaller ridges are evident along the eastern side of the Line Islands, Manihiki Plateau, and Tuomatu Islands, and even larger isolated ridges of this type may have been created by the interaction of the Kerguelen and Reunion hotspots and their adjacent spreading centers (the proposed "second type of hotspot island" of Morgan, 1978). It seems plausible that this type of hotspot–spreading center interaction is presently producing the oblique volcanic ridges near the Pacific–Antarctic Ridge (i.e., the oblique ridges within the Foundation Chain and the oblique Hollister Ridge south of the Eltanin transform system).

The Musicians area is probably the best region in which to study this newly realised type of hotspot volcanic(?) structure. This is because the area records a relatively rare example in which the absolute motion of the Pacific Plate (as shown by the ~320° trend of the Musicians Seamounts) was nearly orthogonal to the relative motion of Pacific–Farallon Plate spreading (as shown by the ~80° trend of the fracture zones). Thus, the hotspot–ridge interaction was immune to overprinting by hotspot–ridge induced volcanism occurring at a later time. In addition, the Musicians Seamount Chain has already been dated and shown to have a simple age progression (Pringle, 1993), perhaps because it is composed of small monogenetic volcanoes. As the Musicians Seamounts were already sampled and dated, our geochemical and geochronological study was free to focus on sampling and dating the enigmatic ridges.

2 $^{40}Ar/^{39}Ar$ Geochronology

John O'Connor and Jan Wijbrans

The high precision $^{40}Ar/^{39}Ar$ analytical data reported here represent the key information for addressing the objectives of the SO 141 and SO 142 projects. Although dredging of the Hawaiian Seamounts and the elongate ridges in the Musicians area was very successful, only a small number of the many rock samples recovered by the individual dredge hauls could be dated (due to limits on available laboratory time and financial resources). Therefore, it was critical that we selected and carefully prepared a wide range of representative samples for irradiation. Evaluating such a large pool of samples by single fusion analyses ensures the best possible chance of: (1) obtaining high precision ages, (2) identifying all important volcanic events such that the history and development of the seamount chains/elongate ridges can be resolved, and (3) allow for follow-up work on unexpected or interesting results without requiring further irradiation of additional samples.

2.1 Sample Preparation

The pool of SO 141 and SO 142 samples selected for $^{40}Ar/^{39}Ar$ dating during logging of the samples onboard the FS *SONNE* were cut into clean rock blocks and then packed while still onboard the ship. The aim of this procedure was to remove the outer weathered surfaces and as much visible alteration as possible using the rock saw. Pieces of these selected and partly processed SO 141 and SO 142 rock samples were then crushed and sieved at the University of Kiel. Sieve fractions were washed with various acids at the Vrije University, Amsterdam, in order to further remove as much as possible of the seawater alteration products (which have a very negative impact on dating analyses).

Whole rock samples (500 to 250 mm size fraction) were treated with 7N HCl prior to immersing for 1 hour in 1N HNO_3 in an ultrasonic bath at 50°C, followed by rinsing in distilled water. Plagioclase (250 to 125 mm size fraction) was separated from crushed whole rock using a magnetic separator. Separated plagioclase was treated with 7N HCl for 30 minutes, 5–8% HF for 5 minutes, 1N HNO_3 for 1 hour, and then washed in distilled H_2O. Various iterations of acid washing were performed on most samples

until the best results were obtained. In the end, 79 rock samples (plus 21 mineral separates) were selected for irradiation. These were hand-picked under a binocular microscope to minimise any possible alteration products, and then loaded into aluminium foil packets and stacked in two quartz vials along with mineral standards (Table 2.1).

2.2 Sample Irradiation

Plagioclase (250 to 125 mm size fraction) and whole rock chips (500 to 250 mm size fraction) were irradiated with Cd-shielding at the Oregon State University (OSU) TRIGA reactor facility in the United States. Cd-shielding significantly reduces the effects of slow neutrons, leading to a major reduction in the ^{40}Ar produced without affecting the production of ^{39}Ar (McDougall and Harrison, 1988). This in turn reduces the impact of the ($^{40}Ar/^{39}Ar$) K correction factor, which is particularly useful in the case of low potassium samples. The K and Ca correction factors for the Cd-shielded position at the OSU TRIGA reactor have previously been determined by Wijbrans et al. (1985). Rock chips or plagioclase separates from each sample were wrapped in aluminum foil and stacked in 9 mm ID quartz tubes. Sanidine from the Taylor Creek Rhyolite, sample TCR 85G003 with an accepted age of 28.34 Ma, was used to measure the flux gradients. TCR was loaded between every five unknowns and also at the top and bottom of each vial. Between four and six replicate analyses were made for each monitor position, typically giving uncertainties of 0.1 to 0.3% (sem.). Using a best fit curve between all of the standards allowed determination of J factors with a similar precision.

2.3 $^{40}Ar/^{39}Ar$ Incremental Heating and Dating

The theory of $^{40}Ar/^{39}Ar$ geochronology is described in Faure (1986), York (1984), and McDougall and Harrison (1988). Sample ages are calculated using the standard age equation. The uncertainty in the age is calculated by partial differentiation of the age equation (Dalrymple and Lanphere, 1969; Dalrymple et al., 1981), and includes uncertainties in the determination of the flux monitor J, blank determination, the regression of the intensities of the individual isotope peaks, the correction factors for interfering isotopes, and the mass discrimination correction.

The argon laserprobe facility at the Vrije University, Amsterdam, has previously been described in considerable detail by Wijbrans et al. (1985). It consists of an 18W argon ion laser, beam optics, a low volume UHV gas inlet system and a Mass Analyser Products (MAP) 215-50 noble gas mass spectrometer. The mass spectrometer is fitted with a modified Nier-type electron bombardment source. During data collection, the mass spectrometer is controlled using a modified version of the standard MAP software written in TurboPascal and allowing data collection for all isotopes of argon using a secondary electron multiplier collector operated at a gain of 60,000. Data reduction allows the choice between a straight linear regression of peak intensities with respect to inlet time, asymptotic curve fitting minimizing standard deviation and sum of squared residuals as criteria for best fit, or an average of peak intensities. The asymptotic extrapolation was very often the most appropriate as the highest peak intensities often showed deviations from straight line behavior with time. Mass fractionation was determined by measuring aliquots of air argon at regular intervals.

High precision $^{40}Ar/^{39}Ar$ ages were determined on both plagioclase separates and whole rock chips via incremental heating with the argon laser probe, using a defocused CW laser beam (York et al., 1981). We encountered difficulties initially both in heating the samples with sufficient uniformity and in producing satisfactorily high peak intensities. Following some experimentation, we solved these problems by using large (13 mm) custom-made sample pans, which allowed us to load significantly more sample in even, single grain layers. Heating such thin layers of sample (under manual control) allowed us to produce predictable analytical results: plagioclase consistently showed excellent plateaux, whereas the whole rock experiments for the older samples typically showed elevated ages in the first 20% of gas released, a good plateau, and anomalously young ages in the final 10–20% when the sample was partly molten and melting.

2.4 Initial Results

The wide range of SO 141 and SO 142 samples irradiated and available for analysis allowed us to overcome significant problems associated with seawater alteration of rock samples (Table 2.1). Many single fusion analyses were conducted in order to distinguish between samples, prior to final sample selection for the very time

consuming incremental heating studies. These single fusion analyses, although numerous, are not reported here as they have no scientific value other than helping with final sample selection. Each incremental heating step reported in Table 2.2 required on average about 40 minutes of laboratory time. Also not reported are the many analyses of the monitor minerals used to calculate J curves, nor the blanks required before and after every few incremental heating steps (each requiring the same amount of lab time as the incremental heating steps).

Our incremental $^{40}Ar/^{39}Ar$ ages for the very altered SO 141 Hawaiian Seamount rocks are of very high quality (Table 2.2). They represent a major advance in the age control of the Hawaiian–Emperor Chain. Initial interpretation of these results suggests that we can make a significant advance in our understanding of the development of the Hawaiian–Emperor Chain, the motion of the Pacific Plate since 81 Ma, and the behaviour of the largest active mantle plume. A manuscript is currently in preparation reporting these SO 141 results.

The incremental $^{40}Ar/^{39}Ar$ ages reported here for the very altered SO 142 rock samples are also of a very high quality (Table 2.2), and range between ~90 Ma and ~44 Ma. These results are highly significant, because they do not support the model of a plume-fed spreading center to the east of the Cretaceous Musicians mantle plume (e.g., see previous discussion of cruise objectives). Our data will require a major change to the current plume models that have been proposed to explain the development of the Musicians Volcanic Elongate Ridges (VERs) and Pacific VERs in general. A second manuscript is currently in preparation reporting these important SO 142 results.

Seamount/Ridge	Vial		Sample	Material	size (µm)	(mg)	Leaching	after	Notes
	A	**1**	**85G003**	**Sanidine**				**1**	
Yuryaku	A	2	SO 141-5DR-1	Leached WR	250-500	80	1 hr HCl (3.5N); 1 hr HNO3 (1N)	**2.5**	weakly weathered
Yuryaku	A	3	SO 141-5DR-3	Leached WR	250-500	80	HCl (3.5N), 1 hr HNO3 (1N), 1 hr HCl (7N), 1 hr HNO3 (	**4.5**	weakly weathered, rare altered olivine and vesicle binaries
Yuryaku	A	4	SO 141-5DR-4	Leached WR	250-500	80	HCl (3.5N); 1 hr HNO3 (1N); 1 hr HCl (7N); 1 hr HNO3 (	**6**	weathered, rare altered olivine and vesicle binaries
Yuryaku	A	5	SO 141-5DR-5	Leached WR	250-500	80	1 hr HCl (3.5N); 1 hr HNO3 (1N)	**9**	weathered, rare altered olivine and vesicle binaries
Yuryaku	A	6	SO 141-5DR-9	Leached WR	250-500	80	1 hr HCl (3.5N); 1 hr HNO3 (1N)	**11**	weathered, rare altered olivine and vesicle binaries
	A	**7**	**85G003**	**Sanidine**				**12**	
Yuryaku	A	8	SO 141-5DR-10	Leached WR	250-500	80	1 hr HCl (3.5N); 1 hr HNO3 (1N)	**14.5**	weathered
Yuryaku	A	9	SO 141-5DR-11	Leached WR	250-500	80	1 hr HCl (3.5N); 1 hr HNO3 (1N)	**16.5**	weathered
Yuryaku	A	10	SO 141-5DR-15	Leached WR	125-250	80	1 hr HCl (3.5N); 1 hr HNO3 (1N)	**18.5**	weathered, rare vesicle binaries
Yuryaku	A	10A	SO 141-5DR-15	plagioclase	125-250	24	1 hr HCl (3.5N); 5 min HF (6-7%);1 hr HNO3 (1N)	**20.5**	apprx. 70% clean grains
Yuryaku	A	11	SO 141-5DR-19	Leached WR	250-500	80	HCl (3.5N), 1 hr HNO3 (1N); 1 hr HCl (7N); 1 hr HNO3 (	**22**	weathered, alteered vesicle binaries
Yuryaku	A	12	SO 141-5DR-20	Leached WR	250-500	80	1 hr HCl (3.5N); 1 hr HNO3 (1N)	**24**	weathered, iddingsite binaries
	A	**13**	**85G003**	**Sanidine**				**25.5**	
Yuryaku	A	14	SO 141-5DR-22	Leached WR	250-500	80	HCl (3.5N); 1 hr HNO3 (1N); 1 hr HCl (7N); 1 hr HNO3 (	**27**	weathered, iddingsite binaries
Yuryaku	A	15	SO 141-5DR-22	plagioclase	125-250	42	1 hr HCl (3.5N); 5 min HF (6-7%);1 hr HNO3 (1N)	**29**	clean, some rare rock binaries
Yuryaku	A	16	SO 141-5DR-26	Leached WR	250-500	80	1 hr HCl (3.5N); 1 hr HNO3 (1N)	**31**	very altered, calcite binaries?
Yuryaku	A	17	SO 141-5DR-26	plagioclase	125-250	20	1 hr HCl (3.5N); 5 min HF (6-7%);1 hr HNO3 (1N)	**32.5**	some alteration coloring
Yuryaku	A	18	SO 141-5DR-26	plagioclase	250-500	15	1 hr HCl (3.5N); 5 min HF (6-7%);1 hr HNO3 (1N)	**33.5**	some alteration coloring
	A	**19**	**85G003**	**Sanidine**				**34.5**	
Yuryaku	A	20	SO 141-5DR-28	Leached WR	250-500	80	1 hr HCl (3.5N); 1 hr HNO3 (1N)	**36.5**	weathered, rare vesicle binaries
Daikakuji	A	21	SO 141-6DR-3	Leached WR	250-500	80	1 hr HCl (3.5N); 1 hr HNO3 (1N)	**38.5**	weathered, some iddingsite-olivine binaries
Daikakuji	A	22	SO 141-6DR-4	Leached WR	250-500	80	c	**40**	weathered, some iddingsite-olivine binaries
Daikakuji	A	23	SO 141-6DR-6	Leached WR	250-500	80	1 hr HCl (3.5N); 1 hr HNO3 (1N)	**42**	weathered, rare iddingsite-olivine binaries
Daikakuji	A	24	SO 141-6DR-7	Leached WR	250-500	80	1 hr HCl (3.5N); 1 hr HNO3 (1N)	**44**	weathered, rare iddingsite-olivine binaries
	A	**25**	**85G003**	**Sanidine**				**45**	
Daikakuji	A	26	SO 141-6DR-8	Leached WR	250-500	80	1 hr HCl (3.5N); 1 hr HNO3 (1N)	**46.5**	weakly weathered, rare iddingsite-olivine binaries
Daikakuji	A	27	SO 141-6DR-10	Leached WR	250-500	80	HCl (3.5N); 1 hr HNO3 (1N); 1 hr HCl (7N); 1 hr HNO3 (	**48.5**	weathered, many iddingsite-olivine binaries
East Daikakuji	A	29	SO 141-7DR-1	Leached WR	250-500	80	HCl (3.5N), 1 hr HNO3 (1N); 1 hr HCl (7N); 1 hr HNO3 (	**50.5**	weathered, many iddingsite-olivine and altered vesicle binarie
East Daikakuji	A	30	SO 141-8DR-5	Leached WR	250-500	80	HCl (3.5N); 1 hr HNO3 (1N); 1 hr HCl (7N); 1 hr HNO3 (	**52**	weathered, many iddingsite-olivine and altered vesicle binarie
	A	**31**	**85G003**	**Sanidine**				**54**	
East Daikakuji	A	32	SO 141-8DR-7	Leached WR	250-500	80	ICl (3.5N); 1 hr HNO3 (1N); 2 x 1 hr HCl (7N); 1 hr HNO:	**56**	weathered, some iddingsite-olivine and altered vesicle binaries
Kamu	A	33	SO 141-9DR-1	Leached WR	250-500	80	HCl (3.5N), 1 hr HNO3 (1N); 1 hr HCl (7N); 1 hr HNO3 (	**58**	weathered, many iddingsite-olivine and altered vesicle binarie
Kamu	A	34	SO 141-9DR-1	plagioclase	125-250	80	1 hr HCl (3.5N); 5 min HF (6-7%);1 hr HNO3 (1N)	**60**	almost100% clean grains
Kamu	A	35	SO 141-9DR-13	Leached WR	250-500	80	1 hr HCl (3.5N); 1 hr HNO3 (1N)	**62**	weathered, some iddingsite-olivine and altered vesicle binaries
Kamu	A	36	SO 141-9DR-13	plagioclase	125-250	80	1 hr HCl (3.5N); 5 min HF (6-7%);1 hr HNO3 (1N)	**64**	almost100% clean grains
Kamu	**A**	**37**	**85G003**	**Sanidine**				**65.5**	
Kamu	A	38	SO 141-9DR-14	Leached WR	250-500	80	1 hr HCl (3.5N); 1 hr HNO3 (1N)	**67**	weathered, iddingsite-olivine and altered vesicle binaries
Kamu	A	39	SO 141-9DR-16	Leached WR	250-500	80	1 hr HCl (3.5N); 1 hr HNO3 (1N)	**69**	weathered, rare iddingsite-olivine binaries
Kamu	A	40	SO 141-9DR-16	plagioclase	125-250	80	1 hr HCl (3.5N); 5 min HF (6-7%);1 hr HNO3 (1N)	**71**	almost100% clean grains
Kamu	A	41	SO 141-9DR-23	Leached WR	250-500	80	1 hr HCl (3.5N); 1 hr HNO3 (1N)	**73**	weathered, some altered vesicle binaries
Kamu	A	41A	SO 141-9DR-23	plagioclase	125-250	80	1 hr HCl (3.5N); 5 min HF (6-7%);1 hr HNO3 (1N)	**75**	almost100% clean grains ?
Kamu	A	42	SO 141-9DR-24	Leached WR	250-500	80	HCl (3.5N); 1 hr HNO3 (1N). 1 hr HCl (7N); 1 hr HNO3 (	**77**	weathered
	A	**43**	**85G003**	**Sanidine**				**78**	
Kamu	A	44	SO 141-9DR-31	Leached WR	250-500	80	ICl (3.5N); 1 hr HNO3 (1N); 2 x 1 hr HCl (7N); 1 hr HNO:	**80**	weathered, some iddingsite binaries
Abbott	A	45	SO 141-11DR-1	Leached WR	250-500	80	1 hr HCl (3.5N); 1 hr HNO3 (1N)	**82**	athered, some iddingsite-olivine and rare altered vesicle bina

Table 2.1: Irradiated SO 141 and SO 142 rock samples

Abbott	A	46	SO 141-12DR-1	Leached WR	250-500	80	·HCl (3.5N); 1 hr HNO3 (1N); 1 hr HCl (7N); 1 hr HNO3 (	**84**	ithered, some iddingsite-olivine and many altered vesicle bina
Abbott	A	47	SO 141-12DR-3	Leached WR	250-500	80	·HCl (3.5N); 1 hr HNO3 (1N); 1 hr HCl (7N); 1 hr HNO3 (	**86**	weathered, some iddingsite-olivine and altered vesicle binaries
Abbott	A	48	SO 141-12DR-4	Leached WR	250-500	80	·HCl (3.5N); 1 hr HNO3 (1N); 1 hr HCl (7N); 1 hr HNO3 (	**88**	weathered, few iddingsite-olivine and altered vesicle binaries
	A	**49**	**85G003**	**Sanidine**				**90**	
Abbott	A	50	SO 141-12DR-7	Leached WR	250-500	80	·HCl (3.5N); 1 hr HNO3 (1N); 1 hr HCl (7N); 1 hr HNO3 (	**91.5**	weathered, some iddingsite-olivine and altered vesicle binaries
Colahan	A	51	SO 141-13DR-1	Leached WR	250-500	80	·HCl (3.5N); 1 hr HNO3 (1N); 1 hr HCl (7N); 1 hr HNO3 (	**93.5**	weathered, some iddingsite binaries
Colahan	A	52	SO 141-13DR-2	Leached WR	250-500	80	·HCl (3.5N); 1 hr HNO3 (1N); 1 hr HCl (7N); 1 hr HNO3 (	**95.5**	weathered, some iddingsite and altered vesicle binaries
Colahan	A	53	SO 141-13DR-7	Leached WR	250-500	80	HCl (3.5N); 1 hr HNO3 (1N); **2 x** 1 hr HCl (7N); 1 hr HNO3	**97**	weathered, some olivine and altered vesicle binaries
Colahan	A	54	SO 141-15DR-1	Leached WR	250-500	80	·HCl (3.5N); 1 hr HNO3 (1N); 1 hr HCl (7N); 1 hr HNO3 (	**99**	weathered, some olivine and altered vesicle binaries
	A	**55**	**85G003**	**Sanidine**				**100.5**	
De Veuster	A	56	SO 141-16DR-1	Leached WR	250-500	80	HCl (3.5N); 1 hr HNO3 (1N), **2 x** 1 hr HCl (7N); 1 hr HNO3	**102**	weathered, some olivine and many altered vesicle binaries
De Veuster	A	57	SO 141-17DR-1	Leached WR	250-500	80	1 hr HCl (3.5N); 1 hr HNO3 (1N)	**104**	weakly weathered
Hancock	A	58	SO 141-20DR-1	Leached WR	250-500	80	HCl (3.5N); 1 hr HNO3 (1N); **2 x** 1 hr HCl (7N); 1 hr HNO3	**106**	weathered, some iddingsite and altered vesicle binaries
ownsend Cromwe	A	59	SO 141-21DR-1	Leached WR	250-500	80	HCl (3.5N); 1 hr HNO3 (1N); **2 x** 1 hr HCl (7N); 1 hr HNO3	**108**	weathered, some olivine and altered vesicle binaries
Helsley	A	60	SO 141-23DR-1	Leached WR	250-500	80	1 hr HCl (3.5N); 1 hr HNO3 (1N)	**110**	weathered, few iddingsite-olivine and altered vesicle binaries
	A	**61**	**85G003**	**Sanidine**				**111.5**	

Table 2.1: Irradiated SO 141 and SO 142 rock samples, continued

Seamount/Ridge	Vial		Sample	Material	Grain-size (µm)	Weight (mg)	Leaching	(mm) Height after	
	A	**X**	**85G003**	**Sanidine**				**1**	
Helsley	A	62	SO 141-23DR-2	Leached WR	250-500	80	1 hr HCl (3.5N), 1 hr HNO3 (1N); 2 x 1 hr HCl (7N), 1 hr HNO3 (1N)	**2.5**	weathered, iddingsite binaries
Smt #63	A	63	SO 141-25DR-1	Leached WR	250-500	80	1 hr HCl (3.5N); 1 hr HNO3 (1N)	**4.5**	weaklyweathered, except for altered vesicle binaries
Kure	A	64	SO 141-26DR-1	Leached WR	250-500	80	1 hr HCl (3.5N); 1 hr HNO3 (1N); 1 hr HCl (7N); 1 hr HNO3 (1N)	**6.5**	weathered, some iddingsite and altered vesicle binaries
Nero	A	65	SO 141-28DR-2	Leached WR	250-500	80	1 hr HCl (3.5N); 1 hr HNO3 (1N); 2 x 1 hr HCl (7N), 1 hr HNO3 (1N)	**8.5**	weathered, some iddingsite and altered vesicle binaries
Midway	A	66	SO 141-29DR-1	Leached WR	250-500	80	1 hr HCl (3.5N); 1 hr HNO3 (1N), 1 hr HCl (7N); 1 hr HNO3 (1N)	**10.5**	weathered, rare iddingsite binaries
	A	**67**	**85G003**	**Sanidine**				**12**	
Midway	A	68	SO 141-29DR-2	Leached WR	250-500	80	1 hr HCl (3.5N), 1 hr HNO3 (1N); 1 hr HCl (7N), 1 hr HNO3 (1N)	**13.5**	weathered, some iddingsite and altered vesicle binaries
Midway	A	69	SO 141-29DR-17	Leached WR	250-500	80	1 hr HCl (3.5N), 1 hr HNO3 (1N)	**15.5**	weathered
Ladd	A	70	SO 141-30DR-1	Leached WR	250-500	80	1 hr HCl (3.5N); 1 hr HNO3 (1N); 1 hr HCl (7N); 1 hr HNO3 (1N)	**17.5**	weathered, iddingsite and altered vesicle binaries
Ladd	A	71	SO 141-30DR-5	Leached WR	250-500	80	1 hr HCl (3.5N); 1 hr HNO3 (1N); 2 x 1 hr HCl (7N); 1 hr HNO3 (1N)	**19.5**	weathered, iddingsite and altered vesicle binaries
Pearl and Hermes	A	72	SO 141-34DR-1	Leached WR	250-500	80	1 hr HCl (3.5N); 1 hr HNO3 (1N); 1 hr HCl (7N); 1 hr HNO3 (1N)	**21.5**	weathered, iddingsite and many altered vesicle binaries
	A	**73**	**85G003**	**Sanidine**				**23**	
Pearl and Hermes	A	74	SO 141-34DR-2	Leached WR	250-500	80	1 hr HCl (3.5N); 1 hr HNO3 (1N)	**24.5**	weathered, rare iddingsite and altered vesicle binaries
Pearl and Hermes	A	75	SO 141-34DR-17	Leached WR	250-500	80	1 hr HCl (3.5N); 1 hr HNO3 (1N); 2 x 1 hr HCl (7N); 1 hr HNO3 (1N)	**26.5**	weathered, altered vesicle binaries
Smts#72-74	A	76	SO 141-37DR-1	Leached WR	250-500	80	1 hr HCl (3.5N), 1 hr HNO3 (1N); 1 hr HCl (7N); 1 hr HNO3 (1N)	**28.5**	weathered
Salmon	A	77	SO 141-38DR-2	Leached WR	250-500	80	1 hr HCl (3.5N); 1 hr HNO3 (1N); 1 hr HCl (7N); 1 hr HNO3 (1N)	**30.5**	weathered
	A	78	x703	Leached WR	250-500	80	1 hr HCl (3.5N), 1 hr HNO3 (1N); 1 hr HCl (7N); 1 hr HNO3 (1N)	**32.5**	rare altered looking olvine binaries
	A	**79**	**85G003**	**Sanidine**				**33.5**	
	A	80	x704	Leached WR	250-500	80	1 hr HCl (3.5N); 1 hr HNO3 (1N)	**36**	rare altered? looking olvine binaries
	A	81	x705	Leached WR	250-500	80	1 hr HCl (3.5N); 1 hr HNO3 (1N); 1 hr HCl (7N); 1 hr HNO3 (1N)	**38**	weathered, rare altered vesicle binaries
	A	82	x707	Leached WR	250-500	80	1 hr HCl (3.5N); 1 hr HNO3 (1N)	**41**	rare altered? looking olvine binaries
Rossini Seamount	A	83	SO 142-1DR-5a	Leached WR	250-500	65	1 hr HCl (3.5N); 1 hr HNO3 (1N); 1 hr HCl (7N); 1 hr HNO3 (1N)	**43**	weathered
Bizet	A	84	SO 142-2DR-1	Leached WR	250-500	65	1 hr HCl (3.5N); 1 hr HNO3 (1N); 1 hr HCl (7N); 1 hr HNO3 (1N)	**44.5**	weathered, rare iddingsite and altered vesicle binaries
	A	**85**	**85G003**	**Sanidine**				**45.5**	
	A	86	SO 142-2DR-1	plagioclase	125-250	65	1 hr HCl (3.5N); 5 min HF (6-7%);1 hr HNO3 (1N)	**47**	almost 100% clean grains
	A	87	SO 142-3DR-4	Leached WR	250-500	65	1 hr HCl (3.5N); 1 hr HNO3 (1N); 1 hr HCl (7N); 1 hr HNO3 (1N)	**49**	weathered, rare iddingsite and altered vesicle binaries
	A	88	SO 142-3DR-4	plagioclase	125-250	16	1 hr HCl (3.5N); 5 min HF (6-7%);1 hr HNO3 (1N)	**51**	almost 100% clean grains
	A	89	SO 142-3DR-4	plagioclase	250-500	19	1 hr HCl (3.5N); 5 min HF (6-7%);1 hr HNO3 (1N)	**52.5**	almost 100% clean grains
	A	90	SO 142-3DR-5	Leached WR	250-500	65	1 hr HCl (3.5N); 1 hr HNO3 (1N); 1 hr HCl (7N); 1 hr HNO3 (1N)	**54**	weathered, iddingsite binaries
	A	**91**	**85G003**	**Sanidine**				**55.5**	
Donizetti	A	92	SO 142-4DR-3	Leached WR	250-500	65	1 hr HCl (3.5N); 1 hr HNO3 (1N); 1 hr HCl (7N); 1 hr HNO3 (1N)	**57**	weathered, iddingsite binaries
Donizetti	A	93	SO 142-4DR-5	Leached WR	250-500	65	1 hr HCl (3.5N); 1 hr HNO3 (1N); 1 hr HCl (7N); 1 hr HNO3 (1N)	**58.5**	weathered, iddingsite and altered vesicle binaries
Donizetti	A	94	SO 142-5DR-1	Leached WR	250-500	65	1 hr HCl (3.5N); 1 hr HNO3 (1N); 1 hr HCl (7N); 1 hr HNO3 (1N)	**60.5**	weathered, iddingsite and altered vesicle binaries
Donizetti	A	95	SO 142-5DR-2	Leached WR	250-500	65	1 hr HCl (3.5N); 1 hr HNO3 (1N); 1 hr HCl (7N), 1 hr HNO3 (1N)	**62.5**	weathered, iddingsite and altered vesicle binaries
Murraz FZ	A	96	SO 142-6DR-4	Leached WR	250-500	80	1 hr HCl (3.5N); 1 hr HNO3 (1N); 1 hr HCl (7N); 1 hr HNO3 (1N)	**64.5**	weathered, iddingsite binaries
	A	**97**	**85G003**	**Sanidine**				**66**	
Bach Ridge	A	98	SO 142-7DR-1	Leached WR	250-500	65	1 hr HCl (3.5N); 1 hr HNO3 (1N); 1 hr HCl (7N); 1 hr HNO3 (1N)	**67.5**	weathered, iddingsite binaries
Bach Ridge	A	99	SO 142-7DR-1	plagioclase	125-250	65	1 hr HCl (3.5N), 5 min HF (6-7%);1 hr HNO3 (1N)	**69.5**	almost 100% clean grains
Bach Ridge	A	100	SO 142-8DR-3	Leached WR	250-500	65	1 hr HCl (3.5N), 1 hr HNO3 (1N); 1 hr HCl (7N); 1 hr HNO3 (1N)	**71.5**	weathered, iddingsite/olivine binaries
Bach Ridge	A	101	SO 142-8DR-3	plagioclase	125-250	65	1 hr HCl (3.5N), 5 min HF (6-7%);1 hr HNO3 (1N)	**73**	almost 100% clean grains
Bach Ridge	A	102	SO 142-8DR-5	Leached WR	250-500	65	1 hr HCl (3.5N), 1 hr HNO3 (1N); 1 hr HCl (7N); 1 hr HNO3 (1N)	**75**	weathered, iddingsite/olivine binaries
	A	**103**	**85G003**	**Sanidine**				**76.5**	
Bach Ridge	A	104	SO 142-8DR-5	plagioclase	125-250	23	1 hr HCl (3.5N); 5 min HF (6-7%);1 hr HNO3 (1N)	**78**	almost 100% clean grains
Bach Ridge	A	105	SO 142-8DR-5	plagioclase	250-500	38	1 hr HCl (3.5N); 5 min HF (6-7%);1 hr HNO3 (1N)	**79.5**	almost 100% clean grains

Table 2.1: Irradiated SO 141 and SO 142 rock samples, continued

	A	106	SO 142-9DR-1	Leached WR	250-500	65	1 hr HCl (3.5N), 1 hr HNO3 (1N); 1 hr HCl (7N); 1 hr HNO3 (1N)	81.5	weathered, iddingsite/olivine binaries
Bach Ridge	A	107	SO 142-9DR-1	plagioclase	125-250	20	1 hr HCl (3.5N), 5 min HF (6-7%);1 hr HNO3 (1N)	83	almost 100% clean grains
Bach Ridge	A	108	SO 142-9DR-3	Leached WR	250-500	65	1 hr HCl (3.5N), 1 hr HNO3 (1N); 1 hr HCl (7N), 1 hr HNO3 (1N)	85	weathered, iddingsite and altered vesicle binaries
	A	**109**	**85G003**	**Sanidine**				86.5	
Bach Ridge	A	110	SO 142-9DR-1	plagioclase	250-500	12	1 hr HCl (3.5N), 5 min HF (6-7%);1 hr HNO3 (1N)	88	almost 100% clean grains
	A	111	SO 142-10DR-2	Leached WR	250-500	65	1 hr HCl (3.5N), 1 hr HNO3 (1N); 1 hr HCl (7N), 1 hr HNO3 (1N)	89.5	weathered, iddingsite binaries
	A	112	SO 142-10DR-2	plagioclase	125-250	65	1 hr HCl (3.5N); 5 min HF (6-7%);1 hr HNO3 (1N)	92	almost 100% clean grains
	A	113	SO 142-10DR-4	Leached WR	250-500	65	1 hr HCl (3.5N); 1 hr HNO3 (1N); 1 hr HCl (7N); 1 hr HNO3 (1N)	94.5	weathered
	A	114	SO 142-11DR-1	Leached WR	250-500	65	1 hr HCl (3.5N), 1 hr HNO3 (1N); 2 x 1 hr HCl (7N), 1 hr HNO3 (1N)	96	weathered, iddingsite binaries
	A	**115**	**85G003**	**Sanidine**				97.5	
	A	116	SO 142-12DR-1	Leached WR	250-500	65	1 hr HCl (3.5N); 1 hr HNO3 (1N); 2 x 1 hr HCl (7N), 1 hr HNO3 (1N)	99	weathered, iddingsite binaries
Beethoven Ridge	A	117	SO 142-13DR-2	Leached WR	250-500	65	1 hr HCl (3.5N), 1 hr HNO3 (1N); 1 hr HCl (7N); 1 hr HNO3 (1N)	101	weathered, iddingsite and altered vesicle binaries
Beethoven Ridge	A	118	SO 142-13DR-2	plagioclase	125-250	65	1 hr HCl (3.5N); 5 min HF (6-7%),1 hr HNO3 (1N)	103	almost 100% clean grains
	A	119	PS051-041-1CC	Leached WR	250-500	80	1 hr HCl (3.5N); 1 hr HNO3 (1N); 1 hr HCl (7N); 1 hr HNO3 (1N)	106	very weathered
	A	120	PS051-041-1CC	plagioclase #1	125-250	65	1 hr HCl (3.5N); 1 hr HNO3 (1N), 2 x 1 hr HCl (7N), 1 hr HNO3 (1N)	108	almost 100% clean grains/white material to be picked
	A	121	PS051-041-1CC	plagioclase #2	125-250	13	1 hr HCl (3.5N); 5 min HF (6-7%);1 hr HNO3 (1N)	110	almost 100% clean grains
	A	122	85G003	Sanidine				111.5	

Table 2.1: Irradiated SO 141 and SO 142 rock samples, continued

Argon Data	Heating steps	Steps used in age calculation*	$^{36}Ar(a)$	$^{37}Ar^*$	^{39}Ar (K)	^{40}Ar (a+r)	Age	2s	^{40}Ar (r) (%)	39Ar (k) (%)	K/Ca
00M0230A	0.18 w	0	0.00462	0.00834	0.01078	1.01635	427.63	31.75	42.66	0.37	0.556
00M0230C	0.3 w	0	0.00466	0.03147	0.01756	0.97662	264.34	18.7	41.52	0.61	0.240
00M0230D	0.35 w	0	0.00210	0.04051	0.01746	0.50649	142.72	13.01	44.92	0.60	0.185
00M0230E	0.4 w	0	0.00085	0.05426	0.01899	0.43144	112.71	11.17	63.13	0.66	0.151
00M0230F	0.45 w	0	0.00059	0.07430	0.02444	0.50703	103.22	8.66	74.39	0.84	0.141
00M0230I	0.5 w	1	0.00422	0.77081	0.21579	4.16116	96.12	1.65	76.93	7.45	0.120
00M0230J	0.55 w	1	0.00107	0.85622	0.21393	4.05280	94.48	1.17	92.78	7.39	0.107
00M0230L	0.6 w	1	0.00017	0.82317	0.19617	3.68010	93.58	1.21	98.64	6.78	0.102
00M0230N	0.65 w	1	0.00010	0.76952	0.18669	3.52037	94.05	1.19	99.18	6.45	0.104
00M0230O	0.8 w	1	0.00007	1.08713	0.28676	5.37565	93.51	1.01	99.61	9.90	0.113
00M0230P	0.9 w	1	0.00022	1.24459	0.34783	6.54831	93.90	1.17	99.01	12.01	0.120
00M0230Q	1.0 W	0	0.00013	1.10475	0.33822	6.21733	91.74	1	99.40	11.68	0.132
00M0230R	1.1 w	0	0.00008	0.61196	0.20053	3.49257	87.04	1.03	99.34	6.93	0.141
00M0230S	1.5 w	0	0.00060	3.53083	0.51285	8.18424	79.91	0.93	97.87	17.71	0.062
00M0230U	3 w	0	0.00027	2.22390	0.13453	2.07151	77.17	1.27	96.27	4.65	0.026
00M0230V	fusion	0	0.00095	4.83767	0.17256	2.64455	76.81	1.45	90.43	5.96	0.015
00M0231B	0.3w	0	0.06635	0.16650	0.13012	10.42787	373.83	25.89	34.72	4.53	0.336
00M0231C	0.35w	0	0.03204	0.18049	0.13415	5.57897	203.62	15.82	37.08	4.67	0.320
00M0231D	0.4w	0	0.01069	0.22070	0.11673	2.70185	116.15	6.14	46.10	4.06	0.227
00M0231E	0.45w	0	0.00584	0.31437	0.13307	2.76937	104.77	3.1	61.60	4.63	0.182
00M0231F	0.5w	0	0.00389	0.48655	0.16696	3.32525	100.39	2.02	74.33	5.81	0.148
00M0231H	0.55w	0	0.00207	0.58019	0.17512	3.37463	97.21	1.67	84.65	6.09	0.130
00M0231I	0.6w	1	0.00078	0.77004	0.20087	3.69951	93.02	1.11	94.12	6.99	0.112
00M0231J	0.65w	1	0.00028	0.83834	0.17382	3.14413	91.40	1.16	97.42	6.05	0.089
00M0231K	0.7w	1	0.00032	1.06551	0.20884	3.81584	92.30	1.13	97.61	7.27	0.084
00M0231L	0.75w	1	0.00028	1.01638	0.18283	3.32528	91.89	1.15	97.54	6.36	0.077
00M0231N	0.8w	1	0.00037	0.88643	0.15109	2.75602	92.15	1.41	96.19	5.26	0.073
00M0231O	0.85w	1	0.00019	0.92372	0.14998	2.70678	91.20	1.57	97.93	5.22	0.070
00M0231P	1.0w	1	0.00024	0.96726	0.16542	3.02377	92.34	1.32	97.68	5.76	0.074
00M0231Q	1.5w	0	0.00074	3.58258	0.45230	6.89648	77.35	0.96	96.92	15.74	0.054
00M0231R	fusion	0	0.00301	10.11716	0.33259	4.46428	68.26	1.71	83.37	11.57	0.014
00M0233B	0.45 w	0	0.01485	0.29914	0.28505	3.39124	61.84	1.86	43.58	2.35	0.410
00M0233C	0.45 w	1	0.00565	1.09278	0.46350	5.19021	58.26	0.66	75.68	3.82	0.182
00M0233D	0.85 w	1	0.00235	1.95813	0.67868	7.59879	58.25	0.37	91.63	5.60	0.149
00M0233E	1.05 w	1	0.00246	2.93070	1.04821	11.65744	57.87	0.39	94.13	8.64	0.154
00M0233F	1.25 w	1	0.00119	2.84853	1.10352	12.30185	58.00	0.38	97.21	9.10	0.167
00M0233G	3.0 w	1	0.00373	6.09057	3.13622	34.91840	57.93	0.28	96.94	25.86	0.221

Table 2.2: 40Ar/39Ar Data, SO 141 and SO 142 cruises

00M0233H	4.5 w	1	0.00239	4.36358	1.89215	21.10427	58.03	0.3	96.76	15.60	0.186
00M0233K	fusion	0	0.01408	13.28549	3.51871	39.97876	59.10	0.33	90.57	29.02	0.114
00M0234A	0.45w	0	0.01473	0.33937	0.06834	1.28920	98.29	13.41	22.85	3.26	0.087
00M0234B	0.65w	0	0.00897	1.16868	0.07042	0.97989	73.01	9.7	26.98	3.36	0.026
00M0234C	0.85w	0	0.00110	0.74766	0.05165	1.07536	108.18	3.64	76.73	2.46	0.030
00M0234D	1.05w	1	0.00318	2.64810	0.12975	1.50136	60.92	2.75	61.54	6.19	0.021
00M0234F	1.25w	1	0.00178	2.92200	0.16792	1.86125	58.40	1.63	77.99	8.01	0.025
00M0234G	3.0w	1	0.00618	8.90308	0.79193	8.80472	58.57	1.04	82.82	37.78	0.038
00M0234H	4.0w	1	0.00178	5.30955	0.33348	3.74392	59.13	1.08	87.68	15.91	0.027
00M0234I	5.0w	0	0.00100	2.53536	0.13348	1.56146	61.57	1.91	84.15	6.37	0.023
00M0234J	fusion	0	0.00397	10.93917	0.34940	4.39615	66.14	1.83	78.92	16.67	0.014
00M0240B	0.3 w	0	0.03814	0.07814	0.39188	10.96435	150.20	6.23	49.3	1.89	2.157
00M0240C	0.35 w	0	0.01355	0.09978	0.25883	5.42908	113.76	3.48	57.5	1.25	1.115
00M0240D	0.4 w	0	0.00971	0.09079	0.28364	5.35967	102.80	2.52	65.1	1.37	1.343
00M0240E	0.45 w	0	0.00869	0.12997	0.35558	6.64366	101.68	1.98	72.1	1.72	1.176
00M0240F	0.5 w	1	0.00244	0.13162	0.37930	6.38120	91.80	1.12	89.8	1.83	1.239
00M0240H	0.55 w	1	0.00332	0.17054	0.46522	7.84457	92.01	1.11	88.9	2.25	1.173
00M0240I	0.6 w	1	0.00194	0.21238	0.51524	8.67694	91.89	1.02	93.8	2.49	1.043
00M0240J	0.65 w	1	0.00177	0.28108	0.56840	9.53749	91.57	1.38	94.8	2.75	0.870
00M0240K	0.7 w	1	0.00098	0.21845	0.47013	7.89970	91.69	0.96	96.5	2.27	0.925
00M0240L	0.75 w	1	0.00352	0.41355	0.85988	14.42330	91.54	1.01	93.3	4.15	0.894
00M0240N	0.85 w	1	0.00214	0.55325	1.11399	18.66342	91.43	0.96	96.7	5.38	0.866
00M0240O	1.1 w	1	0.00456	1.25975	2.84918	47.98867	91.91	0.93	97.3	13.77	0.973
00M0240P	1.5 w	1	0.00343	2.79538	5.14170	86.42109	91.72	0.93	98.8	24.84	0.791
00M0240Q	fusion	1	0.03128	9.51807	7.04439	118.15691	91.54	0.99	92.7	34.04	0.318
00M0241B	0.3w	1	0.49582	0.18867	1.89496	27.25700	79.15	16.33	15.69	13.57	4.319
00M0241C	0.4w	1	0.22794	0.23411	1.07160	15.54764	79.82	13.24	18.75	7.67	1.968
00M0241D	0.45w	1	0.12674	0.27655	0.72608	9.90925	75.18	10.92	20.92	5.20	1.129
00M0241E	0.5w	1	0.11724	0.32315	0.73386	9.96146	74.78	10.05	22.33	5.25	0.977
00M0241F	0.55w	1	0.07551	0.34655	0.59894	8.50817	78.19	7.99	27.60	4.29	0.743
00M0241H	0.65w	1	0.08946	0.58044	0.78583	11.00344	77.09	7.38	29.39	5.63	0.582
00M0241I	0.75w	1	0.06957	0.77940	0.77803	10.78783	76.36	5.71	34.42	5.57	0.429
00M0241J	0.85w	1	0.04580	0.83635	0.69839	9.83039	77.49	4.29	42.08	5.00	0.359
00M0241K	1.0w	1	0.04238	0.98276	0.79621	11.41727	78.91	3.52	47.69	5.70	0.348
00M0241L	1.25w	1	0.03769	1.76187	1.38682	20.27742	80.43	1.95	64.55	9.93	0.338
00M0241N	1.5w	1	0.02096	2.64271	1.99950	29.77019	81.87	1.14	82.78	14.32	0.325
00M0241O	partial fusion	1	0.01345	3.69331	1.36247	20.13101	81.26	1.17	83.51	9.76	0.159
00M0241P	fusion	1	0.03066	6.06047	1.13315	17.01858	82.56	2.05	65.26	8.11	0.080

Table 2.2: 40Ar/39Ar Data, SO 141 and SO 142 Cruises, Continued

00M0242B	0.35w	0	0.03368	0.23776	0.16794	1.85629	62.07	12.96	15.72	4.98	0.304
00M0242C	0.4w	1	0.00617	0.18454	0.13096	0.70906	30.67	4.34	28.00	3.89	0.305
00M0242D	0.45w	1	0.00441	0.25151	0.14485	0.70730	27.68	2.54	35.19	4.30	0.248
00M0242E	0.5w	1	0.00153	0.30507	0.15426	0.73997	27.20	1.12	62.04	4.58	0.217
00M0242F	0.55w	1	0.00057	0.35675	0.14591	0.67935	26.41	0.95	80.02	4.33	0.176
00M0242H	0.65w	1	0.00054	0.65332	0.25137	1.16443	26.27	0.67	87.87	7.46	0.165
00M0242I	0.75w	1	0.00009	0.90113	0.28730	1.34812	26.61	0.54	97.98	8.52	0.137
00M0242J	0.85w	1	0.00014	1.12996	0.35230	1.65287	26.61	0.5	97.63	10.45	0.134
00M0242K	1.0w	0	0.00000	0.65063	0.23582	1.23648	29.71	0.56	100.00	7.00	0.156
00M0242L	1.25w	0	0.00023	1.99239	0.49399	2.06764	23.76	0.45	96.78	14.66	0.107
00M0242N	1.5w	0	0.00032	2.97278	0.54691	2.10825	21.89	0.46	95.68	16.23	0.079
00M0242O	2w	0	0.00038	2.73156	0.26839	0.85635	18.14	0.75	88.28	7.96	0.042
00M0242P	fusion	0	0.00133	2.66386	0.19048	0.71529	21.33	1.17	64.47	5.65	0.031
00M0243B	0.4w	0	0.07450	0.49014	0.26310	3.12024	67.92	18.76	12.41	25.36	0.231
00M0243C	0.45w	0	0.00964	0.31403	0.05941	0.37677	36.64	11.48	11.68	5.73	0.081
00M0243D	0.5w	0	0.00827	0.32234	0.05900	0.42057	41.13	10.16	14.69	5.69	0.079
00M0243E	0.55w	0	0.00290	0.36293	0.04269	0.18210	24.73	5.99	17.53	4.11	0.051
00M0243F	0.65w	1	0.00145	0.54958	0.04813	0.13401	16.18	3.25	23.86	4.64	0.038
00M0243H	0.75w	1	0.00106	0.77747	0.05596	0.16685	17.32	3.37	34.72	5.39	0.031
00M0243I	0.85w	1	0.00043	0.92046	0.05438	0.15278	16.32	3.02	54.36	5.24	0.025
00M0243J	1.0w	1	0.00031	1.33550	0.07193	0.18731	15.13	2.24	67.21	6.93	0.023
00M0243K	1.25w	1	0.00019	2.31074	0.10628	0.28597	15.64	1.97	83.60	10.24	0.020
00M0243L	1.5w	1	0.00013	2.66626	0.09118	0.22615	14.42	2.21	85.30	8.79	0.015
00M0243N	1.75w	1	0.00021	2.89247	0.08025	0.19389	14.05	2.64	76.06	7.74	0.012
00M0243O	2w	1	0.00021	2.36639	0.05034	0.10207	11.79	3.34	62.22	4.85	0.009
00M0243R	fusion	1	0.00087	6.21634	0.05478	0.11706	12.43	5.79	31.32	5.28	0.004
00M0250A	0.4w	1	0.02579	0.26983	0.18241	1.13891	35.61	9.52	13.00	7.75	0.291
00M0250B	0.45w	1	0.00310	0.31467	0.11334	0.55168	27.82	2.29	37.55	4.82	0.155
00M0250C	0.5w	1	0.00071	0.26555	0.08944	0.41169	26.32	1.87	66.37	3.80	0.145
00M0250D	0.55w	1	0.00022	0.27777	0.09127	0.44279	27.73	1.69	87.02	3.88	0.141
00M0250F	0.65w	1	0.00017	0.54461	0.15166	0.73210	27.59	0.83	93.41	6.44	0.120
00M0250G	0.75w	1	0.00015	0.61092	0.16930	0.80785	27.28	0.72	94.86	7.19	0.119
00M0250K	0.85w	1	0.00021	1.01668	0.26851	1.29996	27.68	0.91	95.41	11.41	0.114
00M0250L	1.0w	1	0.00037	1.44259	0.33449	1.58312	27.06	0.74	93.56	14.21	0.100
00M0250N	1.25w	1	0.00042	3.23205	0.43235	2.01275	26.62	0.66	94.17	18.37	0.058
00M0250O	1.5w	1	0.00024	5.93882	0.23624	1.07494	26.02	1.9	93.85	10.04	0.017
00M0250P	1.85w	0	0.00034	8.03681	0.10543	0.42872	23.27	3.7	81.23	4.48	0.006
00M0250Q	fusion	0	0.00095	23.35218	0.17886	0.66986	21.45	5.71	70.56	7.60	0.003

Table 2.2: 40Ar/39Ar Data, SO 141 and SO 142 Cruises, Continued

00M0251A	0.4w	0	0.05248	1.35683	0.43365	3.52358	46.97	8.29	18.51	22.03	0.137
00M0251C	0.45w	1	0.00062	1.15765	0.21226	0.98917	27.09	1.22	84.44	10.78	0.079
00M0251D	0.5w	1	0.00015	1.19737	0.16934	0.81230	27.87	1.22	94.73	8.60	0.061
00M0251E	0.55w	1	0.00018	1.36628	0.16135	0.76900	27.70	1.41	93.62	8.20	0.051
00M0251F	0.65w	1	0.00005	2.14564	0.22400	1.09888	28.50	1.07	98.75	11.38	0.045
00M0251G	0.75w	1	0.00007	2.36134	0.21222	1.02706	28.12	1.01	98.03	10.78	0.039
00M0251I	0.85w	1	0.00019	2.30626	0.17434	0.77898	25.98	2.23	93.31	8.86	0.033
00M0251J	1.0w	1	0.00008	3.48848	0.16640	0.73315	25.62	2.18	96.81	8.45	0.021
00M0251M	1.25w	0	0.00038	5.24170	0.11793	0.42272	20.87	3.86	78.90	5.99	0.010
00M0251N	1.5w	0	0.00023	3.48908	0.04349	0.14996	20.08	9.59	69.05	2.21	0.005
00M0251O	fusion	0	0.00051	5.32774	0.05328	0.21746	23.74	8.78	58.83	2.71	0.004
00M0252A	0.4w	0	0.04245	0.92451	0.54800	5.14841	54.36	5.27	29.10	8.90	0.255
00M0252B	0.45w	0	0.00405	1.12419	0.44114	2.36859	31.27	0.87	66.44	7.16	0.169
00M0252D	0.5w	1	0.00184	1.44346	0.40712	2.10147	30.07	0.84	79.46	6.61	0.121
00M0252E	0.55w	1	0.00068	1.54270	0.38052	1.98016	30.31	0.7	90.77	6.18	0.106
00M0252F	0.65w	1	0.00071	2.68180	0.58533	3.05162	30.37	0.54	93.59	9.50	0.094
00M0252G	0.75w	1	0.00052	3.14561	0.68259	3.50398	29.90	0.53	95.78	11.08	0.093
00M0252H	0.45w	1	0.00026	2.65772	0.57114	2.92386	29.82	0.63	97.47	9.27	0.092
00M0252J	1.0w	1	0.00011	3.00977	0.70602	3.58259	29.56	0.58	99.06	11.46	0.101
00M0252K	1.5w	0	0.00082	7.15958	1.23329	5.39824	25.53	0.43	95.70	20.02	0.074
00M0252L	fusion	0	0.00287	11.75139	0.60360	2.39555	23.16	1.17	73.87	9.80	0.022
00M0253A	0.4w	0	0.14576	0.13610	1.54773	10.15835	38.28	6.33	19.08	6.29	4.890
00M0253B	0.45w	0	0.04412	0.08327	1.76179	10.16476	33.69	1.74	43.81	7.16	9.098
00M0253C	0.5w	0	0.01360	0.04967	1.60087	8.88991	32.44	0.74	68.87	6.51	13.859
00M0253F	0.55w	0	0.00542	0.04239	1.66530	9.06937	31.82	0.42	84.99	6.77	16.894
00M0253G	0.65w	1	0.00533	0.05153	2.40658	12.74082	30.94	0.36	88.99	9.78	20.082
00M0253H	0.75w	1	0.00414	0.06819	2.53096	13.27111	30.64	0.36	91.57	10.29	15.961
00M0253I	0.85w	1	0.00282	0.06521	2.21069	11.65959	30.82	0.39	93.33	8.98	14.578
00M0253J	1.0w	1	0.00281	0.18804	2.51313	13.09653	30.46	0.35	94.04	10.21	5.747
00M0253L	1.25w	1	0.00325	0.81629	3.32146	17.21191	30.29	0.37	94.72	13.50	1.750
00M0253M	1.5w	0	0.00134	0.70557	1.63004	8.16130	29.27	0.35	95.37	6.62	0.993
00M0253N	1.85w	0	0.00205	3.00499	1.66279	8.34743	29.35	0.38	93.23	6.76	0.238
00M0253O	fusion	0	0.00388	4.90899	1.75430	8.79669	29.31	0.4	88.47	7.13	0.154
00M0255B	0.4w	0	0.10220	0.68521	0.29574	4.34883	84.90	22.97	12.59	16.18	0.186
00M0255C	0.45w	0	0.00832	0.59592	0.10579	0.64556	35.72	5.9	20.79	5.79	0.076
00M0255D	0.5w	1	0.00192	0.50474	0.07625	0.34307	26.40	2.97	37.69	4.17	0.065
00M0255E	0.55w	1	0.00093	0.56159	0.07537	0.33631	26.19	3.27	55.12	4.12	0.058

Table 2.2: 40Ar/39Ar Data, SO 141 and SO 142 Cruises, Continued

00M0255F	0.65w	1	0.00067	0.95057	0.11598	0.51575	26.10	1.72	72.33	6.34	0.052
00M0255H	0.75w	1	0.00036	1.27446	0.14013	0.61758	25.87	1.29	85.47	7.66	0.047
00M0255I	0.85w	1	0.00026	1.54658	0.15353	0.69578	26.60	1.41	90.09	8.40	0.043
00M0255J	1.0w	1	0.00021	2.06579	0.17200	0.79502	27.12	1.19	92.87	9.41	0.036
00M0255K	1.25w	1	0.00030	3.43883	0.24743	1.15338	27.35	0.95	92.86	13.53	0.031
00M0255L	1.5w	0	0.00026	4.05461	0.20636	0.86326	24.56	1.19	91.90	11.29	0.022
00M0255N	1.85w	0	0.00042	4.89369	0.12433	0.43912	20.76	2.44	77.92	6.80	0.011
00M0255O	fusion	0	0.00173	12.93934	0.11535	0.38934	19.85	5.71	43.19	6.31	0.004
00M0256A	0.4w	0	0.11313	0.39713	0.53079	10.23979	75.56	9.59	23.45	10.03	0.575
00M0256B	0.45w	0	0.00816	0.40255	0.31557	2.94204	36.91	1.34	54.95	5.96	0.337
00M0256C	0.5w	1	0.00187	0.45286	0.31551	2.69213	33.81	0.56	82.94	5.96	0.300
00M0256E	0.55w	1	0.00074	0.42153	0.27342	2.31667	33.57	0.54	91.32	5.16	0.279
00M0256F	0.65w	1	0.00059	0.74453	0.45532	3.84227	33.44	0.43	95.66	8.60	0.263
00M0256G	0.65w	1	0.00002	1.01709	0.60131	5.11614	33.71	0.39	99.89	11.36	0.254
00M0256H	0.85w	1	0.00013	1.02518	0.56287	4.75412	33.47	0.38	99.21	10.63	0.236
00M0256I	1.0w	1	0.00006	1.21045	0.62160	5.21991	33.28	0.36	99.65	11.74	0.221
00M0256K	1.25w	0	0.00022	1.68724	0.74435	5.96020	31.75	0.39	98.93	14.06	0.190
00M0256L	1.5w	0	0.00038	2.19860	0.47922	3.41583	28.29	0.39	96.78	9.05	0.094
00M0256M	1.8w	0	0.00031	2.56945	0.23737	1.56237	26.14	0.64	94.49	4.48	0.040
00M0256N	fusion	0	0.00108	7.25058	0.15675	0.95625	24.24	2	75.06	2.96	0.009
00M0266B	0.4w	1	0.02493	0.21862	0.18982	2.06617	43.58	6.11	21.91	16.50	0.373
00M0266C	0.45w	1	0.00459	0.09902	0.15966	1.64715	41.33	1.63	54.82	13.88	0.693
00M0266D	0.5w	1	0.00119	0.14452	0.11449	1.13603	39.76	1.11	76.41	9.95	0.341
00M0266E	0.55w	1	0.00030	0.02876	0.03900	0.38902	39.97	2.65	81.37	3.39	0.583
00M0266F	0.65w	1	0.00031	0.04036	0.06645	0.68367	41.21	2.16	88.21	5.78	0.708
00M0266H	0.75w	1	0.00023	0.03412	0.04582	0.47826	41.81	2.15	87.61	3.98	0.577
00M0266I	0.85w	0	0.00015	0.04217	0.06210	0.70028	45.12	2.12	93.95	5.40	0.633
00M0266J	1.0w	0	0.00033	0.12867	0.09683	1.02477	42.38	0.99	91.35	8.42	0.324
00M0266K	1.25w	0	0.00043	0.55071	0.15143	1.51510	40.09	0.82	92.28	13.17	0.118
00M0266L	1.5w	0	0.00038	1.45311	0.12658	1.11226	35.26	1.22	90.84	11.01	0.037
00M0266N	1.8w	0	0.00032	2.19525	0.05230	0.36282	27.89	2.68	79.21	4.55	0.010
00M0266O	fusion	0	0.00035	12.63649	0.04559	0.31004	27.35	9.28	74.77	3.96	0.002
00M0267A	0.4w	0	0.01287	0.39391	0.36775	3.74261	41.78	1.75	49.59	11.08	0.401
00M0267B	0.45w	1	0.00378	0.36669	0.39924	3.66959	37.77	0.82	76.67	12.03	0.468
00M0267C	0.5w	1	0.00144	0.27649	0.33270	2.98869	36.93	0.64	87.56	10.03	0.517
00M0267F	0.55w	1	0.00073	0.24574	0.27882	2.53799	37.41	0.69	92.13	8.40	0.488
00M0267G	0.65w	1	0.00031	0.27397	0.29980	2.68818	36.86	0.51	96.73	9.03	0.471
00M0267H	0.75w	1	0.00038	0.29136	0.27900	2.50551	36.91	0.55	95.75	8.41	0.412

Table 2.2: 40Ar/39Ar Data, SO 141 and SO 142 Cruises, Continued

00M0267I	0.85w	1	0.00041	0.35080	0.27776	2.47843	36.68	0.64	95.30	8.37	0.340
00M0267J	1.0w	0	0.00053	0.52192	0.26438	2.23726	34.81	0.79	93.47	7.97	0.218
00M0267L	1.25w	0	0.00077	1.54924	0.33398	2.66026	32.78	0.55	92.16	10.06	0.093
00M0267M	1.5w	0	0.00057	2.56872	0.23756	1.86458	32.31	0.78	91.72	7.16	0.040
00M0267N	1.8w	0	0.00031	5.24074	0.16020	1.17453	30.19	1.29	92.73	4.83	0.013
00M0267O	fusion	0	0.00174	9.80451	0.08731	0.54011	25.51	4.38	51.30	2.63	0.004
00M0268A	0.4w	0	0.01126	0.01961	0.02530	0.36461	73.79	26.41	9.88	2.09	0.555
00M0268C	0.45w	1	0.00373	0.57882	0.13528	0.80524	30.85	3.15	42.25	11.15	0.100
00M0268D	0.5w	1	0.00074	0.50262	0.09446	0.55139	30.25	2.42	71.65	7.79	0.081
00M0268E	0.55w	1	0.00027	0.49585	0.08450	0.52082	31.93	2.73	86.52	6.97	0.073
00M0268F	0.65w	1	0.00015	0.75581	0.11908	0.74604	32.45	2	94.53	9.82	0.068
00M0268G	0.75w	1	0.00011	0.87145	0.13253	0.81738	31.95	1.84	96.19	10.93	0.065
00M0268J	0.85w	1	0.00006	0.89509	0.12825	0.80618	32.56	1.18	97.92	10.58	0.062
00M0268K	1.0w	0	0.00010	0.94157	0.12108	0.70650	30.24	0.99	95.85	9.98	0.055
00M0268L	1.25w	0	0.00026	1.70947	0.17549	0.80287	23.75	0.99	91.14	14.47	0.044
00M0268M	1.5w	0	0.00022	1.28039	0.09479	0.44126	24.17	1.83	87.19	7.82	0.032
00M0268N	1.8w	0	0.00018	0.70084	0.03650	0.19647	27.91	3.3	78.34	3.01	0.022
00M0268P	fusion	0	0.00128	2.24484	0.06546	0.32635	25.87	3.13	46.25	5.40	0.013
00M0269A	0.4w	1	0.06576	0.41327	0.64562	6.01008	49.69	6.31	23.62	10.13	0.672
00M0269B	0.45w	1	0.01079	0.37032	0.54456	5.05754	49.58	1.44	61.34	8.55	0.632
00M0269C	0.5w	1	0.00458	0.27515	0.36136	3.31326	48.95	1.25	71.02	5.67	0.565
00M0269D	0.55w	1	0.00289	0.27146	0.31586	2.84924	48.17	1.07	76.92	4.96	0.500
00M0269F	0.65w	1	0.00307	0.43852	0.45125	4.11750	48.72	0.93	81.94	7.08	0.442
00M0269G	0.75w	1	0.00229	0.59369	0.52175	4.77465	48.86	0.8	87.60	8.19	0.378
00M0269H	0.85w	1	0.00112	0.65842	0.40306	3.62963	48.09	0.89	91.64	6.33	0.263
00M0269I	1.0w	0	0.00116	0.85123	0.44441	3.82060	45.94	0.8	91.80	6.97	0.224
00M0269J	1.25w	0	0.00138	1.39475	0.56536	4.56317	43.16	0.67	91.79	8.87	0.174
00M0269M	1.5w	0	0.00300	3.98061	0.92783	6.90179	39.82	0.6	88.61	14.56	0.100
00M0269N	1.5w	0	0.00280	4.44267	0.66926	4.83045	38.65	0.7	85.40	10.50	0.065
00M0269O	fusion	0	0.00914	12.05592	0.52191	3.81275	39.11	1.89	58.54	8.19	0.019
00M0275A	0.4w	0	0.03616	0.39664	0.80264	8.28457	59.18	3.13	43.67	13.54	0.870
00M0275B	0.45w	1	0.00257	0.35554	0.51805	3.37717	37.60	0.57	81.67	8.74	0.627
00M0275D	0.5w	1	0.00099	0.34058	0.36040	2.35350	37.67	0.58	88.99	6.08	0.455
00M0275E	0.55w	1	0.00057	0.39828	0.36838	2.42800	38.02	0.62	93.51	6.21	0.398
00M0275F	0.65w	1	0.00056	0.59512	0.46154	3.02052	37.75	0.49	94.76	7.78	0.333
00M0275G	0.75w	1	0.00053	0.76222	0.46139	3.05311	38.17	0.6	95.11	7.78	0.260
00M0275H	0.85w	0	0.00039	0.87274	0.43692	2.98136	39.34	0.61	96.25	7.37	0.215
00M0275J	1.0w	0	0.00047	1.13397	0.44828	3.18743	40.98	0.7	95.84	7.56	0.170

Table 2.2: 40Ar/39Ar Data, SO 141 and SO 142 Cruises, Continued

00M0275K	1.25w	0	0.00029	2.15435	0.64950	4.70787	41.76	0.58	98.22	10.96	0.130
00M0275L	1.5w	0	0.00068	2.65480	0.55416	3.81276	39.67	0.68	94.99	9.35	0.090
00M0275M	1.8w	0	0.00107	4.57646	0.46982	3.15506	38.73	0.81	90.86	7.92	0.044
00M0275N	fusion	0	0.00637	15.98123	0.39758	2.49070	36.15	2.54	56.97	6.71	0.011
00M0282B	0.45w	0	0.00124	0.09852	0.00950	0.18032	77.75	11.5	32.95	0.74	0.041
00M0282C	0.65w	1	0.00153	0.24717	0.01282	0.17570	56.50	12.89	27.99	0.99	0.022
00M0282D	0.65w	1	0.00136	0.55508	0.01942	0.27550	58.45	6.34	40.73	1.51	0.015
00M0282E	1.05w	1	0.00207	0.96565	0.02943	0.40229	56.35	5.89	39.70	2.28	0.013
00M0282F	1.3w	1	0.00158	1.79028	0.05334	0.70534	54.54	3.16	60.13	4.14	0.013
00M0282H	1.5w	1	0.00065	1.87825	0.06554	0.83152	52.36	2.03	81.12	5.08	0.015
00M0282I	2.0w	1	0.00196	4.68715	0.27342	3.40771	51.45	1.15	85.45	21.20	0.025
00M0282J	2.5w	1	0.00009	0.68767	0.02351	0.30435	53.41	4.04	91.71	1.82	0.015
00M0282K	3.5w	1	0.00081	2.37900	0.10494	1.33111	52.35	1.56	84.78	8.14	0.019
00M0282L	6.0w	1	0.00188	6.29721	0.35616	4.50858	52.24	1.03	89.05	27.62	0.024
00M0282N	fusion	0	0.00235	12.02661	0.34150	4.71334	56.89	1.42	87.14	26.48	0.012
00M0283A	0.45w	1	0.00207	0.02894	0.01496	0.20239	64.79	13.41	24.86	0.51	0.222
00M0283B	0.85w	1	0.00641	0.41194	0.07742	0.82751	51.38	4.24	30.41	2.66	0.081
00M0283C	0.85w	1	0.00227	0.68871	0.08569	0.91598	51.39	2.37	57.68	2.94	0.054
00M0283D	1.3w	1	0.00194	1.32567	0.16368	1.73912	51.08	1.2	75.16	5.62	0.053
00M0283G	1.5w	1	0.00104	1.49323	0.18454	1.97040	51.33	1.35	86.53	6.34	0.053
00M0283H	1.7w	1	0.00079	1.79782	0.23511	2.52150	51.55	0.91	91.49	8.08	0.056
00M0283I	2.0w	1	0.00074	2.38349	0.38617	4.14577	51.61	0.64	95.02	13.26	0.070
00M0283J	3.6w	1	0.00024	1.53281	0.17268	1.84956	51.49	1.17	96.28	5.93	0.048
00M0283K	6.0w	1	0.00128	5.22390	0.75630	8.17199	51.94	0.68	95.58	25.98	0.062
00M0283M	fusion	0	0.00216	13.67154	0.83493	9.61574	55.30	0.91	93.77	28.68	0.026
00M0284B	0.65w	0	0.00161	0.34018	0.02256	0.27150	52.86	8	36.39	2.25	0.029
00M0284C	1.0w	0	0.00116	1.13112	0.04650	0.52811	49.91	2.44	60.57	4.65	0.018
00M0284D	1.3w	1	0.00050	1.80556	0.08102	0.87360	47.42	1.44	85.49	8.10	0.019
00M0284E	1.5w	1	0.00077	1.98629	0.10873	1.15948	46.91	1.63	83.58	10.87	0.024
00M0284F	2.0w	1	0.00152	3.88775	0.31346	3.33188	46.75	0.88	88.10	31.33	0.035
00M0284H	3.0w	1	0.00012	0.94124	0.03187	0.34697	47.87	3.96	90.71	3.19	0.015
00M0284I	5.0w	1	0.00035	3.42241	0.18509	2.01565	47.89	1.04	95.06	18.50	0.023
00M0284L	7.0w	1	0.00026	2.39999	0.11033	1.21612	48.46	1.44	93.98	11.03	0.020
00M0284M	9.0w	0	0.00020	1.47126	0.04674	0.54727	51.44	3.03	90.26	4.67	0.014
00M0284N	partial fusion	0	0.00014	1.86751	0.02321	0.33051	62.36	5.34	89.06	2.32	0.005
00M0284O	fusion	0	0.00024	2.92950	0.03108	0.42821	60.36	6	85.98	3.11	0.005
01M0015B	0.4w	0	0.06983	0.48882	0.12388	4.57894	163.22	32.81	18.16	7.02	0.109

Table 2.2: 40Ar/39Ar Data, SO 141 and SO 142 Cruises, Continued

01M0015C	0.45w	1	0.00551	0.58160	0.08533	1.06848	56.96	43.48	39.63	4.84	0.063
01M0015F	0.55w	1	0.00095	0.03615	0.06218	0.61956	45.48	25.71	68.89	3.53	0.740
01M0015H	0.65w	1	0.00061	0.52017	0.10187	0.86479	38.81	15.5	82.69	5.78	0.084
01M0015I	0.75w	1	0.00127	0.57655	0.16120	1.19285	33.88	9.88	76.10	9.14	0.120
01M0015K	1.0w	1	0.00035	0.38925	0.18985	1.74894	42.08	7.95	94.46	10.76	0.210
01M0015L	1.0w	1	0.00102	0.53614	0.23944	2.03163	38.80	6.48	87.12	13.58	0.192
01M0015N	1.25w	1	0.00069	0.79550	0.29065	2.64228	41.54	4.47	92.80	16.48	0.157
01M0015O	1.5w	1	0.00063	0.70403	0.23215	1.91957	37.82	7.39	91.11	13.16	0.142
01M0015Q	2.25w	1	0.00000	0.41114	0.09723	0.84560	39.76	0.62	100.00	5.51	0.102
01M0015R	fusion	1	0.00171	5.25959	0.17995	1.30509	33.21	8.77	72.11	10.20	0.015
01M0043A	0.65w	1	0.09795	4.56520	0.47938	6.07384	61.61	11.53	17.34	2.87	0.045
01M0043B	1.0w	1	0.05393	13.31724	0.98002	11.30946	56.20	3.44	41.51	5.86	0.032
01M0043D	1.3w	1	0.02373	18.54529	1.62471	18.58062	55.70	1.35	72.60	9.71	0.038
01M0043E	1.5w	1	0.01883	13.91289	1.23751	14.17098	55.78	1.42	71.81	7.40	0.038
01M0043F	2w	1	0.01248	26.42576	3.06603	34.43011	54.71	0.83	90.33	18.33	0.050
01M0043H	3.0w	1	0.00161	2.70107	0.21949	2.61968	58.10	3.47	84.63	1.31	0.035
01M0043I	5.0w	0	0.00722	23.65726	1.71293	20.05347	57.00	1.05	90.38	10.24	0.031
01M0043J	7.0w	0	0.00743	28.42736	2.05492	24.28283	57.53	1.01	91.71	12.28	0.031
01M0043L	7.0w	0	0.00715	30.50023	1.56793	19.28839	59.85	1.28	90.12	9.37	0.022
01M0043M	fusion	0	0.02937	121.10586	3.78609	51.90190	66.57	1.84	85.68	22.63	0.013
01M0049B	0.65w	0	0.00987	0.00000	0.00055	0.02471	215.97	1847	0.84	0.00	0.000
01M0049C	1.0w	0	0.00089	0.00000	0.00134	0.02283	84.41	716.7	7.98	0.01	0.000
01M0049E	1.3w	0	0.00000	0.00000	0.00085	0.05324	293.53	130	100.00	0.01	0.000
01M0049F	1.5w	0	0.00033	0.00000	0.00149	0.00000	0.00	0	0.00	0.01	0.000
01M0049G	2.0w	0	0.00051	0.00000	0.00678	0.08746	64.13	47.94	36.57	0.06	0.000
01M0049I	3.0w	0	0.00080	0.07975	0.00531	0.00000	0.00	0	0.00	0.04	0.029
01M0049J	7.0w	1	0.00153	3.67241	0.22640	1.95576	43.21	2.57	81.26	1.87	0.027
01M0049K	10.0w	1	0.00143	12.92145	0.64842	5.69885	43.95	1.34	93.08	5.35	0.022
01M0049M	13.0w	1	0.00124	21.13700	1.05498	9.27826	43.98	1.19	96.20	8.70	0.021
01M0049N	16.0w	1	0.00039	10.20542	0.50945	4.51688	44.33	1.2	97.50	4.20	0.021
01M0049O	19.0w	1	0.00083	14.66379	0.73025	6.43123	44.04	1.24	96.33	6.02	0.021
01M0049S	22.0w	1	0.00086	10.71413	0.55586	4.75974	42.83	1.57	94.95	4.58	0.022
01M0049U	partial fusion	1	0.00203	23.88250	1.20157	10.49123	43.67	1.24	94.58	9.91	0.022
01M0049V	fusion	1	0.00548	141.80197	7.18026	63.04440	43.91	1.09	97.50	59.23	0.022
01M0060B	0.65w	1	0.00686	1.55338	0.07920	0.63313	43.42	15.5	23.79	4.21	0.022
01M0060C	1.0w	1	0.00233	9.31461	0.27070	2.01341	40.43	4.71	74.49	14.39	0.012
01M0060D	1.3w	1	0.00187	10.97707	0.26693	2.13428	43.42	4.84	79.42	14.19	0.010
01M0060F	1.5w	1	0.00096	6.87649	0.16323	1.38581	46.07	2.98	83.01	8.68	0.010

Table 2.2: 40Ar/39Ar Data, SO 141 and SO 142 Cruises, Continued

01M0060H	3w	1	0.00025	2.32067	0.04904	0.44206	48.88	16.49	85.75	2.61	0.009
01M0060I	5w	1	0.00106	5.52701	0.11805	1.05145	48.31	7.3	76.99	6.28	0.009
01M0060K	7w	1	0.00137	4.25758	0.08436	0.72161	46.42	6.3	64.03	4.49	0.009
01M0060L	fusion	1	0.00458	43.57533	0.84926	7.64070	48.79	4.35	84.95	45.15	0.008
01M0068A	0.45w	1	1.01077	9.43263	13.48286	139.92796	55.31	4.66	31.90	17.84	0.615
01M0068B	0.45w	1	0.07643	4.23080	5.07822	48.23374	50.69	1.11	68.11	6.72	0.516
01M0068D	0.5w	1	0.06758	4.69912	5.57102	52.97110	50.74	0.94	72.62	7.37	0.510
01M0068E	0.55w	1	0.02770	2.82315	3.08408	29.19240	50.52	0.85	78.10	4.08	0.470
01M0068G	0.65w	1	0.02359	4.11384	3.52315	33.53027	50.79	0.73	82.79	4.66	0.368
01M0068H	0.75w	1	0.02420	5.85227	4.35019	41.63463	51.07	0.74	85.34	5.76	0.320
01M0068I	0.85w	0	0.02566	6.79499	3.99936	35.94408	48.00	0.7	82.58	5.29	0.253
01M0068J	1.0w	0	0.06916	23.05505	11.65436	100.83211	46.23	0.62	83.15	15.42	0.217
01M0068M	1.25w	0	0.02948	20.34313	6.31051	49.53624	41.99	0.64	85.04	8.35	0.133
01M0068N	1.5w	0	0.03862	33.98018	6.86053	52.52485	40.97	0.71	82.15	9.08	0.087
01M0068O	1.85w	0	0.02572	27.96436	3.03671	22.54773	39.75	1.12	74.79	4.02	0.047
01M0068P	fusion	0	0.15450	111.26956	8.61993	68.03098	42.22	1.57	59.84	11.41	0.033
01M0086B	0.4w	0	0.75113	3.39663	0.77777	63.75500	321.03	40.6	22.31	9.92	0.098
01M0086C	0.45w	0	0.22304	5.22731	0.46041	15.14650	135.78	22.82	18.69	5.88	0.038
01M0086E	0.5w	0	0.07879	3.89119	0.27723	6.53412	98.30	14.17	21.91	3.54	0.031
01M0086F	0.55w	0	0.02932	3.54584	0.16098	2.89825	75.57	10.53	25.07	2.05	0.020
01M0086H	0.65w	0	0.04761	12.00859	0.41337	6.82731	69.44	6.17	32.67	5.27	0.015
01M0086I	0.75w	0	0.00654	12.05496	0.32006	4.36907	57.59	2.45	69.35	4.08	0.011
01M0086J	0.85w	0	0.01470	9.65066	0.23934	3.54810	62.45	4.11	44.96	3.05	0.011
01M0086L	1.0w	0	0.00927	11.02842	0.27264	3.94966	61.05	3.22	59.03	3.48	0.011
01M0086M	1.25w	0	0.02777	24.44048	0.82484	10.86662	55.61	2.73	56.97	10.53	0.015
01M0086N	1.85w	1	0.01549	42.69725	1.28802	13.79832	45.35	1.81	75.09	16.44	0.013
01M0086P	fusion	1	0.01653	73.28377	2.80188	30.49033	46.05	1.33	86.19	35.75	0.016
01M0088B	0.4w	0	0.34620	3.71063	0.48719	35.00939	288.92	31.12	25.50	14.28	0.056
01M0088C	0.45w	0	0.04032	2.43450	0.13045	3.62351	117.23	16.64	23.32	3.82	0.023
01M0088E	0.5w	0	0.02263	2.64981	0.12939	2.81554	92.48	9.41	29.63	3.79	0.021
01M0088F	0.55w	1	0.00699	2.64453	0.09539	1.65518	74.12	7.29	44.50	2.80	0.016
01M0088G	0.65w	1	0.00555	3.52936	0.10154	1.78050	74.89	6.96	52.06	2.98	0.012
01M0088I	0.75w	1	0.01034	5.40063	0.16960	3.05984	77.00	5.02	50.04	4.97	0.014
01M0088J	0.85w	1	0.00678	13.38456	0.32435	5.72513	75.37	3.09	74.06	9.51	0.010
01M0088K	1.0w	1	0.00432	11.39135	0.27038	4.79145	75.66	3.07	78.95	7.92	0.010
01M0088M	1.25w	0	0.00577	8.50661	0.24508	3.69294	64.54	3.16	68.43	7.18	0.012
01M0088N	1.85w	0	0.00693	31.84706	0.53782	7.07604	56.48	3.16	77.55	15.76	0.007
01M0088O	fusion	0	0.02199	60.25420	0.92081	11.46201	53.48	3.51	63.82	26.99	0.007

Table 2.2: 40Ar/39Ar Data, SO 141 and SO 142 Cruises, Continued

01M0098B	0.4w	0	1.22533	3.74481	2.80975	42.06125	78.94	13.18	10.41	5.14	0.323
01M0098C	0.45w	1	0.16392	1.36137	0.82774	8.04173	51.63	6.15	14.24	1.51	0.261
01M0098D	0.5w	1	0.10419	1.32770	0.99689	9.53186	50.82	3.33	23.64	1.82	0.323
01M0098F	0.55w	1	0.11833	1.58963	1.56085	14.97417	50.99	2.36	29.98	2.85	0.422
01M0098G	0.65w	1	0.04742	1.41758	1.25902	11.98070	50.58	1.21	46.09	2.30	0.382
01M0098H	0.75w	1	0.09783	2.42415	2.12796	20.07444	50.15	1.46	40.98	3.89	0.377
01M0098J	0.85w	1	0.05801	3.37232	2.56082	23.69900	49.21	0.8	58.03	4.68	0.327
01M0098K	1.0w	1	0.02087	1.22678	0.80850	7.46069	49.07	1.17	54.75	1.48	0.283
01M0098L	1.5w	1	0.15934	21.75962	9.83047	88.75025	48.02	0.58	65.34	17.98	0.194
01M0098N	1.8w	0	0.07733	26.97737	6.84176	58.87529	45.80	0.47	72.04	12.51	0.109
01M0098O	2.1w	0	0.10026	36.26944	6.76381	57.78899	45.48	0.57	66.11	12.37	0.080
01M0098P	2.4w	0	0.07453	27.32340	4.15275	35.16189	45.07	0.68	61.49	7.59	0.065
01M0098Q	fusion	0	0.32134	112.84201	14.14843	123.22507	46.35	0.83	56.48	25.87	0.054
01M0124B	0.4w	0	0.97224	1.43091	1.16166	33.12101	127.19	42.93	10.34	3.14	0.349
01M0124C	0.45w	0	0.39620	1.55001	0.79970	13.46804	76.21	25.9	10.32	2.16	0.222
01M0124D	0.5w	1	0.10020	0.75161	0.40395	3.86900	43.74	13.43	11.56	1.09	0.231
01M0124F	0.55w	1	0.09894	1.26328	0.94780	9.07306	43.71	5.57	23.68	2.56	0.323
01M0124G	0.65w	1	0.09037	2.36659	1.53793	14.43101	42.86	3.18	35.08	4.15	0.279
01M0124H	0.75w	1	0.03199	1.53705	0.79997	7.57121	43.22	2.36	44.47	2.16	0.224
01M0124J	0.85w	1	0.04678	1.93722	0.95993	9.00539	42.85	2.87	39.45	2.59	0.213
01M0124K	1.0w	1	0.02553	2.61573	1.78197	16.56367	42.46	1.09	68.71	4.81	0.293
01M0124L	1.4w	1	0.04304	6.78918	4.25031	39.73671	42.70	0.77	75.75	11.48	0.269
01M0124M	1.4w	1	0.01877	9.16817	5.08045	47.29132	42.52	0.53	89.50	13.72	0.238
01M0124O	1.6w	1	0.01795	17.90291	7.92746	73.54271	42.38	0.47	93.27	21.41	0.190
01M0124P	1.8w	0	0.00693	13.47777	4.26289	37.25873	39.95	0.48	94.79	11.51	0.136
01M0124Q	2.0w	0	0.00640	17.20598	3.16061	26.04883	37.70	0.5	93.23	8.54	0.079
01M0124R	fusion	0	0.02240	48.54562	3.95212	32.39665	37.50	0.89	83.03	10.67	0.035
01M0125B	0.4w	0	0.20812	1.06238	0.88749	20.91034	99.92	11.42	25.37	3.00	0.359
01M0125C	0.45w	0	0.11403	1.19189	0.80461	14.51767	77.01	7.12	30.11	2.72	0.290
01M0125D	0.5w	0	0.12871	1.73460	1.18078	17.54091	63.64	5.48	31.56	3.99	0.293
01M0125F	0.55w	0	0.08025	2.06718	1.45176	16.95039	50.21	2.88	41.68	4.91	0.302
01M0125G	0.65w	0	0.02322	1.22810	0.64097	6.83476	45.91	2.31	49.90	2.17	0.224
01M0125H	0.75w	1	0.03411	1.97603	1.40907	13.40352	41.01	1.33	57.08	4.77	0.307
01M0125I	0.85w	1	0.01489	1.13918	0.87990	8.11355	39.77	1.06	64.84	2.98	0.332
01M0125J	1.1w	1	0.04282	4.97083	2.68439	25.01413	40.18	0.97	66.41	9.08	0.232
01M0125L	1.3w	1	0.01356	2.25138	1.02124	9.46187	39.95	0.88	70.25	3.45	0.195
01M0125M	1.5w	1	0.03231	6.59271	2.53200	23.28928	39.67	0.82	70.92	8.56	0.165
01M0125N	1.7w	0	0.02090	10.94603	3.14062	26.10257	35.88	0.61	80.87	10.62	0.123

Table 2.2: 40Ar/39Ar Data, SO 141 and SO 142 Cruises, Continued

01M0125O	2.0w	0	0.02110	18.99566	3.07140	23.38306	32.90	0.66	78.95	10.39	0.070
01M0125P	2.3w	0	0.04611	24.76106	3.22230	25.85895	34.66	1	65.49	10.90	0.056
01M0125Q	fusion	0	0.08874	106.80680	6.63942	46.51148	30.29	1.18	63.95	22.46	0.027
01M0135B	0.45w	0	0.16680	2.42367	0.80072	11.01917	77.87	13.64	18.27	8.92	0.142
01M0135C	0.5w	0	0.04302	1.00332	0.23250	2.96418	72.25	12.89	18.91	2.59	0.100
01M0135D	0.55w	0	0.03254	1.80231	0.29014	2.31186	45.49	8.53	19.38	3.23	0.069
01M0135F	0.65w	0	0.01530	1.58274	0.20643	1.29047	35.79	5.58	22.20	2.30	0.056
01M0135G	0.75w	0	0.01921	2.40179	0.32486	1.78982	31.58	4.24	23.97	3.62	0.058
01M0135H	0.85w	0	0.02562	4.44950	0.49535	2.44736	28.34	3.72	24.43	5.52	0.048
01M0135I	1.0w	0	0.01188	4.72384	0.43515	1.71862	22.69	2.58	32.87	4.85	0.040
01M0135K	1.2w	1	0.01808	13.03753	1.14188	3.37233	17.00	1.71	38.70	12.72	0.038
01M0135L	1.4w	1	0.01022	11.68795	0.86593	2.50038	16.62	1.33	45.29	9.65	0.032
01M0135M	1.6w	1	0.00454	13.48029	0.79598	2.16269	15.64	1.29	61.72	8.87	0.025
01M0135N	1.8w	1	0.00681	12.86158	0.69961	1.92068	15.80	1.67	48.82	7.79	0.023
01M0135O	2.0w	1	0.00729	13.76123	0.64025	1.70058	15.29	1.85	44.10	7.13	0.020
01M0135Q	fusion	1	0.02452	80.14766	2.04877	5.61372	15.77	2.75	43.66	22.82	0.011
01M0146B	0.65W	0	0.00056	0.00000	0.00371	0.14430	184.27	138.2	46.54	0.03	0.000
01M0146C	1.0w	1	0.00033	0.00000	0.00571	0.06791	58.40	98.35	41.03	0.04	0.000
01M0146D	1.3w	1	0.00045	0.00000	0.01922	0.20008	51.20	29.2	59.91	0.13	0.000
01M0146F	1.5w	1	0.00023	0.33155	0.02316	0.23557	50.03	10.32	77.43	0.16	0.030
01M0146G	3w	1	0.00119	0.58846	0.07208	0.57884	39.62	4.51	62.14	0.49	0.053
01M0146H	5w	1	0.00112	2.46006	0.17637	1.55100	43.34	1.64	82.41	1.21	0.031
01M0146I	7w	1	0.00223	9.83552	0.57538	4.93162	42.26	1.17	88.22	3.93	0.025
01M0146K	9w	1	0.00387	37.75033	2.09600	18.39740	43.26	1.18	94.14	14.33	0.024
01M0146L	partial fusion	1	0.00367	36.48971	1.93637	17.00407	43.28	1.19	94.01	13.24	0.023
01M0146M	partial fusion	1	0.00388	48.06535	2.51434	22.20345	43.52	1.15	95.09	17.19	0.022
01M0146N	fusion	1	0.01663	141.25807	7.20463	63.98826	43.77	1.15	92.87	49.26	0.022
01M0156B	0.4w	0	0.25474	0.22851	0.42345	8.95148	106.73	34.48	10.63	1.56	0.797
01M0156C	0.45w	0	0.30263	0.77762	0.44896	10.15700	113.99	38.56	10.20	1.65	0.248
01M0156D	0.55w	0	0.37255	1.72808	0.72604	14.90459	103.73	29.56	11.92	2.67	0.181
01M0156F	0.65w	0	0.14857	0.57541	0.25445	5.26624	104.56	33.59	10.71	0.93	0.190
01M0156G	0.75w	0	0.20002	1.21101	0.43843	7.31109	84.71	26.6	11.01	1.61	0.156
01M0156H	0.85w	0	0.31715	2.66401	0.84311	12.16704	73.54	22.06	11.49	3.10	0.136
01M0156I	1.0w	0	0.31315	2.28487	0.84013	13.13276	79.52	21.76	12.43	3.09	0.158
01M0156J	1.2w	0	0.21071	7.15678	1.64442	15.69513	48.97	7.71	20.13	6.04	0.099
01M0156K	1.4w	0	0.10704	4.33884	1.17032	9.51188	41.79	5.65	23.12	4.30	0.116
01M0156M	1.6w	1	0.02704	5.60877	1.36480	8.71033	32.89	1.61	52.15	5.02	0.105
01M0156N	1.8w	1	0.08934	9.67024	2.22436	14.42304	33.41	2.56	35.33	8.17	0.099

Table 2.2: 40Ar/39Ar Data, SO 141 and SO 142 Cruises, Continued

01M0156O	2.0w	1	0.00902	9.62458	1.74551	11.23429	33.17	0.97	80.83	6.41	0.078
01M0156P	2.2w	1	0.05202	16.51740	2.76366	17.68424	32.98	1.4	53.50	10.16	0.072
01M0156Q	2.4w	1	0.06713	47.05263	5.44695	34.25253	32.41	1.06	63.33	20.02	0.050
01M0156T	2.8w	0	0.01869	15.37906	1.85930	10.86474	30.14	0.95	66.29	6.83	0.052
01M0156U	fusion	0	0.06373	61.22932	5.02039	25.84343	26.58	1.18	57.85	18.45	0.035
01M0169C	single fusion	1	0.01113	10.30200	0.65505	5.89706	44.85	1.59	64.19	9.71	0.027
01M0169D	single fusion	1	0.02964	11.93939	0.82012	7.43814	45.18	2.48	45.93	12.15	0.030
01M0169E	single fusion	1	0.01621	9.21106	0.65832	5.95324	45.05	2.03	55.41	9.76	0.031
01M0169F	single fusion	1	0.00771	9.12018	0.64382	5.72610	44.31	1.44	71.54	9.54	0.030
01M0169H	single fusion	1	0.02293	10.71851	0.73559	6.64389	44.99	2.27	49.51	10.90	0.030
01M0169I	single fusion	1	0.02764	10.48512	0.64666	5.98719	46.11	2.92	42.30	9.58	0.027
01M0169J	single fusion	1	0.00860	10.89498	0.60359	5.41211	44.67	1.62	68.06	8.95	0.024
01M0169K	single fusion	1	0.04409	14.02895	1.10620	10.18997	45.88	2.64	43.89	16.39	0.034
01M0169L	single fusion	1	0.04079	11.84309	0.87830	7.96862	45.19	3.13	39.80	13.02	0.032
01M0170A	0.4w	0	1.14627	4.33502	3.72191	54.71306	81.81	19.65	13.91	17.43	0.369
01M0170B	0.5w	0	0.20697	3.97756	1.92876	18.50042	53.80	7.05	23.22	9.03	0.209
01M0170C	0.55w	0	0.04939	2.88062	1.00057	8.73023	49.01	3.44	37.43	4.69	0.149
01M0170D	0.65w	1	0.02213	2.48961	0.56026	4.64043	46.55	2.99	41.50	2.62	0.097
01M0170F	0.75w	1	0.01498	0.00443	0.54444	4.31853	44.61	2.17	49.38	2.55	52.837
01M0170G	0.85w	1	0.02273	0.00780	1.06840	8.38146	44.12	1.61	55.52	5.00	58.881
01M0170H	1.0w	1	0.01138	0.00369	0.55069	4.43023	45.23	1.81	56.84	2.58	64.193
01M0170I	1.2w	1	0.01257	0.00712	0.93949	7.42464	44.44	1.09	66.65	4.40	56.701
01M0170K	1.4w	1	0.00807	0.00869	1.22233	9.46956	43.58	0.76	79.89	5.73	60.473
01M0170L	1.6w	1	0.03149	0.05193	6.82530	53.00663	43.68	0.55	85.06	31.97	56.520
01M0170M	1.8w	0	0.00865	0.01484	1.62986	12.25501	42.31	0.62	82.74	7.63	47.215
01M0170N	2.0w	0	0.00543	0.01070	0.94463	7.04028	41.94	0.68	81.43	4.42	37.950
01M0170P	fusion	0	0.00419	0.00000	0.41268	3.33042	45.37	1.07	72.90	1.93	0.000
01M0173B	0.45w	1	0.18108	0.80602	0.48976	5.22958	56.04	22.42	8.90	1.04	0.261
01M0173C	0.55w	1	0.13809	1.01435	0.48714	5.02948	54.22	17.22	10.97	1.03	0.207
01M0173D	0.65w	1	0.12113	1.20274	0.52452	5.49374	54.99	14.12	13.31	1.11	0.188
01M0173E	0.75w	1	0.17847	1.88861	1.02329	10.80756	55.44	10.59	17.01	2.17	0.233
01M0173G	0.85w	1	0.20880	2.21728	1.53369	15.83067	54.20	8.33	20.42	3.26	0.297
01M0173H	1.0w	1	0.19655	3.61311	2.29773	23.32669	53.33	5.31	28.65	4.88	0.273
01M0173I	1.2w	1	0.18616	7.65674	4.51163	45.33569	52.79	2.61	45.18	9.58	0.253
01M0173J	1.4w	1	0.08759	7.00722	3.86646	38.50724	52.33	1.58	59.80	8.21	0.237
01M0173K	1.6w	1	0.10218	16.40122	7.71207	76.78536	52.31	1.05	71.78	16.38	0.202
01M0173M	1.8w	0	0.03917	16.02226	5.75490	52.83859	48.29	0.69	82.03	12.22	0.154
01M0173N	fusion	0	0.15761	137.01487	18.87896	176.87422	49.27	0.89	79.16	40.10	0.059

Table 2.2: 40Ar/39Ar Data, SO 141 and SO 142 Cruises, Continued

01M0174A	0.40 W	1	0.29198	2.06061	2.51597	24.14823	50.74	7.09	21.87	5.68	0.525
01M0174B	0.5w	1	0.23625	5.38601	5.48363	53.42213	51.49	2.69	43.35	12.38	0.438
01M0174C	0.55w	1	0.05265	2.58941	2.19013	21.64033	52.22	1.63	58.18	4.95	0.364
01M0174E	0.6w	1	0.07123	6.86503	5.34422	54.24392	53.62	1.08	72.04	12.07	0.335
01M0174F	0.65w	1	0.03698	7.04590	4.73357	48.09597	53.67	0.86	81.49	10.69	0.289
01M0174G	0.7w	1	0.01618	5.44071	3.23718	32.39201	52.87	0.87	87.14	7.31	0.256
01M0174H	0.8w	1	0.01905	7.88230	4.61784	46.25053	52.92	0.74	89.15	10.43	0.252
01M0174I	0.95w	0	0.01616	11.45287	5.27011	49.19165	49.37	0.56	91.15	11.90	0.198
01M0174K	1.10 W	0	0.01276	13.41021	4.00954	34.65003	45.75	0.58	90.18	9.05	0.129
01M0174L	1.25 W	0	0.01852	24.22538	4.68145	38.05762	43.07	0.61	87.42	10.57	0.083
01M0174M	1.40 W	0	0.00621	10.26831	1.17746	8.98381	40.45	0.82	83.03	2.66	0.049
01M0174N	1.60 W	0	0.00394	9.37072	0.68842	5.32822	41.03	1.11	82.07	1.55	0.032
01M0174O	2.00 W	0	0.00272	6.94041	0.33525	2.43933	38.60	1.75	75.21	0.76	0.021
01M0174Q	fsn	0	0.04204	77.13850	2.58530	18.29044	37.54	2.25	59.55	5.52	0.014
01M0175A	0.45w	1	0.07066	0.87349	0.08782	1.41849	83.01	50.33	6.36	1.40	0.043
01M0175B	0.65w	1	0.08598	1.36209	0.16939	2.32676	70.83	31.4	8.39	2.70	0.053
01M0175C	0.75w	1	0.08987	2.31713	0.25697	2.92295	58.85	21.71	9.91	4.10	0.048
01M0175D	0.85w	1	0.05426	2.09703	0.20230	2.23115	57.09	18.03	12.21	3.23	0.041
01M0175F	1.0w	1	0.03260	2.23052	0.15396	1.72837	58.09	13.54	15.21	2.46	0.030
01M0175G	1.2w	1	0.08940	5.35853	0.54961	6.05445	57.02	9.87	18.65	8.77	0.044
01M0175H	1.4w	1	0.06306	6.76166	0.53620	5.73892	55.43	7.32	23.55	8.55	0.034
01M0175I	1.5w	1	0.03999	7.05754	0.50445	5.25573	53.98	5.56	30.78	8.05	0.031
01M0175J	1.6w	1	0.01999	6.92614	0.38151	4.04711	54.94	3.9	40.66	6.09	0.024
01M0175L	2.0w	1	0.01848	11.12523	0.45530	4.49805	51.22	4.1	45.17	7.26	0.018
01M0175M	2.0w	1	0.01807	12.42232	0.43506	4.32992	51.59	4.39	44.77	6.94	0.015
01M0175N	2.2w	1	0.01253	8.95535	0.27744	2.67532	50.01	5.64	41.94	4.43	0.013
01M0175O	4.5W	1	0.03563	25.08332	0.64420	6.57573	52.90	4.85	38.44	10.28	0.011
01M0175P	fusion	1	0.05279	115.69819	1.61407	14.67436	47.19	4.96	48.47	25.75	0.006
01M0186B	0.45w	0	0.81620	1.04868	1.49233	63.67123	187.01	26.53	20.89	1.55	0.612
01M0186C	0.55w	0	0.21698	0.97497	0.57182	16.97213	132.12	19.19	20.93	0.59	0.252
01M0186D	0.65w	0	0.30846	1.94777	1.38956	30.33886	98.12	11.39	24.97	1.45	0.307
01M0186E	0.75w	0	0.27097	1.97927	1.27034	27.61881	97.72	11.01	25.65	1.32	0.276
01M0186G	0.85w	0	0.14893	1.47326	1.26024	19.74850	70.96	6.31	30.97	1.31	0.368
01M0186H	1.0w	0	0.06449	1.42237	0.79679	11.50023	65.46	4.8	37.64	0.83	0.241
01M0186I	1.2w	0	0.22357	4.34340	3.04198	41.82691	62.41	3.92	38.77	3.16	0.301
01M0186J	1.4w	0	0.31545	12.79961	7.65502	96.72389	57.43	2.25	50.92	7.96	0.257
01M0186K	1.5w	0	0.09755	8.95306	4.77495	54.55615	52.01	1.28	65.43	4.97	0.229
01M0186M	1.7w	1	0.04274	11.29913	6.29081	68.79768	49.81	0.74	84.49	6.54	0.239

Table 2.2: 40Ar/39Ar Data, SO 141 and SO 142 Cruises, Continued

01M0186N	1.9w	1	0.03723	11.95699	8.07708	88.01082	49.64	0.64	88.89	8.40	0.290
01M0186O	2.1w	1	0.03189	14.14000	10.09690	109.85485	49.56	0.58	92.10	10.50	0.307
01M0186P	2.3w	1	0.02134	8.16780	6.89169	75.00400	49.58	0.63	92.24	7.17	0.363
01M0186Q	3.0w	1	0.01048	6.95428	5.44797	59.38552	49.65	0.68	95.04	5.67	0.337
01M0186S	3.5w	1	0.01316	7.92233	7.85750	85.20843	49.40	0.59	95.63	8.17	0.426
01M0186T	fusion	0	0.19088	22.11463	29.20658	328.54735	51.22	0.65	85.35	30.39	0.568
01M0194B	0.45w	1	0.00636	0.00000	0.13766	1.16273	44.15	3.38	38.24	0.84	0.000
01M0194C	0.55w	1	0.00452	0.00000	0.11790	1.01826	45.13	4	43.25	0.72	0.000
01M0194D	0.65w	1	0.00582	0.46069	0.16218	1.37319	44.25	2.17	44.38	0.98	0.151
01M0194E	0.75w	1	0.00784	1.14785	0.35673	3.08135	45.14	1.19	57.08	2.17	0.134
01M0194G	0.85w	1	0.01489	1.57269	0.67317	5.80759	45.08	1.16	56.90	4.09	0.184
01M0194H	1.0w	1	0.01685	3.04989	1.01489	8.68048	44.70	0.85	63.55	6.16	0.143
01M0194I	1.2w	1	0.02595	6.13919	1.86011	15.88135	44.62	0.62	67.44	11.29	0.130
01M0194J	1.4w	1	0.02037	10.18568	1.89749	16.15237	44.49	0.58	72.85	11.52	0.080
01M0194K	1.8w	1	0.02465	31.97099	2.53936	21.45940	44.17	0.85	74.66	15.42	0.034
01M0194L	2.6w	1	0.01441	18.23515	1.58133	13.32249	44.04	0.82	75.77	9.60	0.037
01M0194N	3.5w	1	0.01193	24.80472	1.38523	11.56655	43.65	1.12	76.64	8.41	0.024
01M0194O	fusion	1	0.03853	149.61045	4.74594	40.47192	44.57	1.74	78.04	28.81	0.014
01M0196B	0.45w	1	0.00627	0.33005	0.04808	0.41177	47.40	22.36	18.19	0.52	0.063
01M0196C	0.55w	1	0.01428	0.35620	0.14497	1.01508	38.84	9.57	19.39	1.57	0.175
01M0196D	0.65w	1	0.00827	0.10054	0.20438	1.51521	41.10	5.83	38.27	2.22	0.874
01M0196E	0.75w	1	0.00730	0.10694	0.15094	1.14279	41.96	7.63	34.62	1.64	0.607
01M0196G	0.85w	1	0.01172	1.20178	0.34440	2.39956	38.65	2.81	40.94	3.73	0.123
01M0196H	1.0w	1	0.00629	0.72750	0.31071	2.13319	38.09	2.07	53.44	3.37	0.184
01M0196I	1.2w	1	0.01640	4.57144	1.22083	8.36907	38.03	1.14	63.32	13.23	0.115
01M0196J	1.4w	1	0.00564	6.69657	1.00458	6.87508	37.97	0.88	80.48	10.89	0.065
01M0196L	1.8w	1	0.00546	9.68115	1.01968	6.80799	37.05	1.05	80.85	11.05	0.045
01M0196M	2.6w	1	0.00401	11.19174	0.85120	5.64792	36.83	1.09	82.65	9.23	0.033
01M0196N	3.5w	1	0.00313	15.35085	0.67359	4.59117	37.82	1.63	83.21	7.30	0.019
01M0196O	fusion	1	0.01280	128.63523	3.25126	24.16261	41.20	2.51	86.47	35.25	0.011

Table 2.2: 40Ar/39Ar Data, SO 141 and SO 142 Cruises, Continued

3 Geochemistry of the Hawaiian Chain

Tim Worthington and Peter Stoffers

The Hawaiian–Emperor Seamounts form a chain that consists of more than 107 volcanoes, stretches more than 5800 km from Meiji (near the Aleutian Trench) to Loihi (SE of Hawaii), and represents a total volume of erupted magma in excess of 10^6 km^3 (Clague and Dalrymple, 1989). Seamounts along the chain show a progressive SE-younging from Meiji (~90 Ma) to Loihi (active), and this is consistent with NW movement of the Pacific Plate over a stationary mantle plume (Figs 1.1, 1.2). However, a major change in Pacific Plate motion is required at ~43 Ma (at Yuryaku–Daikakuji Seamounts) together with a few smaller changes (e.g., ~25 Ma near Smt 72). Both volcano spacing and volume vary irregularly along the chain from near continuous large volume volcanic ridges (southern Emperors and the Hawaiian Islands) to widely separated small discrete seamounts (e.g., Abbott to Halsley). For much of its length the Hawaiian–Emperor Chain is essentially linear, but some sections appear to consist of two or more sub-parallel chains (e.g., between Smt 63 and Smt 72, and the Kea and Loa trends on Hawaii).

Most studied Hawaiian volcanoes evolve with time through an initial akalic phase (small volume), a dominant tholeiitic phase that represents the passage of the volcano over the centre of the plume (>95% of the lavas), a late-stage alkalic phase which caps the volcano, and a rejuvenated (post-erosional) alkalic phase that may persist for as long as 6 m.y. after the tholeiitic phase has ceased (Clague and Dalrymple, 1989). These observations are biased towards the well-exposed and well-studied youngest volcanoes of the Hawaiian Chain (Kauai–Loihi). In particularly, it is not known whether the small discrete seamounts found on some sections of the Hawaiian–Emperor Chain follow the same evolutionary path.

Furthermore, there are distinct geochemical differences (major and trace elements, and Sr-Nd-Pb isotopes) between the tholeiites of adjacent young Hawaiian volcanoes (e.g., Mauna Kea and Mauna Loa). These have been attributed by different workers to differences in volcano–plume geometry (e.g., Lassiter et al., 1996), plume composition (e.g., Frey et al., 1994), or melt generation processes (e.g., different lithospheric thickness). Similarly, although some studies have shown that the Sr isotopic

composition of the Hawaiian Chain is broadly constant, values of $^{87}Sr/^{86}Sr$ progressively decrease from the Hawaiian–Emperor bend northwards along the Emperor Chain towards Meiji (Lanphere et al., 1980). This variation, and concomitant changes in Nd-Pb isotopes and trace element abundances, may reflect either proximity of the northern Emperors to a now subducted paleo-spreading centre (Keller et al., 2000), or changes in melting due to variations in lithospheric thickness (Regelous et al., 2001).

The ~43 Ma age of the Hawaiian–Emperor bend was determined from an age date on an alkalic Yuryaku lava that may be from the late-stage or rejuvenated stage of activity at this seamount. Therefore, the prime aim of the geochemistry program was to identify tholeiitic lavas from Yuryaku and Daikakuji in order to obtain the true age of the Hawaiian–Emperor bend. Secondary aims included identifying tholeiitic lavas from other Hawaiian Chain seamounts for age dating, establishing whether both large and small seamounts evolve through the 4 volcanic phases, determining whether there geochemical changes along the Hawaiian Chain, and resolving whether or not the progressive change in isotopic and trace element composition of tholeiites along the Emperor Chain terminates at the ~43 Ma bend.

3.1 Samples and Processing

Cruise SO 141 of the FS *SONNE* visited 17 Hawaiian Seamounts between the ~43 Ma Hawaiian–Emperor bend near Yuryaku and the ~25 Ma bend near Smt 72 (Fig. 1.2). Dredging concentrated on steep collapse scarps of the mid–upper seamount flanks. It was hoped that this would bias sample collection in favour of recently exposed (and thus relatively fresh) tholeiitic lavas from the main shield-building phase, and avoid both the late-stage alkalic and rejuvenated stage alkalic lavas that are concentrated near the summits of the recently extinct Hawaiian volcanoes.

A total of 350 samples were recovered by the dredging program, with better sample recovery at the older seamounts near the Hawaiian–Emperor bend. Recovered material ranged from aphyric to olivine-rich (15% phenocrysts) basalts, rare trachytic lavas, and numerous breccias and deeply weathered hyaloclastite. Crusts of Fe-Mn oxides were more common on the younger seamounts at the eastern end of the study area, and rarely found on the older seamounts. This surprising result might reflect; (1) stripping and

non-recovery of thicker Fe-MnOx crusts from the western lavas during dredging (whereas thinner crusts were recovered still attached to the lavas), (2) recent collapses or slumping preferentially occurring at the older western seamounts, or (3) greater hydrothermal activity on the generally larger seamounts at the eastern end of the study area.

All recovered lavas have undergone significant but variable degrees of marine weathering. Olivine phenocrysts were completely pseudomorphed by iddingsite, with only rare relic cores occasionally found in a few lavas from the younger eastern volcanoes. In contrast, plagioclase and pyroxene were generally unaltered. The groundmass was pervasively altered with the development of chlorite and other fine grained clay minerals. A few lavas had very thin crusts of partly palagonised glass, but it proved impossible to separate any relic fresh glass from secondary carbonates and associated Fe-Mn oxides. Vesicular lavas were characterised by partial to complete infilling of vesicles by zeolite minerals, sometimes in association with carbonates.

The freshest 76 lavas were selected for geochemical analyses. Blocks of the freshest available material were cut from these lavas, cleaned, and coarse crushed. Attempts were made to minimise zeolite contamination by hand-picking the coarse-crushed chips, but this usually proved futile on account of the zeolite abundance and thin in-grown rims on many vesicles. No attempt was made to remove iddingsite. The coarse chips were then boiled in deionised water in an ultrasound bath for 1 hour (or longer where necessary), dried, and fine crushed in an agate mortar. Loss on ignitions were determined by roasting 4 g of sample powder in a furnace at 1000°C for 6 hours. Standard fused glass disks (lithium metaborate flux) were prepared for major element analysis using the Philips PW 1400 XRF spectrometer at the University of Kiel. Trace elements were determined by dissolving 250 mg of powder with HF and HNO_3 acids, drying, re-dissolving the precipitate in 2N HNO_3, and analysed using the VG PlasmaQuad ICP-MS at the University of Kiel.

3.2 Major and Trace Element Analyses

Major and trace element analyses of the 76 selected lavas are provided in Table 3.1. Although loss on ignition values are reasonable (0.7 to >5 wt.%, average 2.7 wt.%), the more mobile elements have clearly been affected by the pervasive marine weathering

and possibly sub-aerial weathering prior to submergence of the volcano. For example, K_2O/P_2O_5 ranges from less than 0.5 to greater than 3 for our lavas, whereas fresh basalts from Mauna Loa consistently have K_2O/P_2O_5 ~1.6 (Yang et al., 1996). Low values of K_2O/P_2O_5 may reveal leaching of K_2O or scavenging of P_2O_5 during growth of zeolites (± carbonates ± phosphates). Nevertheless, major element discrimination diagrams clearly show some lavas from Yuryaku, Daikakuji, Halsley and Midway are tholeiitic (Figs 3.1, 3.2).

Not all elements are mobile during weathering. Some pairs of geochemically similar elements are tightly constrained to near primordial ratios in nearly all of our recovered lavas (e.g., Zr/Hf = 36.7 ± 1.9, Nb/Ta = 15.4 ± 0.9; Fig. 3.3). Elements such as these, which are immobile during weathering, provide an alternative method for classifying deeply weathered lavas as either tholeiitic or alkalic. The classification relies on the principle that tholeiites are generated by higher degrees of partial melting of the source than alkalic lavas, and therefore the more incompatible element of any element pair is less enriched in the tholeiites (effectively it is "diluted"). Several studies of young lavas from Mauna Loa and Mauna Kea confirm the general applicability of the principle (e.g., Rhodes, 1996). Nevertheless, it is necessary to assume that there are no major changes in the source composition for the chosen elements. We have used this technique to verify the classification of our lavas, are able to confirm that some lavas from Yuryaku, Daikakuji and Midway are tholeiitic, and further suggest that some others (in particular from Abbott) are probably deeply weathered tholeiites (Figs 3.4, 3.5).

Other elements that are immobile during marine weathering can be used to investigate the source composition of the Hawaiian plume. Values of $(Nb/Th)_{Prim}$ are remarkably constant at 2.3 ± 0.4 in all dredged lavas, whether tholeiitic or alkalic (Fig. 3.6). The non-primitive value of $(Nb/Th)_{Prim}$ ~2 (cf. primitive mantle = 7.6) is a characteristic of most young Hawaiian lavas and has been used to argue for recycling of old oceanic crust through subduction followed by upwelling in the Hawaiian plume (Hofmann, 1986). Clearly, this is also a feature that has characterised the Hawaiian plume since ~43 Ma. Likewise, the majority of our samples have low values of $(Th/La)_{Prim}$ and $(Th/Ba)_{Prim}$ that overlap with the young Hawaii field of Hofmann and Jochum (1996) and are distinct from most other mantle plumes excepting Iceland. However, anomalously high $(Th/Ba)_{Prim}$ values in several of our samples probably

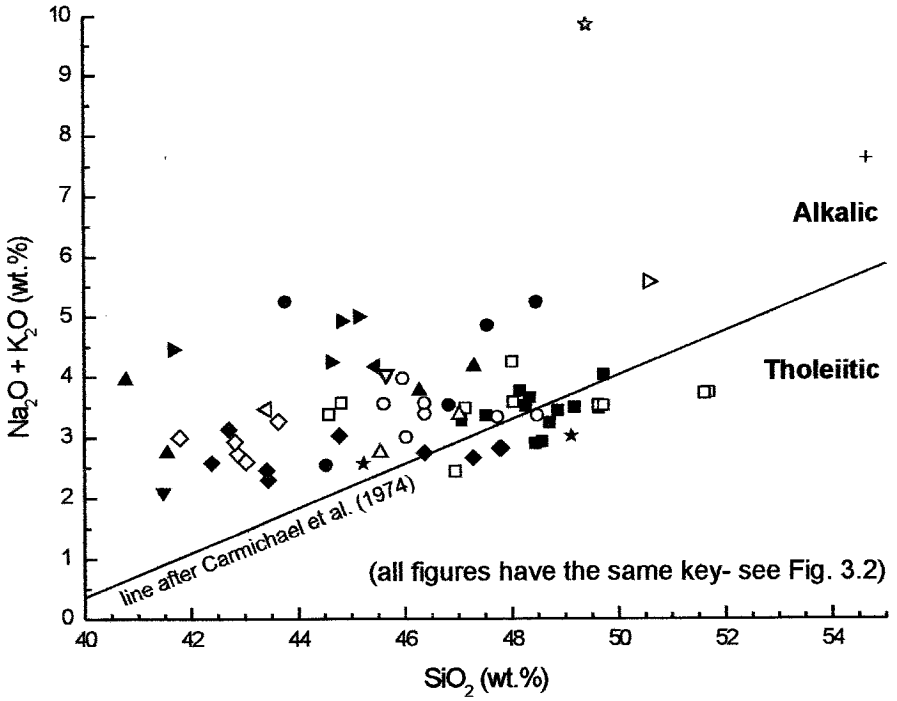

Fig. 3.1: Total Alkalis vs. Silica for Western Hawaiian Ridge lavas

All analyses normalised to 100 wt.% anhydrous

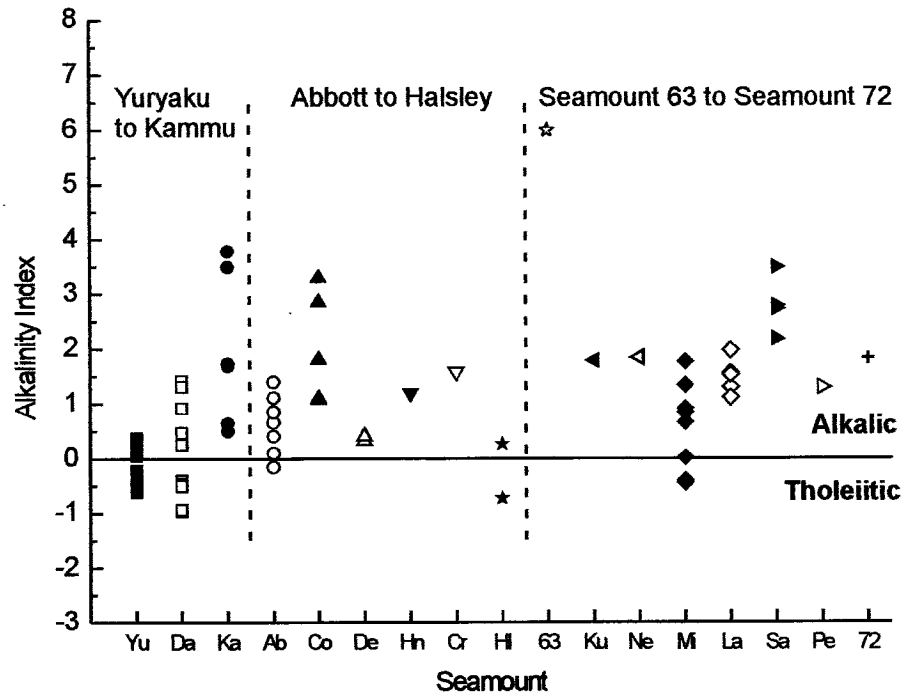

Fig. 3.2: Alkalinity Index for Western Hawaiian Ridge lavas

Alkalinity index = total alkalis - ((silica*0.37)-14.43)
Some lavas from Yuryaku, Daikakuji, Abbott, Halsley and Midway are tholeiites

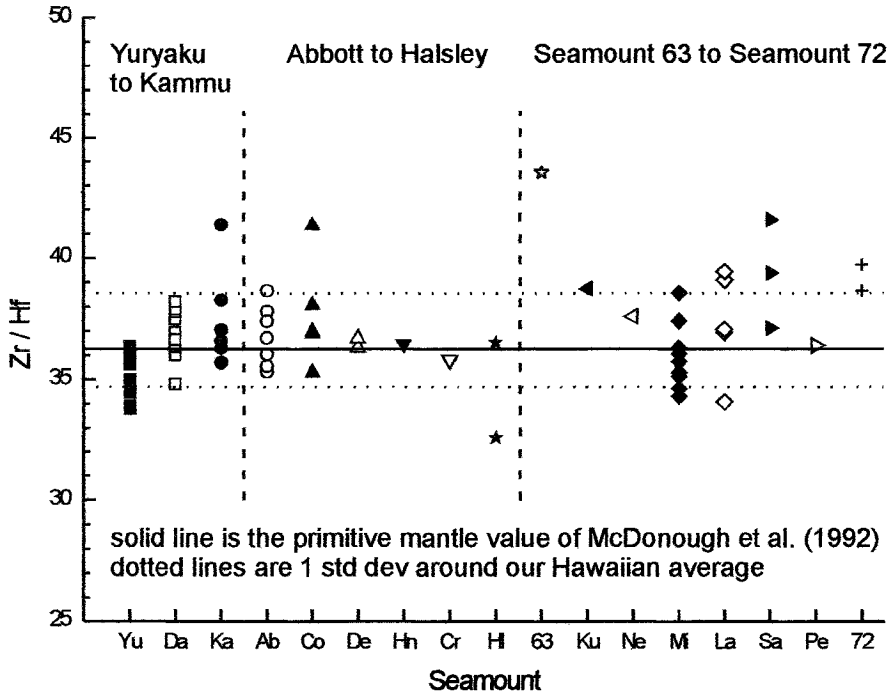

Fig. 3.3: Zr/Hf for Western Hawaiian Ridge lavas

Most lavas are confined within the band, indicating that the Zr and Hf (and other high-field strength elements) were immobile in most lavas during marine weathering

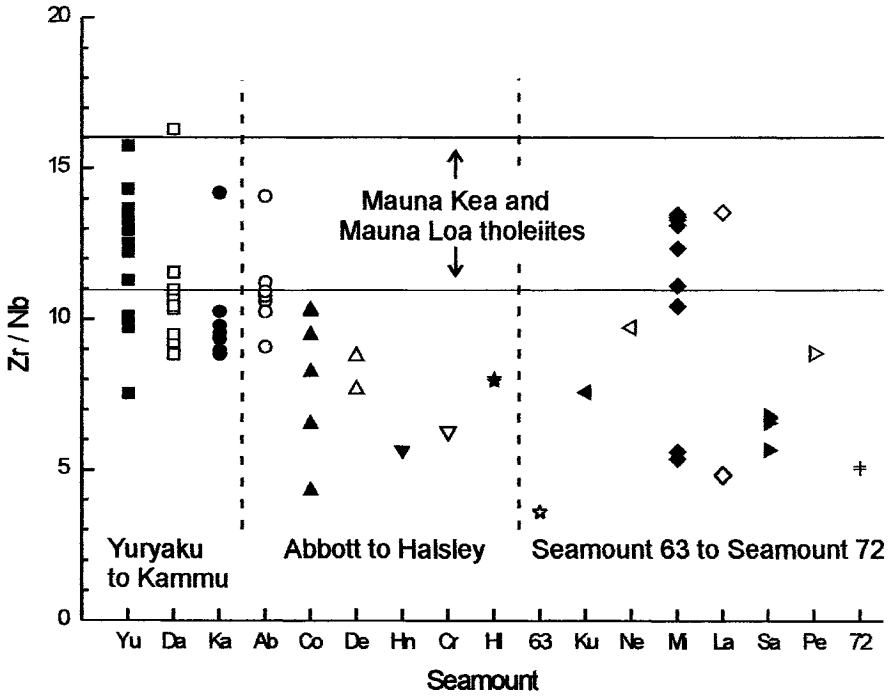

Fig. 3.4: Zr/Nb for Western Hawaiian Ridge lavas

Some additional lavas from Yuryaku, Daikakuji, Kammu, Abbott, Midway and Ladd are revealed as deeply weathered tholeiites when immobile elements are compared to present day tholeiites from Mauna Kea and Mauna Loa

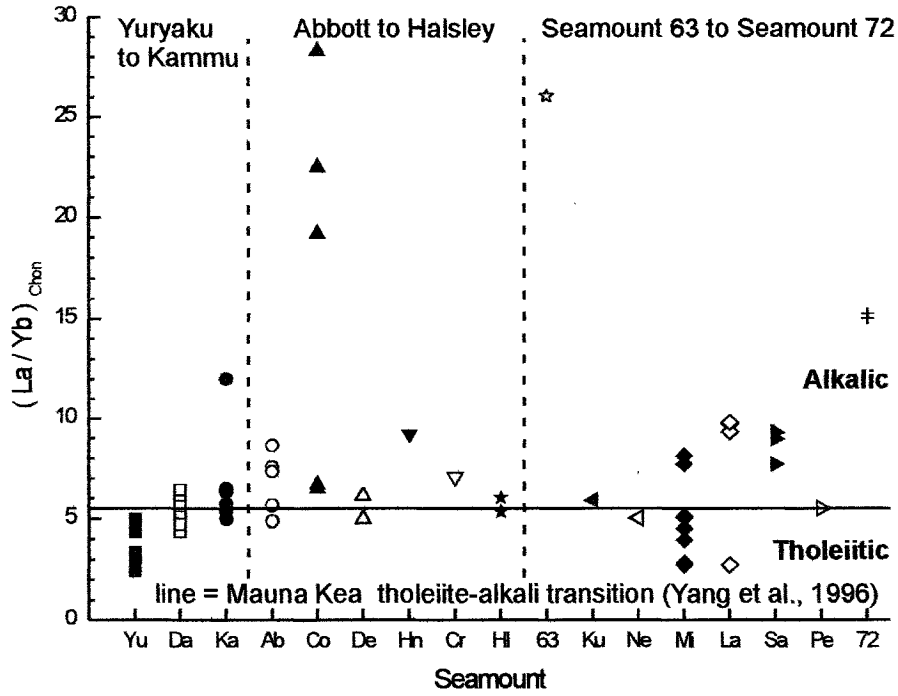

Fig. 3.5: $(La/Yb)_{chon}$ for Western Hawaiian Ridge lavas

Further confirmation from immobile elements that some Yuryaku, Daikakuji, Kammu, Abbott, Halsley, Midway and Ladd lavas are tholeiitic, and that others may be transitional in character

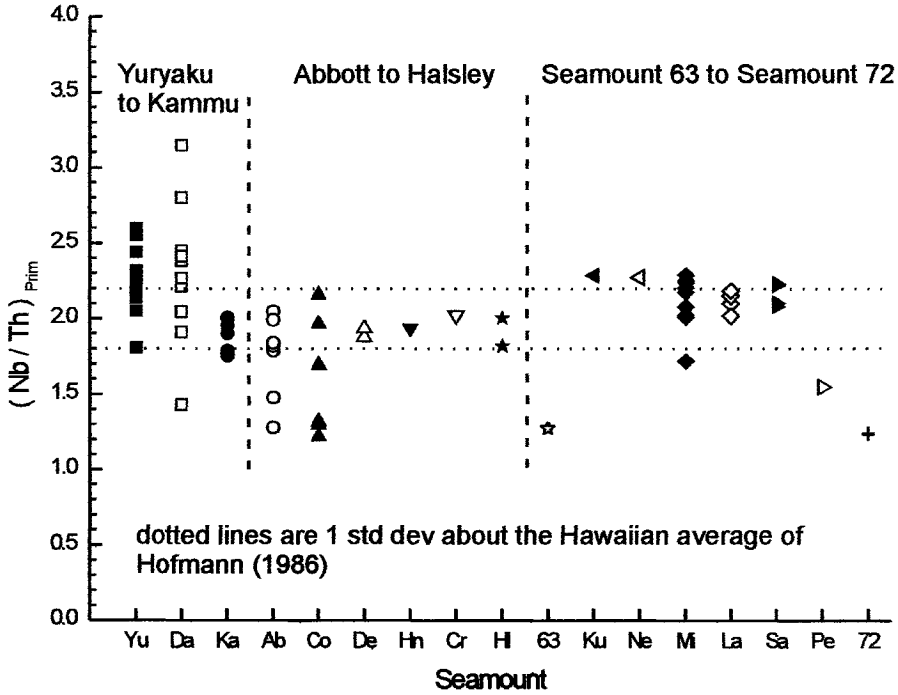

Fig. 3.6: $(Nb/Th)_{prim}$ for Western Hawaiian Ridge lavas

These highly incompatible elements are tightly constrained in most lavas, indicating that they have not been significantly affected by marine weathering. They further reveal that the characteristic non-primitive nature of some highly incompatible element ratios in Hawaiian lavas has persisted back to the Hawaiian-Emperor bend

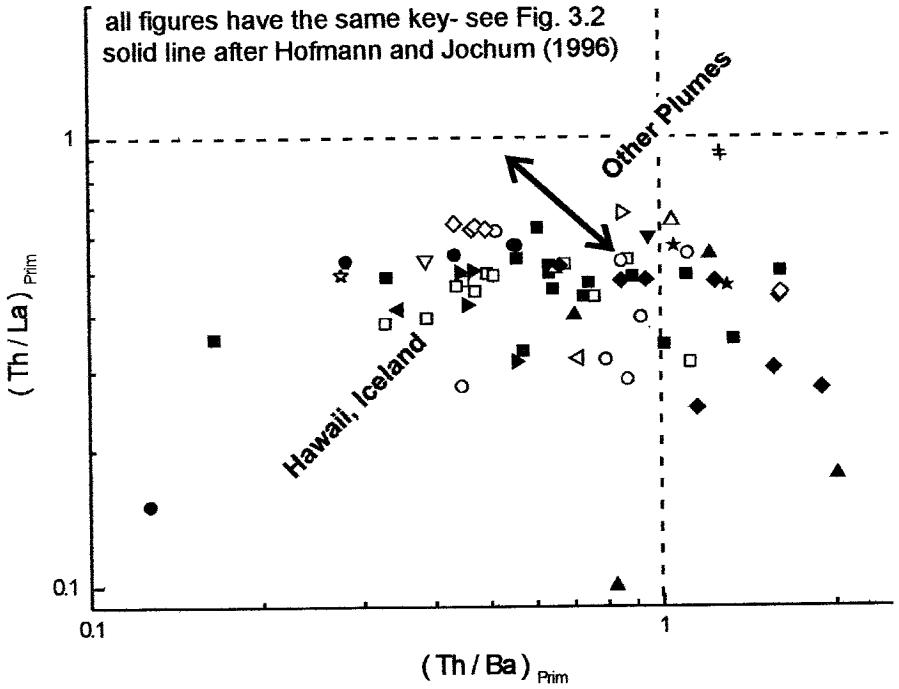

Fig. 3.7: $(Th/La)_{prim}$ vs $(Th/Ba)_{prim}$ for Western Hawaiian Ridge lavas

Hawaii and Iceland are unique among mantle plumes in plotting to the left side of the dividing line on this diagram (arrowed line). Samples plotting to high values of $(Th/Ba)_{prim}$ have probably been affected by Ba mobility during marine weathering

reflect the high mobility of Ba during marine weathering and low temperature hydrothermal alteration processes (Fig. 3.7).

3.3 Sr, Nd and Pb Isotope Analyses

Isotopic analyses of 10 lavas for Sr, Nd, and Pb were completed. Approximately 250 mg of powder was leached in ultrapure 6N HCl at 120°C for 1 hour, followed by dissolution in HF. Standard ion exchange techniques were used to produce Sr and Nd concentrates (modified after White and Patchett, 1984), and Pb concentrates (modified after Manhes et al., 1978; we used 1N HBr for washing and 6N HCl for elution). The concentrates were analysed using the Finnigan MAT 262 mass spectrometer at GEOMAR (Kiel). Both Sr and Pb were analysed in static mode on single Re filaments, whereas Nd was analysed in dynamic mode on a Re filament with a second Re

ionisation filament. Applied mass fractionation corrections for Sr and Nd were $^{86}Sr/^{88}Sr$ = 0.1194 and $^{146}Nd/^{144}Nd$ = 0.7219. For Pb, the analyses were fractionation-corrected using repeated measurements of NBS 981 normalised to its accepted values (Todt et al., 1996). The relative precision of the NBS 981 runs was <1 ‰ (2N), and Pb blanks were negligible (<50 pg). The isotopic determinations are reported in Table 3.2.

The samples selected for isotopic analysis were the freshest and most tholeiitic/least alkalic lavas from Yuryaku, Daikakuji, Abbott, Halsley, Midway and Ladd. Two samples were analysed for Yuryaku, Daikakuji, Abbott and Midway, and in each case these represent different lithologies. Both $^{87}Sr/^{86}Sr$ and $^{143}Nd/^{144}Nd$ show the expected close inverse relationship, and it is apparent that each seamount has a distinct value (where two samples were analysed from the same seamount). Conversely, ratios within the Pb isotope system show considerable scatter, probably reflecting ingrowth of ^{206}Pb and ^{207}Pb resulting from addition of U during the early stages of marine weathering. The results presented here will be age corrected using the confirmed results from the $^{40}Ar/^{39}Ar$ dating program. In addition, ingrowth in the Pb isotope system will be modelled using these age dates and ICP-MS analyses.

3.4 Provisional Results

Tholeiitic lavas interpreted to represent the main shield building phase of volcanism have been identified in our samples from Yuryaku, Daikakuji, Abbott, Halsley and Midway. Age dating of these tholeiites should provide the time at which the volcano overlay the Hawaiian plume, and thus has the potential to reveal the time at which the motion of the Pacific Plate changed. Ratios of incompatible elements that are immobile during marine weathering support our identification of the weathered tholeiites. It is clear that tholeiitic lavas have been erupted from both the larger seamounts and the smaller more widely spaced seamounts. Other incompatible element ratios indicate that the recycled oceanic crustal component in the Hawaiian plume was present in all sampled Hawaiian Seamounts.

Radiogenic isotope analyses of the freshest samples are within the range of published Hawaiian–Emperor values, but the Pb-isotope results reveal significant ingrowth due to U-addition during marine weathering. A full assessment of the isotope

results awaits the availability of confirmed age dates for both age corrections and Pb ingrowth modelling.

A rigorous analysis of geochemical changes along the studied section of the Hawaiian–Emperor Chain is in progress, combining variations in those elements immobile during marine weathering with the isotope determinations.

Table 3.1: Whole Rock Major (XRF) and Trace Element (ICP-MS) Analyses, Hawaiian Ridge: Yuryaku to Salmon

Seamount	Yuryaku	Yuryaku	Yuryaku	Yuryaku	Yuryaku	Yuryaku	Yuryaku	Yuryaku	Yuryaku	Yuryaku	Yuryaku	Yuryaku	Yuryaku	Yuryaku	Yuryaku	Daikakuji	Daikakuji	Daikakuji	Daikakuji	Daikakuji	Daikakuji	Daikakuji
Sample	5/1	5/3	5/4	5/5	5/9	5/10	5/11	5/15	5/17	5/19	5/20	5/22	5/24	5/26	5/28	6/3	6/4	6/5	6/6	6/7	6/8	6/10
SiO_2	48.75	44.77	46.41	45.65	47.10	46.47	47.90	46.16	45.47	46.82	46.90	47.45	47.05	47.07	45.55	46.84	50.00	46.62	47.32	48 63	46 35	44.53
TiO_2	3.07	3.08	3.24	2.93	3.03	2.77	2.90	3 13	2.79	2.69	3.13	2.86	3.27	2 88	2.94	3.49	3.11	3.67	2.73	2.83	2.78	2.47
Al_2O_3	14.55	14.47	15.50	14.80	14.68	15.42	14.41	15.07	13.58	13.18	12.82	13.37	13.30	15.83	14.86	14.18	14.06	13.12	12.91	13 07	11.53	9.86
Fe_2O_3	11.24	11.99	12.08	12.71	12.12	11.02	12.69	13.47	12.57	12.31	12.26	11.14	11.61	11.83	13.04	12.35	10.46	12.87	11.67	11 23	11 77	13.79
MnO	0.15	0.15	0.13	0.16	0.14	0.11	0.14	0 24	0.16	0.11	0.16	0.16	0.14	0.16	0.18	0.12	0.10	0.13	0.15	0 14	0.15	0.15
MgO	5.81	4.92	4.40	4.59	5.59	4.68	5.76	5.64	5.94	7.62	7.10	6.42	6.20	5 36	4.50	5.60	4.75	6.67	6.71	8.13	8.07	13.33
CaO	10.91	10.66	10.57	11.14	11.15	10.44	8.36	7.95	9.01	8.81	11.28	11.58	11.45	10 54	11.42	9.91	10.10	10.08	10.14	9.97	10.18	8.09
Na_2O	2.54	2.87	2.82	2.64	2.27	2.74	2.92	2.94	2.76	2.61	2.42	2.29	2.53	2.89	2.56	3.06	2.76	2.57	2 50	2 66	2 26	1.91
K_2O	0.88	0.63	0.81	0.59	0.58	0.92	0.96	0.56	1.03	0.72	0.39	1.05	0.60	0.54	0.62	1.07	0.86	0.91	0.87	0.78	0.57	0.40
P_2O_5	0.34	0.34	0.43	0.88	0.33	0.33	0.32	0.35	0.33	0.35	0.38	0.81	0.47	0 43	1.14	0.74	0.53	0.45	0.36	0.37	0 33	0.33
LOI	0.73	2.09	1.76	2.38	1.74	2.00	4.01	5.07	3.12	4.45	1.27	2.39	1.25	2 14	2.46	1.93	2.40	2.08	1.85	1.63	1.63	5.70
Total	98.97	95.97	98.15	98.47	98.73	96.90	100.37	100.58	96.76	99.67	98.11	99.52	97.87	99.67	99.27	99.09	99.13	99.17	97.21	99.44	95.62	100.56
Sc	42.2	42.6	38.5	37.7	36.5	41.8	38.9	34.5	41.6	44.1	34.4	38.4	38.6	37.0	42.1	35.4	34 9	34.1	37.2	31.7	35.1	27.5
Cr	111.4	150.5	146.5	202.0	162.0	326.4	216.6	161.8	220.9	633.9	585.4	336.9	555.1	237.2	190.9	95.7	252.1	413.4	326 4	350.7	593 7	828.9
Co	42.9	48.2	44.5	49.4	41.0	56.3	57.0	55.4	52.8	64.5	60.7	42.6	50.9	50.7	47.9	37.1	46 7	42.4	49.1	47.1	54.0	72.2
Ni	57.7	96.5	83.3	80.4	78.5	107.3	103.8	159.2	115.0	409.1	233.1	129.6	170.8	136.3	98.9	63.1	113 0	221.2	94.0	140.3	225.5	488.0
Cu	49.7	128.2	111.3	131.1	118.5	112.3	144.3	167.6	156.0	130.7	69.9	105.9	93.6	141.2	154.0	70.0	102.9	66.7	114 2	89.1	93.0	122.3
Zn	161.8	205.4	162.6	150.6	151.1	175.0	193.9	160.6	176.0	130.0	155.1	244.5	303.6	130.0	158.1	238.8	142.3	214.3	156 4	159.2	137 4	197.3
Ga	26.5	26.9	27.4	26.6	24.7	27.2	25.8	25.6	25.1	22.3	22.9	26.1	26.1	26.6	26.8	27.3	25 4	23.3	23.5	22.6	22 6	16 6
Rb	10.3	9.0	9.8	15.2	9.7	12.8	52.1	24.1	80.1	11.9	6.5	55.3	9.8	8.0	16.3	12.5	21 0	8.1	23 1	12.6	13 4	7.4
Sr	366.0	361.5	366.0	369.3	334.8	341.3	308.1	325.6	312.0	298.8	459.7	417.5	504.0	453.3	389.6	631.4	495.9	537.3	405.4	452.4	481 6	293.5
Y	35.5	34.2	37.5	40.9	30.2	31.4	27.4	31.4	31.8	32.5	26.9	49.8	31.0	27.3	42.2	34.2	24.9	30.1	25.0	25.4	24 7	21.3
Zr	173.4	170.9	177.1	160.2	151.3	153.1	156.4	160.1	155.9	131.4	151.2	167.8	181.4	150.1	163.4	217.6	149.3	171.6	136.0	178.2	176.7	146.5
Nb	13.1	12.7	13.6	11.7	11.2	10.7	12.5	13.1	12.5	8.3	15.5	14.9	18.0	19.9	12.4	24.6	14.1	18.5	14 7	16.7	17 1	15.4
Cs	0.10	0.24	0.16	0.56	0.30	0.32	4.53	2.74	7.38	0.84	0.36	4.94	0.40	0.26	0.59	0.28	1.37	0.12	1 58	0 34	0.35	0.58
Ba	87.0	61.8	81.6	40.4	44.0	73.8	97.2	36.4	165.9	31.3	83.6	141.1	107.3	156.4	334.1	241.7	132.3	174.8	132 5	138.7	134.6	98.4
La	11.22	11.37	13.60	15.39	9.93	9.15	10.23	11.81	11.32	9.24	13.30	24.46	15.25	15.28	15.71	23.04	12 61	15.18	13.20	13.98	14.07	12.96
Ce	27.25	24.74	27.89	25.56	22.96	22.55	24.50	26.08	24.96	18.07	30.96	32.66	34.22	33.56	25.89	46.73	29.70	30.61	30 30	33.19	33.95	29.45
Pr	4.09	4.08	4.57	4.37	3.70	3.54	3.76	4.03	3.85	3.19	4.66	5.71	5.13	4.67	4.37	6.52	4 28	4.76	4.49	4.83	4.86	4.25
Nd	20.39	20.54	22.55	21.74	18.39	18.03	18.51	19.67	18.88	16.62	22.43	26.79	24.58	21.38	21.52	29.82	20 58	23.06	21.47	22 84	22 87	19.82
Sm	6.43	6.38	6.84	6.55	5.84	5.80	5.63	5.87	5.73	5.51	6.24	7.14	6.87	5.84	6.43	7.63	5.79	6.49	6.05	6 27	6.15	5.32
Eu	2.21	2.20	2.34	2.20	2.06	2.03	1.96	1.99	1.95	1.90	2.07	2.30	2.26	1.95	2.18	2.49	1.98	2.16	1.99	2.06	2.02	1.73
Gd	7.49	7.54	7.97	7.71	6.87	6.80	6.40	6.69	6.56	6.46	6.62	8.13	7.28	6 30	7.65	7.78	6.22	6.77	6.32	6.45	6.32	5.48
Tb	1.22	1.22	1.28	1.25	1.10	1.11	1.01	1.08	1.06	1.04	1.02	1.26	1.11	0.99	1.23	1.17	0.95	1.04	0.96	0.98	0 95	0.83
Dy	7.30	7.27	7.64	7.59	6.59	6.69	5.97	6.51	6.34	6.29	5.81	7.66	6.45	5.82	7.48	6.88	5.42	5.97	5.43	5 58	5 44	4 76
Ho	1.40	1.38	1.44	1.47	1.25	1.27	1.11	1.24	1.20	1.21	1.07	1.54	1.19	1.09	1.47	1.24	1.00	1.11	0.99	1.02	1.00	0.87
Er	3.54	3.47	3.70	3.81	3.13	3.24	2.80	3.16	3.07	3.10	2.68	4.07	2.97	2.76	3.84	3.13	2.48	2.78	2.48	2.56	2.50	2 17
Tm	0.46	0.44	0.47	0.49	0.40	0.41	0.36	0.40	0.39	0.41	0.34	0.53	0.37	0.35	0.50	0.40	0.32	0.35	0.31	0.33	0.32	0.28
Yb	2.75	2.68	2.88	3.07	2.40	2.51	2.12	2.48	2.35	2.47	2.02	3.27	2.28	2.13	3 11	2.42	1.91	2.10	1.87	1.95	1.93	1.67
Lu	0.38	0.37	0.41	0.44	0.34	0 34	0.29	0.35	0.33	0.35	0.28	0.48	0.32	0.30	0.45	0.35	0.27	0.30	0.26	0 27	0.27	0.23
Hf	4.87	4.94	5.09	4.63	4.46	4.44	4.51	4 60	4.33	3.69	4.47	4.82	4.99	4.29	4.59	5.80	4 09	4.76	3.91	4 84	4.78	4.03
Ta	0.85	0.86	0.90	0.80	0.78	0.73	0.84	0.88	0.81	0.58	1.09	0.96	1.19	1.29	0.82	1.59	0.93	1.23	0.99	1.14	1.15	1.01
Tl	0.05	0.01	0.02	0.10	0.02	0.03	0.10	0.37	0.19	0.03	0.02	0.31	0.07	0 02	0.41	0.05	0.04	0.05	0.04	0.04	0.03	0.02
Pb	0.81	1.20	1.30	1.21	0.92	0.76	0.97	0.81	0.98	0.87	0.91	2.30	1.57	1.15	1.18	1.79	1.17	1.38	2.06	1.23	1.16	0.99
Th	0.66	0.66	0.71	0.65	0.58	0.56	0.65	0.70	0.66	0.38	0.75	0.97	0.83	1.14	0.66	1.31	0.70	0.69	0.62	0.82	0.82	0.80
U	3.12	1.39	1.69	1.52	1.79	2 58	0.63	0.57	0.84	0.80	0.38	1.08	1.13	0.62	1.65	0.83	0.71	0.59	0.48	0 47	0.34	0.33

Table 3.1: Whole Rock Major (XRF) and Trace Element (ICP-MS) Analyses, Hawaiian Ridge: Yuryaku to Salmon (continued)

Seamount	Daikakuji	Daikakuji	Daikakuji	Daikakuji	Kammu	Kammu	Kammu	Kammu	Kammu	Kammu	Kammu	Abbott	Abbott	Abbott	Abbott	Abbott	Abbott	Abbott	Colahan	Colahan	Colahan	Colahan
Sample	6/11	7/1	8/5	8/7	9/1	9/13	9/14	9/16	9/23	9/24	9/31	11/1	12/1	12/2	12/3	12/4	12/5	12/7	13/1	13/2	13/6	13/7
SiO_2	49 89	42.85	42.66	45.41	45.90	41.90	45.12	45.54	36.86	46.56	42.70	44 38	43 70	47.35	44.41	44.64	44 48	45.48	43.97	39.57	38.03	36 28
TiO_2	3.09	3.80	3.67	3.74	2.43	2.66	2.28	3.66	2.30	3.82	2.48	3 33	3.73	3 31	3.68	3.02	3.37	3.15	3.04	3.30	3.95	5 11
Al_2O_3	14.07	13.62	13.47	13.78	18.63	17.79	13.53	14.97	12.11	14.76	13.11	13 37	13.36	15 53	12 76	15.05	13.77	13.73	13.36	8.93	9 66	8 78
Fe_2O_3	10.48	14.96	13.74	14.18	8.65	10.40	12.70	12.99	9.51	14.25	12.61	12 72	13 14	11.78	14 51	12.14	12.16	13.85	12.00	13 60	13.56	14.51
MnO	0.10	0.15	0.16	0.17	0.11	0.25	0.18	0.15	0.23	0,20	0.13	0 18	0.16	0 13	0 16	0.18	0.22	0.17	0 13	0 16	0.16	0 15
MgO	4.84	4.39	4.52	5.20	1.94	0.82	6.69	3.28	3.11	3.19	5.27	4 70	5 08	4 27	6.83	4.62	4 49	5.36	5.01	9.73	6.96	9 81
CaO	10.06	10.59	11.80	9.80	10.31	12.76	12.16	8.99	18.50	9.57	14.48	12 09	11 42	11.08	9 53	12.65	12.05	10.40	12 05	15 99	13.89	14.75
Na_2O	2.73	2.60	2.43	2.52	3.99	3.90	2.77	3.74	2.78	3.47	1.96	2.87	2 67	2 70	2.47	2.43	2.79	2.36	2.57	1.61	1.81	1 54
K_2O	0.88	0.81	0.80	0.83	0.97	1.14	0.64	1.22	0.86	1.29	0.49	0 97	0.74	0 58	0 78	0.49	0.64	0.82	1 01	1.01	1.88	0 85
P_2O_5	0.54	1.85	2.44	0.72	1.81	4.16	0.34	0.67	7.72	0.83	2.68	1.95	1 84	0.95	0.64	1.79	1 98	0.46	1.89	1 34	3 38	3 50
LOI	2.15	4.39	3.95	3.69	2.62	2.95	3.57	1.39	6.51	1.44	3.06	3.01	3.80	2.54	4 26	3.00	2.92	3.33	2.85	4.73	7.26	4 49
Total	98.83	100.01	99.64	100.04	97.56	98.73	99.96	96.60	100.49	99.38	98.97	99 57	99 64	100 22	100 03	100.01	98 87	98.61	97 88	99 97	100.54	99 77
Sc	36.0	39.9	38.5	37.0	12.9	15.7	29.2	25.1	21.2	29.5	41.4	34.4	31.6	37 7	31 8	34.9	35.4	35.4	32.4	43.3	36.2	32.3
Cr	258.5	611.0	428 5	516.6	5.3	7.2	402.9	78.8	114.7	40.7	876.6	533.9	347.4	138.8	542.3	173.3	103.3	136.8	151.3	848.7	668.5	664.9
Co	48.6	51.1	44.7	52.4	33.8	65.4	57.0	40.8	46.5	56.1	43.3	69.7	53.0	31.1	71.4	39.4	48.3	47.4	34.6	81.5	72.9	69.7
Ni	119.3	128.1	93.1	150.5	27.6	107.0	178.6	65.9	60.0	61.9	131.5	132.0	100.9	37.5	190 1	69.4	85.9	56.8	85.5	345.7	183.1	329.8
Cu	112.1	121.6	87.0	64.5	40.3	164.1	87.3	58.8	77.2	66.4	175.1	63.9	103.0	50.7	114.8	82.0	107 7	44.4	72.1	103.9	99.5	65.4
Zn	147.3	264.0	214.5	199.4	157.6	154.3	142.5	186.1	138.5	179.8	196.9	185.6	201.5	172.4	254 4	167.0	169.3	147.2	161.0	191.6	191.4	164.2
Ga	26.5	26.5	24.8	26.2	27.6	30.6	21.2	28.8	26.8	29.5	24.2	26.5	27.3	28.6	27.4	28 3	31.8	24.3	23.8	19.5	19.3	19.2
Rb	22.6	12.3	13.6	11.7	37.9	26.0	16.5	23.9	11.1	23.3	10.9	10.4	13.2	8.8	13.3	7.1	8.5	17.2	15.7	25.5	34.2	13.6
Sr	513.7	683.6	674.2	603.5	819.2	1108.2	371.8	569.7	778.4	538.4	478.8	695.2	640.1	581.2	483 9	559.7	665.7	436.7	550.4	757.2	372.5	435.1
Y	26.6	69.0	41.8	32 9	32.2	69.1	22.3	35.0	377.8	35.8	75.0	29.9	52.4	39.5	33.8	71.2	79 3	49.1	37.1	51.6	228.8	92.9
Zr	155.4	283.4	258.7	260.4	204.1	226.1	129.4	261.0	136.2	242.8	149.9	228.9	261.1	248.8	269.1	191.3	243.5	201.9	213.3	241.7	237.9	293.7
Nb	14.9	25.8	15.9	22.5	21.3	23.1	14.4	29.4	13.3	25.9	10.6	21.6	23.2	23.1	26 2	13.6	26 7	18.5	22.5	56.1	36.4	35.6
Cs	1.44	0 37	0.58	0.40	3.31	1.52	1.26	0.82	0.25	0.34	0.46	0 31	0 67	0 13	0 54	0.25	0 31	0.50	0.37	0.53	0.62	0 19
Ba	128.0	118.6	143.2	123.7	424.1	4172.6	166.5	258.0	155.6	230.4	427.5	278.3	159.9	112.1	147.7	119.6	294 6	107.0	145.5	343.2	254.8	88.1
La	13.52	42.82	25.12	20.52	22.77	41.23	13.38	25.32	259.45	22.37	36.44	23 43	40.51	22 94	24 03	36.70	47.93	25.16	25.90	77.40	213.79	102 37
Ce	29.99	52.25	48.02	46.84	45.70	48.29	29.21	56.84	31.59	51.34	26.76	52.95	58.79	46 88	56 33	40.01	49 72	40.77	45.47	137.99	95.64	86 80
Pr	4.44	9.92	7.24	6.94	6.46	9.09	4.20	7.94	54.27	7.16	6.58	7 35	10 38	6.75	8 06	8.25	10 18	7.28	7.11	19 17	42.30	19.49
Nd	21.23	45.51	34.05	32.47	29.19	40.86	19.23	35.83	259.89	32.81	31.16	33 21	46 73	31 32	36 96	37 90	46.37	34.11	32.20	80.19	197.48	87 36
Sm	5.94	11.03	9.03	8.78	7.33	9.61	5.12	9.17	51.68	8.67	7.65	8 39	11.42	8.29	9.65	9.45	11.08	9.04	8.09	16.83	37.20	17.25
Eu	2.00	3.46	2.85	2.79	2.42	3.11	1.72	2.98	16.54	2.83	2.44	2.70	3 59	2.75	3.04	2.92	3.38	2.85	2.62	4.92	11 12	5.18
Gd	6.33	11.84	9.11	8.74	7.35	10.64	5.47	9.22	63.53	9.04	9.45	8 20	11 85	8.82	9 56	11.28	12.40	10.27	8.40	15.22	41.50	17 90
Tb	0.96	1.73	1.37	1.31	1.10	1.55	0.83	1.38	7.49	1 38	1.40	1 22	1 69	1 34	1 39	1.71	1.80	1.60	1.24	2.02	4.23	2 12
Dy	5.51	10.22	7.77	7.33	6.24	9.27	4.78	7.69	41.56	7.87	8.83	6 75	9.46	7.68	7 59	10.37	10.72	9.73	7.13	10.35	20.30	10.95
Ho	1.02	2.04	1.45	1.33	1.17	1.91	0.90	1.40	8.67	1.44	1.89	1 22	1 73	1 41	1 31	2.09	2 13	1.87	1.33	1 78	3.72	2.01
Er	2.53	5.47	3.68	3.27	2.99	5.19	2.28	3.44	21.78	3.58	5.21	2 94	4.27	3 53	3 11	5.50	5 64	4.70	3.37	4.12	8.54	4.73
Tm	0.32	0.71	0.46	0.41	0.39	0.70	0.30	0.44	2.53	0.46	0.68	0 36	0 53	0 45	0.36	0.71	0.71	0.58	0.44	0.47	0.92	0.54
Yb	1.91	4.44	2.86	2.43	2.34	4.35	1.79	2.63	14.44	2.77	4.24	2.13	3 13	2 71	2 12	4.32	4.36	3.43	2.65	2 70	5.05	3.04
Lu	0.27	0.67	0.41	0.34	0.34	0.68	0.25	0.36	2.33	0.38	0.66	0 29	0 45	0 38	0.28	0.63	0.65	0.46	0.38	0.36	0 84	0.47
Hf	4.11	7.48	6.77	7.10	5.33	5.46	3.56	7.05	3.81	6.63	4.20	6 35	7 39	6.58	7 19	5.21	6.30	5.68	5.60	5.84	6.44	7 96
Ta	0.95	1.75	1.08	1.57	1.39	1.41	0.94	1.90	0.97	1.65	0.72	1 43	1 54	1 42	1.67	0.86	1 64	1.23	1.43	3 18	2.63	2.42
Tl	0.05	0.30	0.16	0.06	0.08	0.46	0.02	0.07	0.06	0.24	0.04	1 50	0 81	0 03	1 17	0.08	0.48	0.31	0.11	0 47	0.17	0.06
Pb	1.76	2.28	1.60	1.47	1.92	9.00	0.97	1.83	1.31	1.62	2.47	1.71	2 09	1 63	1 67	2.75	3 74	2.58	2.61	4.83	1 79	1.90
Th	0.73	1.59	1.31	1.30	1.43	1.52	0.87	1.72	0.88	1.53	0.65	1 72	1 53	1.49	1.51	1.25	1.58	1.18	1.23	5.00	2.53	2 13
U	0.74	1.13	1.33	0.79	1.23	1.85	0.37	0.74	2.18	0.81	1.00	1 02	0 89	0 81	0.55	0.71	0.78	0.50	1 18	0 94	1.51	1.06

Table 3.1: Whole Rock Major (XRF) and Trace Element (ICP-MS) Analyses, Hawaiian Ridge: Yuryaku to Salmon (continued)

Seamount	Colahan	Colahan	De Veust	De Veust	Hancock	Cromwell	Halsley	Halsley	Smt 63	Kure	Nero	Midway	Midway	Midway	Midway	Midway	Midway	Midway	Midway	Midway	Ladd	Ladd
Sample	15/1	15/2	16/1	17/1	20/1	21/1	23/1	23/2	25/1	26/1	28/2	29/1	29/2	29/7	29/12	29/17	29/20	29/22	29/24	29/28	30/1	30/3
SiO_2	43.58	41.35	43.42	45.17	39.38	43.82	47.99	44.18	47 20	43 80	41.95	47 04	43.10	45.18	47 02	45.66	41.74	40.70	41.15	42 35	42.53	41 58
TiO_2	3.43	3.67	2.83	2.92	3.20	3.35	3.05	2.67	1.08	3 06	3.41	2.37	2.68	2 29	2.38	2.70	2.29	2.95	2.57	2 51	3.51	3 27
Al_2O_3	12.24	11.96	11.81	13.06	12.19	13.41	13.62	12.59	15 18	16 42	15.39	14.14	12.44	13.55	14.14	13.73	11.26	13.17	13.03	13.62	14.23	13 12
Fe_2O_3	14.05	15.22	13.35	12.27	13.37	13.51	12.64	15.07	13.53	13 66	14.42	12.43	13.47	12 33	11.99	12.46	14.12	11.91	11.95	12.89	13.20	14.03
MnO	0.20	0.25	0.17	0.16	0.18	0.14	0.16	0.19	0 31	0 24	0.13	0 15	0.17	0.15	0 15	0.15	0.17	0.14	0.15	0 15	0.16	0 16
MgO	6.91	6.43	11.03	5.25	7.85	4.48	6.23	6.48	2 36	2 86	3.08	6.47	8.40	6 20	6.50	6.12	12.53	4.57	5.26	5.45	7.22	9.48
CaO	7.72	9.06	9.80	12.25	14.93	11.77	10.66	12.80	4.54	11 21	12.87	12.26	12.60	12.27	12.54	13.39	11.28	15.20	16.56	15.25	12.79	11.98
Na_2O	2.03	1.14	1.89	2.68	1.29	2 81	2.35	2.09	5 71	3 11	2.86	2.32	1.87	2 01	2.31	2.30	1.42	2.48	2.13	2.04	2.35	1.90
K_2O	1.81	1.08	0.73	0.56	0.71	1.07	0.60	0.42	3 69	0.91	0.49	0.45	1.05	0 53	0.47	0.40	0.79	0.51	0.38	0 36	0.84	0.75
P_2O_5	0.19	0.31	0.32	1.74	1.87	1.60	0.42	1.21	1.93	1 09	2.04	0.77	0.50	1.07	0.95	1.58	0.50	3.68	3 92	2.94	0.64	0.71
LOI	8.25	11.80	3.88	2.71	5.56	2.48	1.29		3 51	2.03	2.91	1.68	3.65	1.93	1.63	1.50	4.03	2.70	2.46	2.26	2.58	2.56
Total	100.41	104.27	99.23	98.77	100.53	98.44	99.01	97.70	99 04	98 39	99.55	100.08	99.93	97.51	100.08	100 01	100 13	98.01	99.56	99.82	100.05	99.54
Sc	33.8	42.3	30.7	35.9	37.9	30.3	46.0	33.1	3.7	33.0	34.8	47.0	35.0	43.3	42.1	40.6	34 8	34 8	42.1	42.3	30.3	29.0
Cr	855.0	683.6	476.8	227.3	357.8	343.4	892.7	151.6	4.5	126.1	495.5	270.9	445.7	249.7	250.4	468.5	736.1	230.8	404.0	600.0	360.2	451.5
Co	79.0	89.3	67.2	47.5	56.5	46.7	96.2	45.1	14.7	48.9	32.5	46.5	58.4	43.0	44.4	42.2	79.0	38.1	43.9	46.3	58 1	65.6
Ni	190.4	288.0	375.4	82.2	102.5	63.9	305.1	106.2	16.8	98.5	53.3	74.7	172.1	66.3	84 3	91.2	451.2	63.9	78.1	100.9	142.2	245.9
Cu	101.6	155.5	102.0	101.6	99.0	60.6	87.0	121.0	24.2	137.5	126.8	121.2	143.4	115.1	120.4	102.4	148.5	76 0	87.2	111.1	77.0	79.1
Zn	221.7	261.9	158.8	151.7	145.1	168.1	201.6	126.5	255.2	203.5	202.7	155.8	141.8	145.1	148.4	148.0	160.4	160.9	152.0	162.5	139.7	142.2
Ga	17.9	22 1	20.5	25.7	19.3	25.4	24.2	23.9	24.1	27.5	25.7	25.3	21.4	22.7	23.1	22 6	19.5	22 8	22.6	22.1	23.9	20.8
Rb	24.2	17.1	10.8	10.1	9.9	15.2	8.5	10.1	108.4	13.5	6.6	10.4	13.0	12.7	10.6	7.2	10.3	8.6	7.7	6.3	12.8	12.4
Sr	112.9	132 3	272.7	559.6	243.3	721.1	469.6	418.6	3043.0	690.8	696.8	324.5	389.0	308.4	311.5	370.8	283.0	574.1	536.1	443.6	791.3	690.1
Y	26.7	40.5	28.0	34.8	28.3	39.2	35.1	27.2	54.8	45.9	66.3	34.0	28.3	31.6	30.4	49.9	28.2	33.7	59.7	51.2	25.9	25.0
Zr	278.8	314 1	174.2	166.9	187.4	176.4	139.6	170.9	341.3	203.8	238.5	152.4	152.3	139.0	142 6	168.2	134.8	199.7	151.7	143.7	184.2	166.0
Nb	27.0	30.6	22.7	19.0	33.1	28.1	17.4	21.5	94 6	26.8	24.5	11.3	28.3	10.4	10.6	13.6	24.1	15.2	14.5	12.9	38.3	34.2
Cs	0.25	0.31	0.18	0 53	0.18	0.41	0.33	0.29	1.44	0.27	0.24	0.41	0.24	0 48	0.40	0.28	0.19	0.26	0.30	0 23	0.27	0.29
Ba	75.6	65.0	113.7	147 8	176.8	351.7	72.1	100.3	2633.6	332.3	148.4	31.6	182.8	28.4	55.0	33.9	114.1	70.3	61.8	40 1	411.5	333.4
La	18.96	26.92	18.56	19.15	28 25	25.88	20.34	18.70	149.24	28.22	33.49	11.49	23.73	10 46	9.90	23.67	22.55	18.52	29.05	20.90	28.24	25.32
Ce	60.11	60.53	44.01	40.19	54.45	45.56	38.32	41.34	274.59	47.24	44.36	25.25	44.77	22 45	22.79	30.59	38 74	39 47	31 64	27.98	60.36	51.76
Pr	7.05	8.70	5.96	5.60	7.24	6 51	5.57	5.64	34.67	7.13	8.01	3.90	6.41	3 46	3.47	5.57	5.57	5.70	5.83	4 76	7.92	6.85
Nd	33.00	40.72	27.07	25.62	31.08	29.13	25.08	25.36	131.08	31.84	37.41	19.12	28.32	17 09	17.15	26.33	24 47	26.85	26.93	22 41	34.22	29.68
Sm	8.67	10.23	6.92	6.80	7.06	7.23	6.48	6.46	23.64	7.71	9.60	5.73	6.81	5.12	5.20	6.93	5.81	7.29	6.91	6 08	8.06	6.92
Eu	2.62	3.07	2.25	2.32	2.28	2 44	2.16	2.15	7.06	2.54	3.11	2.04	2.20	1 78	1.80	2.27	1.85	2.33	2.25	2 03	2.64	2.22
Gd	8.18	9.98	7.14	7.38	6.94	7.56	6.89	6.69	18.91	8.19	10.76	6.82	6.90	6.00	6.07	8.08	5.92	7.62	8 01	7.24	7.74	6.89
Tb	1.18	1.42	1.07	1.14	1.01	1.11	1.05	1.03	2.50	1.23	1.60	1.11	1.01	0.97	0.99	1.24	0.87	1.15	1 24	1.14	1.10	0.95
Dy	6.35	7.87	6.05	6.63	5.63	6.30	6.16	5.84	12.64	7 22	9.60	6.69	5.63	5.93	5.97	7.55	4 91	6.49	7.68	7 09	5 96	5.18
Ho	1.10	1.44	1.10	1.24	1.03	1 20	1.19	1.07	2.14	1.43	1.94	1.30	1.04	1.16	1.15	1.53	0.93	1.21	1.62	1 47	1.05	0.93
Er	2.68	3.55	2.71	3.18	2.60	3.07	3.09	2.69	5.16	3.78	5.20	3.39	2.62	3.02	2.99	4.13	2.34	3.08	4.44	4.01	2.57	2.29
Tm	0.33	0.45	0.34	0.42	0 34	0 40	0.41	0.35	0 65	0.51	0.70	0.45	0.34	0.40	0.39	0.55	0.30	0.39	0 59	0.54	0.33	0.29
Yb	1.94	2.68	2.03	2.56	2 05	2 45	2.54	2.08	3.83	3.19	4.45	2.78	2.05	2.46	2.43	3.48	1.86	2.42	3.84	3 52	1.95	1.73
Lu	0.27	0.38	0.28	0.36	0.29	0 36	0.37	0.29	0.53	0.48	0.68	0.40	0.29	0 35	0.34	0.52	0.27	0.35	0 60	0 55	0.27	0.25
Hf	7.90	8.49	4.80	4.55	5.14	4 92	4.28	4.68	7 83	5.26	6.34	4.40	4.19	3.94	3.95	4.79	3 49	5 34	4.42	4.02	4.99	4.25
Ta	1.98	2.13	1.41	1.15	2.12	1.84	1.20	1.34	5.00	1.65	1.62	0.74	1.72	0.66	0.68	0.94	1.33	0.95	0 94	0 84	2.43	2.06
Tl	1.73	0.82	0.74	0.26	0.37	0.18	0.08	0.03	0.09	0.68	0.03	0.01	0.18	0.01	0.01	0.03	0.17	0.02	0 06	0.09	0.18	0.11
Pb	5.50	4.03	1.85	1.46	2 31	1.81	0.70	1.25	6.27	2 39	1.39	0.80	1.68	0 63	0.85	1.96	1.40	1.38	2 10	1.77	1.77	1.59
Th	2.61	2.78	1.43	1.16	2.01	1 64	1.12	1.27	8.75	1.38	1.27	0 61	1.46	0.55	0.56	0.77	1.28	1.04	0.85	0 75	2 15	1.87
U	0.64	0.66	0.37	0 83	1 04	0.96	0.88	0.45	1 46	1.07	1.32	0.61	0.51	0 69	0.87	0.81	0 44	1.62	1.86	1.33	0.61	0.65

Table 3.1: Whole Rock Major (XRF) and Trace Element (ICP-MS) Analyses, Hawaiian Ridge: Yuryaku to Salmon (continued)

Seamount	Ladd	Ladd	Ladd	P&Herm	P&Herm	P&Herm	P&Herm	Smt 72	Salmon	Salmon
Sample	30/5	30/5 2	30/7	34/1	34/1	34/2	34/17	37/1	38/1	38/2
SiO_2	41 46	40.55	41.41	43.53	42.74	43.01	39.76	49.39	48.68	53.17
TiO_2	3.45	3.39	3.21	3.43	3.45	3.87	3.35	3 28	1.44	1.56
Al_2O_3	13.52	12.76	12.94	16.92	16.70	17.60	15.59	16 32	16.72	18.76
Fe_2O_3	13.86	14.49	13.88	13.08	13.26	13.82	12.77	10.62	6.37	6.74
MnO	0.17	0.18	0.16	0.50	0.41	0.21	0.21	0.15	0.20	0.20
MgO	7.40	7.84	9.65	2.60	2.58	3.53	3.12	3 46	1.77	1.95
CaO	13.06	13.38	11.75	9.44	9.47	9.12	12.19	8.52	6.21	6.54
Na_2O	1.99	2.04	1.70	3.61	3.58	3.11	3.26	3.38	4.82	4.78
K_2O	0.85	0.87	0.80	1.21	1.12	0.99	1.01	2.06	2.96	2.62
P_2O_5	1.06	1.53	0.74	2.13	2.07	1.13	4.19	0.48	0.82	0 97
LOI	2.79	3.24	2.80	3.75	4.07	3.09	4.30	1.85	1.64	2.18
Total	99.61	100.27	99.04	100.20	99.45	99.48	99.75	99.51	91.63	99.47
Sc	29.6	38.0	32.3	19.3	18.9	15.6	16.7	34.0	7.4	5.9
Cr	372.2	232.8	525.7	4.3	2.8	5.3	2.3	35.2	0.6	0.7
Co	55.7	39.9	70.9	163.5	133.2	38.4	30.5	31.3	12.2	11 5
Ni	143.4	63.5	279.7	53.6	51.2	17.4	22.4	33.0	12.4	13.5
Cu	80.7	103.5	93.0	57.4	62.6	51 9	49.6	74.2	11.8	17.0
Zn	145.9	134.1	156.6	209.4	222.4	238.6	215.2	173.0	145.8	146.4
Ga	22.7	21.5	22.8	22.6	23.8	24.5	20.1	28.4	26.8	26.4
Rb	14.1	8.9	15.3	13.9	13.5	11 2	13.0	267.6	69.9	51.4
Sr	779.4	279.3	720.7	1040.2	1109.2	1353.0	1075.6	400.5	1158.5	1158.4
Y	28.4	29.1	27.1	43.9	46.6	73.5	90.0	35.8	45.7	48.1
Zr	181.7	130.6	181.7	305.5	326.4	330.3	286.3	217.2	535.7	542.3
Nb	37.9	9.6	37.6	46.5	48.5	58.4	42.1	24.5	106.3	105.9
Cs	0.34	0.36	0.33	0.21	0.20	0.16	0.26	2 69	0.35	0 33
Ba	388.7	27.3	342.0	460.2	458.1	600.7	353.5	181.6	668.1	655.9
La	29.42	9.94	27.37	41.36	43.01	65.75	63.05	23.29	92.53	93 59
Ce	59.91	21.86	55.81	81.72	84.91	102.69	78.04	46.36	179.53	177.71
Pr	8.00	3.38	7.38	11.44	11.88	16.54	13.60	6.83	21.97	21.85
Nd	34.88	16.53	32.20	49.74	51.89	71.10	59.78	30.62	81.63	81.41
Sm	8.12	4.98	7.51	11.36	11.79	15.47	12.85	7.71	14.65	14.53
Eu	2.64	1.74	2.41	3.61	3.67	4.74	4.04	2.50	4.16	4.14
Gd	7.77	5.93	7.20	10.87	11.06	15.51	13.50	8.19	12.02	11.97
Tb	1.11	0.96	1.03	1.53	1.56	2.15	1.90	1.26	1.71	1.71
Dy	6.07	5.78	5.63	8.42	8.67	12.15	11.18	7.35	9.43	9.44
Ho	1.09	1.12	1.01	1.54	1.58	2.34	2.30	1.38	1.76	1.78
Er	2.69	2.89	2.48	3.88	3.97	6.08	6.30	3.52	4.62	4.75
Tm	0.35	0.39	0.31	0.50	0.50	0.79	0.86	0.46	0.64	0.65
Yb	2.11	2.41	1.87	3.08	3.09	4.73	5.46	2.82	4.06	4.17
Lu	0.30	0.34	0.27	0.45	0.45	0.69	0.86	0.39	0.59	0.60
Hf	4.90	3.83	4.61	7.76	7.85	8.90	7.27	5.97	13.86	13.65
Ta	2.42	0.64	2.24	2.91	2.96	3.94	2.70	1.60	7.40	7.29
Tl	0.24	0.01	0.08	0.13	0.12	0.28	0.33	0.07	0.20	0.14
Pb	1.60	0.67	1.62	2.76	2.80	4.56	2.89	2.03	8.00	7.70
Th	2.21	0.53	2.03	2.45	2.57	3.30	2.36	1.86	10.14	10.03
U	0.81	0.52	0.74	1.33	1.39	0.87	2.21	1.37	1.52	1.69

Table 3.2: Sr, Nd and Pb isotope analyses, Hawaiian Ridge: Yuryaku to Ladd

Seamount	Yuryaku	Yuryaku	Daikakuji	Daikakuji	Abbott	Abbott	Halsley	Midway	Midway	Ladd
Sample	5/1	5/9	6/4	6/7	12/2	12/7	23/2	29/1	29/12	30/5 (2)
$^{87}Sr/^{86}Sr$	0.703512	0.703500	0.703780	0.703799	0.703498	0.703483	0.703572	0.703531	0.703520	0.703358
	0.000007	0.000007	0.000006	0.000006	0.000007	0.000007	0.000007	0.000007	0.000007	0.000007
$^{143}Nd/^{144}Nd$	0.513050	0.513062	0.512943	0.512942	0.513020	0.513021	0.512987	0.513064	0.513058	0.513015
	0.000008	0.000001	0.000009	0.000007	0.000008	0.000009	0.000006	0.000014	0.000007	0.000005
$^{206}Pb/^{204}Pb$	19.084	19.321	18.775	18.168	18.545	18.643	18.788	18.973	19.093	18.442
	0.004	0.004	0.004	0.003	0.004	0.005	0.006	0.006	0.007	0.010
$^{207}Pb/^{204}Pb$	15.425	15.444	15.417	15.380	15.410	15.415	15.441	15.451	15.452	15.406
	0.003	0.003	0.003	0.003	0.003	0.004	0.005	0.005	0.006	0.008
$^{208}Pb/^{204}Pb$	37.885	37.872	38.027	37.716	38.015	38.159	38.116	38.144	38.121	38.098
	0.007	0.008	0.008	0.006	0.008	0.010	0.012	0.013	0.014	0.020

All isotope values are present day (i.e., not age corrected).
Errors reported are 2 SEM.

4 Geochemistry of the Musicians Seamounts

Yucheng Pan and Rodey Batiza

To the northwest of the Hawaiian Islands is a Cretaceous submarine mountain range known as the Musicians Seamounts (Fig. 1.3). Three populations of seamounts were recognised in the Musicians province (Rea and Naugler, 1971; Pringle, 1992); (1) the Musicians Horst, an elevated block of crust elongated in an east–west direction located to the north of the Murray Fracture Zone, (2) the Southern Ridges, a series of five large east–west trending ridges located in the southern part of the province, and (3) individual seamounts scattered throughout the province but mainly represented by the western seamounts, which are linearly distributed and show the age progression expected from a hotspot (Pringle, 1992). We report the results of the 13 new dredges from the FS *SONNE* Cruise SO 142 (HULA II), combined with the previous 35 dredges summarised by Pringle (1992).

4.1 Samples and Analyses

Like the previous dredges, the new dredges recovered rocks that are generally altered. Alteration is pervasive in the groundmass of all samples, although we do find fresh glasses in 4 of the 13 dredges. Fresh glass was not reported in the previous 35 dredges (Pringle, 1992). Crystals in the samples are mainly plagioclase xenocrysts and phenocrysts, and appear to be fresh. Pyroxene crystals also appear to be fresh, whereas olivine crystals are generally completely altered.

Electron microprobe major element compositions of the four samples with fresh glass are listed in Table 4.1. All the fresh glasses are tholeiite, and are similar to normal mid-ocean ridge basalts (e.g., K_2O/TiO_2 <0.14) and to transitional mid-ocean ridge basalts (K_2O/TiO_2 >0.14 but <0.4).

Whole rock major element compositions determined by XRF are listed in Table 4.2. Whole rocks contain significant amounts of H_2O and volatiles (loss on ignition, LOI), mostly as a result of alteration. Compared to fresh glasses, the whole rocks have significantly lower MgO contents. The fresh glasses of the four samples have an average MgO of 7.43 wt.%, whereas the whole rocks of the same four samples have an average MgO of only 3.65 wt.%. In detail, the crystallised center, the middle glassy part

(with the fresh glass), and the outside glassy part of one piece of 4DR-1 have MgO contents of 1.84, 6.42, and 2.11 wt.% respectively (Table 4.2). Magnesium is the element that is most easily and abundantly leached out from basalts to ocean water during alteration (e.g., Alt, 1995; Elderfield et al., 1997; Iskhakov, 1998). The average whole rock MgO contents for the 13 new dredges and the previous 35 dredges are 3.55 wt.% and 2.57 wt.%, respectively. Because of the alteration, interpretations will be based on a relative base (how the data compare to each other) and not to an absolute base.

The ICP-MS trace element compositions of the 13 new dredges are listed in Table 4.3. Only XRF trace element compositions were given for the previous 35 dredges (Pringle, 1992).

Crystal compositions are listed in Table 4.4. The An# [=100Ca/(Ca+Na) of plagioclase] ranges from 57 to 87 with an average of 72. The Wo# [=100Ca/(Ca+Mg+Fe) of pyroxene] ranges from 47 to 51 with an average of 48. The En# [=100Mg/(Mg+Fe) of pyroxene] ranges from 25 to 30 with an average of 28. The Fo# [=100Mg/(Mg+Fe) of olivine] for the only fresh olivine crystal found is 86. K-feldspar and apatite were also found.

4.2 Geochemical Trends

There are systematic geochemical trends from the hotspot to the mid-ocean ridge in the Musicians province. For example, MgO and Fe_2O_3 (as total iron) increase while incompatible elements like TiO_2, Na_2O, P_2O_5, and Zr decrease from the hotspot to the mid-ocean ridge (Fig. 4.1). In addition, there are systematic isotopic trends: $^{87}Sr/^{86}Sr$ decreases and $^{143}Nd/^{144}Nd$ increases from the hotspot to the mid-ocean ridge (Fig. 4.2). The Southern Ridges, where a lot data exist, have similar geochemical and isotopic trends (Fig. 4.3). For seamounts on the hotspot track, both MgO and $^{143}Nd/^{144}Nd$ increase whereas K_2O and $^{87}Sr/^{86}Sr$ decrease from the older seamounts in the north to the younger seamounts in the south (Fig. 4.4).

4.3 Provisional Interpretations

MgO variation diagrams for lavas from the Musicians Seamounts are shown in Figure 4.5. Fractionation was modeled using the MELTS program (Ghiorso and Sack,

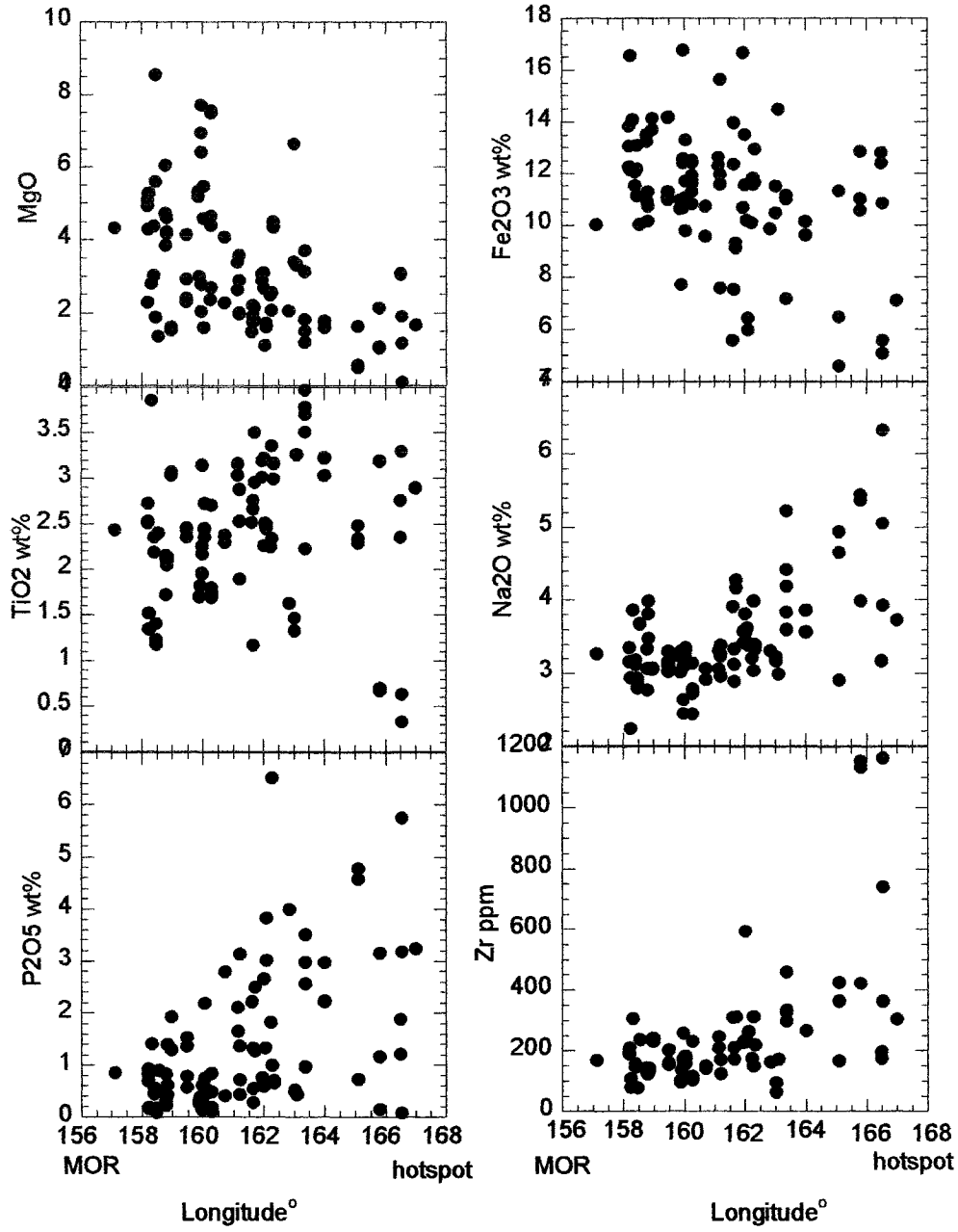

Fig. 4.1: Geochemical Trends from the Hotspot Towards the Mid-Ocean Ridge (MOR) for the Musicians Province.

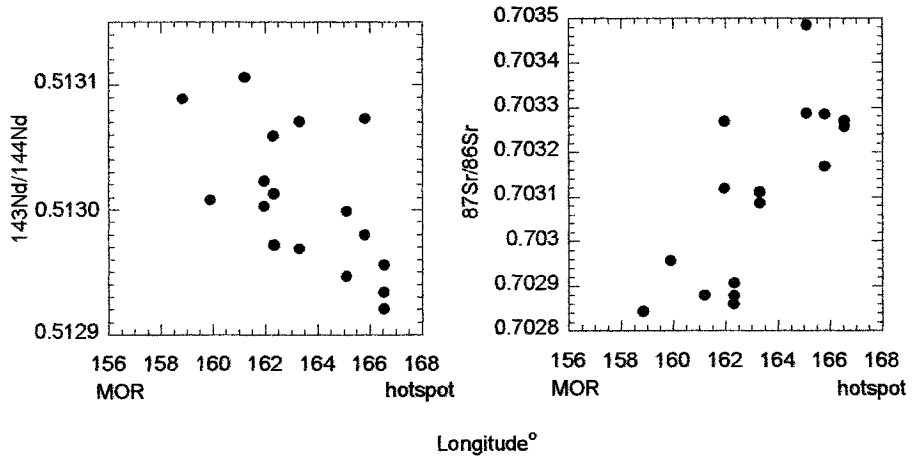

Fig. 4.2: Variations of Nd and Sr Isotopes with Longitude, Musicians Province.

Isotopic data were measured either on fresh plagioclase (for $^{87}Sr/^{86}Sr$) or pyroxene (for $^{143}Nd/^{144}Nd$) crystals or on strongly leached whole rocks (most likely with only fresh crystals left; Pringle, 1992).

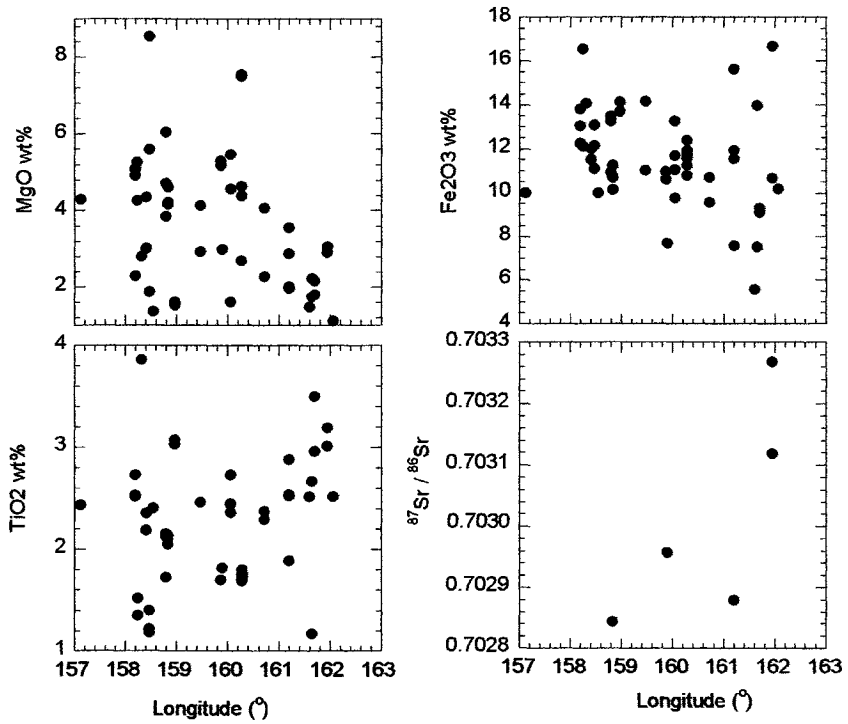

Fig. 4.3: Geochemical Trends within the Southern Ridges.

MgO and Fe_2O_3 decrease, whereas TiO_2 and $^{87}Sr/^{86}Sr$ increase from east (close to the mid-ocean ridge) to west (close to the hotspot).

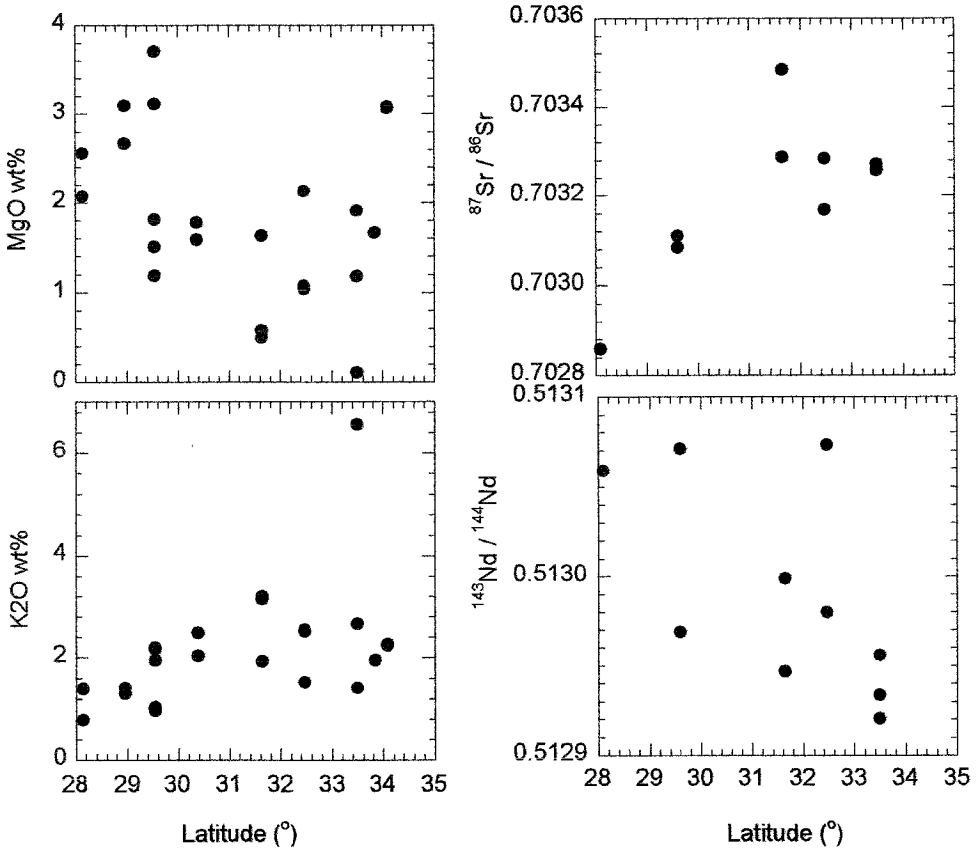

Fig. 4.4: Geochemical Trends for the Seamounts on the Hotspot Track.

MgO and $^{143}Nd/^{144}Nd$ increase, whereas K_2O and $^{87}Sr/^{86}Sr$ decrease from the north (older seamounts) to the south (younger seamounts).

1995). Samples from seamounts on the hotspot track generally require fractionation under higher pressure (or H_2O content) than those from the Horst and the Southern Ridges (Fig. 4.5). For the Southern Ridges alone, samples that are closer to the hotspot require fractionation under higher pressure than those closer to the mid-ocean ridge (Fig. 4.6). Multiple parent magmas and alteration are two possible explanations for the bad fits concerning Ca, Na, K, and P. That K and P concentrations are much higher than those from MELTS (over-enrichment) indicates that, besides fractionation, other processes such as melting and mixing are required to explain the data (Pan and Batiza, 1998).

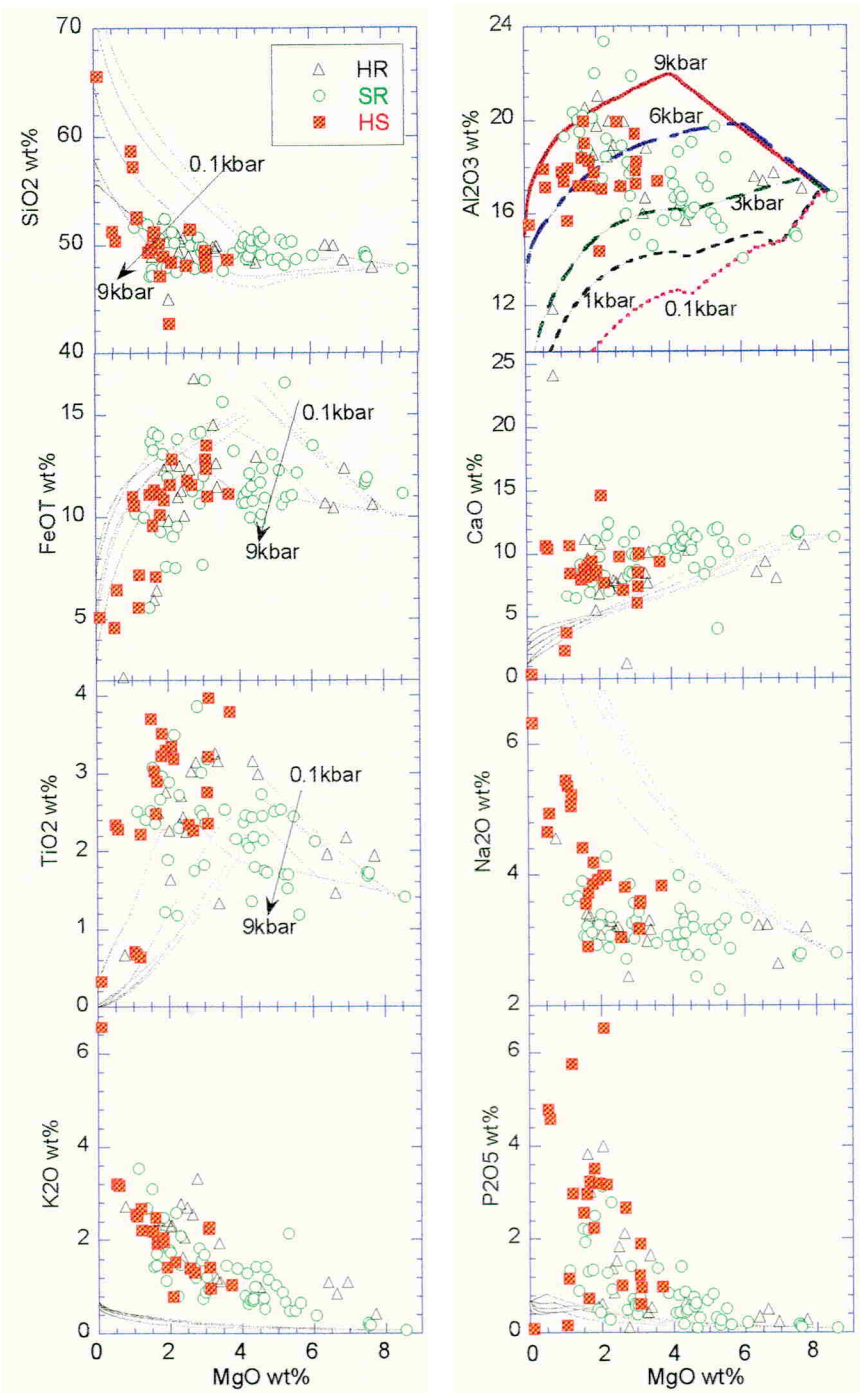

Fig. 4.5: MgO Variation Diagrams for Lavas from the Musicians Seamounts.

HR = the Musicians Horst; SR = the Southern Ridges; HS = hotspot seamounts from the western part of the Musicians Province.

MELTS runs shown have 0.5 wt.% H_2O, QFM buffer, fractionating solid, and different pressures from 0.1 to 9 kbar. H_2O has a similar effect to pressure (i.e., the effect of high pressure could be achieved by a high H_2O content).

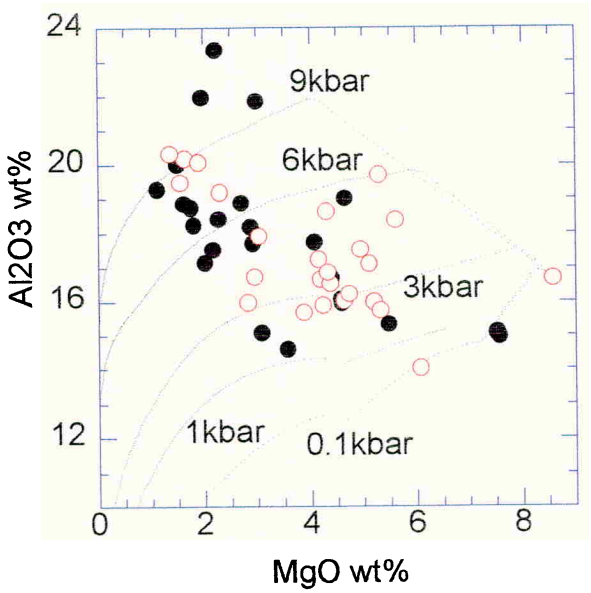

Fig. 4.6: Al_2O_3 vs. MgO Variation Diagram for Lavas from the Southern Ridges.

The filled and unfilled circles are samples close to the hotspot (longitude > 159.9°) and close to the mid-ocean ridge (longitude < 159.9°) respectively. Although with much scatter, samples close to the hotspot require fractionation under higher pressure than those close to the mid-ocean ridge.

The over-enrichment (relative to fractionation alone) of incompatible elements like K, P, and Zr, and especially the isotopic trends of Nd and Sr in the lavas of Musicians Seamounts, require mixing. The simplest mixing scenario to explain the geochemical trends involves two-end members: one from the mid-ocean ridge and the other from the hotspot. However, mixing is unlikely between magmas from the mid-ocean ridge and the hotspot, because magma cannot travel the large distances required in the upper mantle and/or crust. The mixing trend within the hotspot end-member itself also suggests that the type of mixing required is far more complicated than simple magma mixing.

Solid-state mixing facilitated by mantle melting related to upwelling could explain all of the geochemical trends within the Musicians Seamounts lavas. The mantle contained at least two end-members on a relatively small scale: a depleted, mid-ocean

ridge mantle-like component and an enriched component. Melts from these two end-members mixed together during melting. Due to the thick lithosphere at the hotspot, mantle upwelling and melting stopped at depth and the magma so produced would likely experience high pressure fractionation as it moved through the thick lithosphere (Fig. 4.5). During the interaction of the hotspot and mid-ocean ridge, part of the upwelling mantle at the hotspot was channelised to the mid-ocean ridge. Because lithosphere got thinner towards the mid-ocean ridge, the enhanced upwelling of this channelised mantle enhanced melting in the sub-lithospheric channel between the hotspot and the mid-ocean ridge. Enhanced melting resulted in the dilution of incompatible elements from the enriched mantle component. Consequently, from the hotspot to the mid-ocean ridge the lithosphere got thinner, fractionation pressure got lower (Fig. 4.6), melting fraction got larger, and the concentrations of compatible elements like Mg increased while those of the incompatible elements decreased (Figs 4.1, 4.3). Similarly, from the hotspot to the mid-ocean ridge, $^{87}Sr/^{86}Sr$ decreased and $^{143}Nd/^{144}Nd$ increased because the contribution of the depleted mantle end-member, which had low $^{87}Sr/^{86}Sr$ and high $^{143}Nd/^{144}Nd$, increased due to enhanced melting (Figs 4.2, 4.3).

Solid-state mixing can also explain the geochemical trends for lavas from the seamounts along the hotspot track. As the hotspot and its interaction with the mid-ocean ridge matured, melting at the hotspot was likely to increase. This melting increase could explain the increase of Mg and $^{143}Nd/^{144}Nd$ and the decrease of K and $^{87}Sr/^{86}Sr$ from the older to the younger seamounts (Fig. 4.4). Another possible explanation is that the hotspot mantle at the initial stage of upwelling contained more of the enriched end-member, whose abundance decreased during further upwelling. The enriched end-member, which contains abundant heat-producing elements, is probably an important reason for the initiation of the hotspot. Similarly, its depletion might be important for the cessation of a hotspot.

We are continuing our work on a method to quantify the geochemical trends in the Musicians Seamounts in relation to the mantle components, melting, and channelised flow from the hotspot to the mid-ocean ridge.

Table 4.1: Electron Microprobe Analyses of Fresh Glass, Musicians Seamounts (wt.%)

Sample	Point	SiO_2	TiO_2	Al_2O_3	Fe_2O_3*	MnO	MgO	CaO	Na_2O	K_2O	P_2O_5	Total	K_2O/TiO_2
4DR-1	1	46.90	1 92	16 86	10.69	0.09	7.70	10 65	3.17	0 43	0.27	98 68	0.22
	2	47.13	1.98	16.91	10.57	0 15	7.73	10.89	3 18	0.37	0 23	99.14	0.19
	3	47.41	1.89	16 94	10 70	0.16	7.61	10.80	3.24	0 40	0.33	99 49	0.21
	4	48 09	1.91	17 08	10 70	0 17	7 60	10 48	3.15	0 45	0.27	99.91	0.24
	5	48.24	1.88	17.17	10.70	0.19	7.79	10.46	3.26	0.44	0.30	100.43	0.23
	6	48 40	2.04	17 03	10.69	0.23	7 81	10.60	3.28	0.38	0.25	100.72	0.19
	7	46 98	1.86	16.85	10 48	0.12	7.77	10.64	3.22	0.38	0.41	98 71	0.21
	8	47.94	1.97	17.02	10.58	0.17	7 66	10.59	3.04	0.44	0.28	99.69	0.23
	9	47 60	1 90	17.02	10.41	0.13	7.70	10.61	3.24	0.40	0.26	99 26	0.21
	10	47.97	1.88	16.96	10 92	0.13	7.72	10.62	3.21	0.43	0.26	100.10	0.23
	11	48.50	2.05	17.00	10 27	0.12	7.76	10 67	3.15	0.44	0.19	100.14	0.21
	12	47.50	1.83	17.08	10 61	0.15	7 61	10.73	3 22	0 41	0.31	99.44	0.22
	13	47.89	1.95	16.97	10.74	0.13	7 67	10 51	3.18	0.44	0.26	99.73	0.22
	14	47.36	2.05	16.97	10.43	0.18	7.67	10.79	3.25	0.41	0 32	99.44	0 20
	15	47.69	2.01	17 12	10.61	0 18	7 77	10.77	3.14	0 43	0 24	99.95	0 22
	16	48.03	1.91	16 95	10.43	0 16	7.74	10.59	3.14	0.43	0.29	99.67	0.23
	17	48.34	1 93	17.02	10.67	0.17	7.71	10.77	3.13	0.37	0 38	100 49	0.19
8DR-10	1	49.51	1 72	15.14	11.84	0.18	7 58	11.49	2 81	0.19	0.22	100 68	0.11
	2	49.04	1.72	15.05	12.19	0.15	7.60	11.86	2.79	0.19	0 14	100.74	0.11
	3	49.08	1 72	15.04	12.07	0 19	7.63	11.81	2.93	0.19	0.09	100.75	0.11
	4	49.24	1.73	15.12	12.00	0.19	7 59	11.65	2.71	0 18	0.21	100 62	0 11
	5	48.96	1 74	14.90	12 15	0.18	7 53	11.60	2.85	0.19	0.15	100.24	0 11
	6	49.11	1 71	15.02	11 70	0.21	7 66	11 82	2.81	0.18	0.15	100.35	0.11
	7	49.07	1 78	15 07	11.94	0.20	7.64	11.61	2.82	0.21	0.10	100 43	0.12
	8	49 32	1 75	15 09	12.02	0.19	7.48	11.83	2.82	0.19	0.09	100 79	0 11
	9	49.01	1.82	14.99	11.88	0 21	7 53	11.75	2.64	0 19	0 18	100.21	0 11
	10	48.55	1.67	14.97	12 03	0.19	7 70	11.73	2.86	0.18	0.07	99 96	0.11
	11	48.96	1.65	14.93	12 19	0.16	7 60	11.80	2.78	0 22	0 14	100 42	0.13
	12	48.78	1 76	15.03	11.67	0.17	7.60	11.83	2 71	0 19	0 16	99 89	0.11
	13	48.91	1.70	14.81	11.81	0.20	7 59	11.85	2.84	0.17	0.10	99.97	0 10
	14	48.76	1 69	14.97	12.05	0.20	7.59	11.72	2.71	0.19	0.14	100.03	0.11
	15	49.26	1.70	15.08	11.90	0.23	7.50	11.67	2.80	0.17	0.02	100.32	0 10
8DR-11	1	49.36	1.76	15.10	11.78	0.19	7.49	11.63	2.75	0 21	0.24	100.50	0 12
	2	49.70	1 71	15.19	11.99	0 21	7.53	11.56	2.90	0.27	0.24	101 29	0 16
	3	49.92	1 77	15.12	11.43	0.23	7.60	11 42	2.78	0 22	0.21	100.71	0.12
	4	49.28	1.65	14.95	11.77	0.18	7 59	11.55	2.80	0.22	0 15	100 15	0.13
	5	49.39	1.78	15.10	11.63	0.20	7.54	11.51	2.78	0.22	0.21	100.36	0.13
	6	49.08	1.64	15.18	11 77	0.14	7.57	11 48	2.77	0.21	0.21	100.04	0.13
	7	49.23	1 73	15.12	11.52	0.18	7 61	11.31	2.76	0.24	0.13	99.83	0.14
	8	49.37	1.69	15.08	11.44	0.15	7.36	11.45	2 64	0 21	0.24	99 62	0.12
	9	48.92	1 81	15.09	11.62	0.25	7 45	11.39	2.89	0 23	0.12	99 75	0 13
	10	49.04	1 81	14.99	11.46	0.20	7.45	11.53	2.87	0.21	0 19	99 76	0.12
	11	49.44	1.66	15.00	11.34	0.14	7.50	11.66	2.77	0 18	0.19	99 89	0 11
	12	49.29	1.65	15.16	11.59	0.12	7.54	11.48	2.77	0.22	0.13	99.95	0.14
	13	49.86	1.84	15.43	11.70	0.19	7 57	11.49	2.66	0.26	0.13	101 12	0.14
8DR-20	1	49.15	1 80	15.12	11.65	0.15	7.72	11.73	2.63	0.16	0.15	100.26	0.09
	2	49.21	1.75	14.89	11.96	0.15	7 61	11.36	2.82	0 18	0.12	100 06	0.10
	3	49.10	1.66	15.02	11.71	0.23	7.65	11.70	2.83	0.18	0.13	100.21	0 11
	4	49.85	1.66	15.75	11.38	0.18	7.16	12.00	2.67	0 16	0 16	100.97	0.10
	5	48.17	1.63	15.05	12.21	0.18	7 61	11.75	2.82	0 18	0 15	99 73	0.11
	6	48.45	1.63	14.78	11 71	0.21	7.45	11.76	2.76	0.15	0.18	99 08	0.09
10DR-1	1	49.00	2.18	13.82	13.52	0.15	6.67	10.93	3.33	0 40	0.24	100 23	0 18
	2	48.80	2.13	14.01	13.38	0.20	5.89	11.05	3.34	0 40	0.26	99 46	0 19
	3	48.84	2.11	14.02	13 64	0.24	5.98	10.99	3.36	0.43	0.23	99.83	0.21
	4	49.04	2.10	14.06	13.50	0.16	6.07	11.10	3.45	0.39	0.22	100.09	0 18
	5	48.93	2.12	13.85	13.52	0.20	6.02	11.18	3.34	0.41	0.27	99.84	0.19
	6	49.32	2.13	14.16	13.44	0.19	5.97	11.02	3.12	0.39	0.19	99.94	0.18
	7	49.03	2.13	14.02	13.55	0.24	5.93	11.09	3.34	0.39	0.15	99.89	0.18
	8	48.77	2.14	14.10	13.37	0.22	5.91	11.08	3.37	0 42	0.24	99.60	0 19
11DR-8	1	47.70	1.38	16.66	11.61	0.18	8.64	11.52	2.78	0.06	0.09	100 62	0 04
	2	47.90	1.37	16.80	10.96	0.20	8.62	11.42	2.74	0.07	0.03	100.11	0 05

Sample	Point	SiO_2	TiO_2	Al_2O_3	Fe_2O_3*	MnO	MgO	CaO	Na_2O	K_2O	P_2O_5	Total	K_2O/TiO_2
	3	48.11	1.46	16.76	10.97	0 14	8.69	11.37	2.79	0 09	0.13	100.51	0.06
	4	48 31	1.53	16.93	10.98	0 17	8 53	11.37	2.83	0.08	0.03	100 76	0 05
	5	48.26	1 41	16.76	11.20	0.19	8 69	11.44	2.92	0.05	0.00	100 92	0 04
	6	47.47	1.29	16.60	11.25	0.19	8.73	11 46	2.77	0.09	0.05	99 90	0 07
	7	48.11	1.49	16.77	11 18	0 21	8 60	11.23	2.85	0.08	0.17	100 68	0 06
	8	48.56	1 40	16.81	11.26	0.14	8.64	11.37	2.88	0 07	0.24	101.38	0.05
	9	47.97	1 36	16.71	11 04	0.16	8.54	11.34	2.82	0.08	0.08	100.11	0.06
	10	47.92	1.47	16 85	11.31	0.15	8 67	11 21	2.75	0.07	0 09	100 48	0 05
	11	48.05	1.36	16.76	11.22	0.17	8 50	11.36	2.75	0.07	0 15	100 39	0.05
	12	47.90	1.40	16.64	11.16	0.16	8.63	11.47	2.78	0.06	0.06	100.26	0.04
	13	47.65	1.39	16.68	10.98	0 16	8 31	11.27	2 76	0.07	0 12	99.41	0.05

* Total iron is expressed as Fe_2O_3 in accordance with XRF data.

Table 4.2: Whole Rock XRF Major Element Compositions, Musicians Seamounts (wt.%)

Sample	Lat(°)	Lon(°)	SiO_2	TiO_2	Al_2O_3	Fe_2O_3	MnO	MgO	CaO	Na_2O	K_2O	P_2O_5	LOI	Total
1DR-5	32.32	163.10	46.20	3 02	14 84	13.44	0.10	3.07	7.85	2 77	1.10	0 41	5 97	98 80
3DR-1	32 25	161.13	44 65	2.85	15.01	11.37	0.11	3.04	6 89	2.98	1 75	1 49	8 38	98.56
3DR-10	32 25	161.13	44.30	2.74	15.55	11.12	0.06	2.38	7.26	2.76	2 30	1.92	8 26	98.68
4DR-1c*	32.26	159.96	45.57	2.05	17.90	11.36	0.18	1.84	6 19	2 80	2 08	0.56	8 33	98.90
4DR-1g*	32.26	159.96	44 91	2.01	16.38	11 47	0.16	6.42	7.41	2.44	1 02	0.23	6.58	99.05
4DR-1r*	32 26	159.96	37 96	2.39	15.15	12 75	0.23	2.11	0.90	1.86	2.53	0.10	22.66	98.65
4DR-2	32 26	159.96	45.80	1.80	16.08	9 79	0.10	5.87	7.85	2.95	1.01	0.32	7.10	98.68
5DR-4	32.29	159.47	46.35	2.15	16.77	9.98	0.08	2.11	6.76	3.00	2 53	1.25	7.56	98.58
5DR-7	32.29	159.47	45 61	2.21	16.91	10.22	0.13	2 18	7.13	2.86	1.87	1.39	8.39	98.93
7DR-1	26.61	160.72	47.22	2.26	16.85	10.17	0.12	3.87	10.49	2.77	0 78	0.40	4.10	99.08
7DR-4	26.61	160.72	44.04	2.13	17.08	8.86	0.15	2.11	11.52	2 84	1.37	2.59	5 73	98 46
8DR-1	26 62	160.27	47.46	1.66	17.94	10.70	0.10	2.56	10.37	2.58	1 15	0.46	4.14	99.15
8DR-5	26 62	160.27	47.66	1.70	15.78	10.21	0.12	4.15	10.47	2.62	1.36	0.46	4.10	98.67
8DR-30	26.62	160.27	44.67	1.60	17.31	11.28	0.25	4.23	8.04	2.22	1 30	0.10	8.15	99.18
9DR-1	26.66	159.47	46.65	2.29	16.02	10.24	0.11	3.85	8.95	2.88	1.20	0.74	5.44	98 41
9DR-4	26.66	159.47	46.54	2.30	15.62	13.23	0.14	2.74	7.91	2.82	1.58	0.54	5.49	98.94
10DR-1	26.57	158.79	46.54	2.04	14.83	12.53	0.18	3.65	9.79	2.90	1.32	0.80	3.95	98.56
10DR-9	26.57	158.79	48.76	1.66	15.62	10.53	0 13	4 55	10.91	2.67	1 12	0.31	2.75	99.03
11DR-2	26.68	158.47	45.17	1 10	17.06	11.28	0.16	5.20	9 39	2 66	0 61	0.16	5.95	98.77
11DR-6	26.68	158.47	45.50	1.17	19.05	12.43	0.15	1.79	10.54	2.79	1.08	0.47	3 70	98.66
12DR-3	26.70	158.24	45.96	1.27	17.49	11.38	0.15	4.02	9.98	2.76	0.67	0.17	4.85	98.75
12DR-7	26.70	158.24	39.57	1.25	16.19	13.61	0.20	4.34	3.24	1.84	1.76	0 14	16.85	99.01
13DR-3	26.18	158.41	46.50	2.20	16.74	11.24	0.11	2.83	9.17	2.98	1 14	0.53	5.31	98.77
13DR-4	26.18	158.41	46.81	2.06	15.56	10.84	0.13	4.11	10.29	2.93	0.95	0.42	4.43	98.55

*4DR-1c, 4DR-1g, and 4DR-1r are the crystallised center, middle glassy part, and outside glassy part (respectively) of sample 4DR-1.

Table 4.3: ICP-MS Trace Element Compositions, Musicians Seamounts (ppm)

	1DR -5	3DR -1	3DR -10	4DR -1c	4DR -1g	4DR -1r	4DR -2	5DR -4	5DR -7	7DR -1	7DR -4	8DR -1	8DR -5	8DR -30	9DR -1	9DR -4	10DR -1	10DR -9	11DR -2	11DR -6	12DR -3	12DR -7	13DR -3	13DR -4
Y	42	61	105	45	25	11	35	66	77	34	178	32	34	20	34	35	38	32	26	33	28	12	45	39
Zr	162	221	190	158	155	197	138	182	184	144	132	99	109	98	144	150	138	121	72	73	74	90	146	138
Hf	4	5	4	4	4	4	3.5	5	4	4	3	3	3	2	4	3	3	3	1	1	1	2	4	4
Nb	14	23	24	11	12	12	10	15	15	11	11	4	5	4	10	10	9	7	5	5	3	1	11	10
Ta	1 5	2	2	1	3	1.5	1	1 5	1.5	1	1	0.5	0 5	0 5	1	1	1.5	0.5	5	<0.5	3	<0.5	1	1
Rb	19	41	35	37	17	42	19	44	42	18	35	20	19	21	16	35	24	24	12	17	13	30	30	23
Cs	0.6	2 5	1.7	1.4	0.8	1.5	1 3	2.2	2.3	1.2	2 2	0 8	0 8	0.8	0.7	1.1	1	0.8	0.7	0 7	1 3	1.1	2.1	1.8
Sr	240	318	318	299	226	112	239	284	314	302	380	202	194	160	251	249	256	257	153	191	167	123	272	252
V	415	160	205	195	185	50	198	155	140	215	150	210	260	150	210	200	240	240	205	218	210	110	210	255
Co	48	30	23	49	54	57	37	22	29	35	31	32	44	61	42	33	47	48	53	62	60	73	32	39
Ni	35	75	75	105	140	135	185	80	80	60	100	70	105	130	85	50	45	55	205	158	165	210	65	45
Cu	110	125	150	120	90	260	135	160	190	90	175	165	160	150	190	165	120	105	180	200	200	340	125	95
Zn	270	235	190	155	135	345	295	190	210	170	145	120	130	125	185	145	125	95	240	143	235	250	150	160
Ga	24	23	22	22	17	9	20	22	22	23	22	21	20	15	22	22	20	19	18	19 5	19	10	22	22
Ba	45	136	150	197	76	99	76	133	158	64	69	40	45	45	61	87	93	59	20	45	32	53	69	61
Pb	10	15	10	5	5	15	15	15	15	10	10	5	15	20	15	20	10	5	20	15	15	15	15	15
Th	1	1	1	<1	<1	<1	<1	1	1	<1	<1	<1	<1	<1	<1	<1	<1	<1	<1	<1	<1	<1	<1	<1
U	1	0 5	0 5	0.5	<0 5	0.5	<0.5	0.5	0.5	<0.5	1	<0.5	<0 5	<0.5	0.5	0.5	<0.5	<0.5	<0 5	<0 5	<0 5	0.5	0.5	<0.5
W	44	11	10	6	59	10	16	8	6	18	20	18	12	35	10	7	10	19	8	37	14	12	16	13
La	15	36	69	16	9	11	17	37	49	16	106	7	10	5	10	12	13	9	5	8	8	9	15	14
Ce	29	45	43	25	25	29	23	32	34	27	28	15	16	14	24	24	22	19	10	9	10	10	25	25
Pr	5	7	14	5	3	3	5	7	8	5	20	3	3	2	4	4	4	3	2	2	3	2	4	4
Nd	23	32	59	24	15	13	23	32	37	21	88	13	14	8	18	19	17	15	10	10	12	8	21	20
Sm	7	7	13	6	4	3	5	8	8	5	19	4	4	3	5	5	5	4	3	3	3	2	6	6
Eu	2.2	2.5	3.8	2.0	1 5	0.8	1.8	2.4	2.4	1.8	5.8	1.4	1.5	1.0	1.7	1.9	1.7	1.5	1.2	1 2	1.3	0.7	1 9	1.8
Gd	8	9.3	16.4	7.6	4.9	3.7	6.65	10.2	11.2	7.1	25.2	5.4	5.7	3 6	6.7	6.2	6.8	5.7	4.1	4.55	4.8	2 8	7.1	6.5
Tb	1.3	1 3	2.4	1.2	0.8	0 6	1.1	1.5	1 7	1	3 7	0.9	0 9	0.6	1 1	1	1	0 9	0 6	0.75	0.7	0 5	1	1
Dy	7.2	7.8	12.6	6.5	4.7	3.6	5.8	8.6	9.4	6.1	20.3	6	5.8	3.8	6	6.3	6.2	5.5	4.2	4.7	4 4	2.9	6.7	6.2
Ho	1 4	1.6	2.7	1.4	1	0.6	1.3	1.9	2.2	1.2	4.5	1.2	1.2	0.8	1.3	1.2	1.3	1.2	1	1.05	0.9	0.5	1 5	1 4
Er	4 1	4.4	7	4	2.5	1.7	3.45	5 2	5.7	2.9	11.7	3.4	3.4	2.2	3.4	3.6	3.9	3.3	2.9	3.2	2 8	1 5	4.3	3.8
Tm	0.6	0.7	0.9	0.6	0.4	0.3	0.5	0.7	0.8	0.4	1.6	0.5	0.5	0.4	0.5	0.5	0.5	0.5	0.4	0.45	0.4	0.2	0.6	0.5
Lu	0.5	0.7	0.9	0.6	0 4	0 3	0.5	0.8	0.8	0.5	1 6	0.5	0.5	0.4	0.5	0.5	0.6	0.5	0.4	0 5	0.4	0.3	0 6	0 6

Table 4.4: Electron Microprobe Analyses of Plagioclase, Pyroxene, Olivine and K-feldspar (Musicians Seamounts)

Sample	Mineral	Point	SiO_2	TiO_2	Al_2O_3	FeO	MnO	MgO	CaO	Na_2O	K_2O	P_2O_5	Total	An#
3DR-1	pl	49	50.87	0.08	31 24	0.46	0.00	0.13	14.76	3.07	0.14	0.00	100.74	72
	pl	62	54 25	0.16	27.27	1.32	0.02	0.41	11.65	4.85	0.26	0.04	100 22	57
	or	61	65.06	0.00	18.09	0.03	0.00	0 02	0.00	0.09	16.40	0.02	99.72	
4DR-10	cpx	37	48.91	2.00	17.58	9.95	0.11	7.01	10.52	3.35	0.71	0.35	100.51	
	cpx	39	48.32	2 13	17 01	9.90	0.15	7.76	10.88	3.24	0.43	0.36	100 19	
	cpx	41	48.99	2.00	17.32	9.85	0.10	7.06	10.34	3.31	0 66	0.26	99.89	
	cpx	42	49.05	1.93	18.01	9 55	0.13	6.63	9.87	3.41	0.74	0 24	99.55	
	cpx	44	48.31	1.91	17.18	9.82	0.16	7.48	10.63	3.24	0.50	0.27	99 51	
	cpx	40	49.80	1.83	18.62	9 02	0.10	5 62	9.31	3.30	1.08	0 21	98 90	
	cpx	38	48.54	2.06	17.41	9 95	0 07	6.40	9.98	3 38	0.79	0.28	98.86	
4DR-2	pl	34	51.71	0.06	30.36	0.55	0.03	0.19	13.97	3.67	0.11	0.05	100.70	68
5DR-4	pl	59	51.70	0 17	29.88	0.63	0.01	0.18	13.68	3 47	0.60	0 08	100.39	67
	or	60	65.53	0.01	18.03	0.18	0 01	0.00	0.04	0.18	16.20	0.00	100.18	
5DR-7	pl	46	51.30	0.11	30.84	0.55	0.07	0.18	14.20	3.65	0.10	0.00	100.99	69
8DR-10	pl	82	48 45	0 01	32 74	0 53	0.00	0.16	16.57	2.31	0.02	0.00	100.78	81
	pl	84	48.60	0 02	32 35	0.56	0.03	0.18	16.38	2 36	0 04	0.05	100.56	80
	pl	83	47.97	0.10	32.75	0.54	0 00	0.18	16.76	2.15	0.03	0.04	100 51	82
8DR-11	pl	171	52 45	0 05	29.73	0 60	0.00	0.17	13.35	4.02	0.06	0 00	100.45	65
	pl	172	52 18	0 07	29.85	0 61	0.00	0.16	13.55	3.85	0.09	0.00	100.35	66
8DR-20	pl	107	48 58	0 05	32 04	0 59	0 00	0 18	16 15	2 46	0 05	0 00	100 09	80
	pl	106	50 61	0 33	28 57	2.02	0.01	0.41	13.04	3 52	0.18	0.08	98 78	65
	pl	105	48 27	0.03	32.91	0.41	0.00	0.19	16.78	2.31	0.03	0.05	100 98	82
	pl	122	50.12	0.05	31.02	0.47	0 00	0.21	15 15	3.02	0 01	0.03	100.08	74
	pl	108	48 89	0 00	31.77	0.65	0.01	0.14	15.88	2.65	0 02	0.00	100.01	78
	pl	112	52.65	0.06	29.92	0.56	0.06	0.21	13.79	3.80	0 04	0 03	101 12	67
	pl	111	49.85	0.02	32.01	0.48	0.00	0.18	15.67	2.64	0 04	0 01	100 90	76
	pl	117	48 25	0.05	33.06	0.45	0.03	0.18	16.55	2.21	0.02	0.03	100.83	81
	pl	118	49.45	0.08	32.05	0.44	0.00	0.20	15.86	2.50	0 01	0 00	100.60	78
	cpx	120	49.16	1.70	14.90	10.89	0.12	7 58	11.78	2.68	0.20	0.21	99.22	
	cpx	121	49.14	1 68	15.03	10.61	0.16	7.67	11.66	2.82	0 18	0 23	99 17	
	cpx	119	49.17	1.70	14.82	10.30	0.09	7.52	11.73	2.82	0 17	0.21	98.54	
8DR-21	pl	187	49.95	0.04	31.30	0.55	0.06	0.16	15 23	2 94	0 03	0.00	100.25	75
	pl	186	51.28	0.03	30.33	0.49	0 01	0.19	14.14	3.47	0.06	0.00	100 00	69
	pl	182	50.50	0.03	31.69	0.56	0.00	0.15	15 18	2.96	0 06	0.00	101 13	74
	pl	185	50.40	0.12	31 03	0.58	0 04	0.24	14.93	3.02	0 05	0 00	100.42	73
	pl	184	50 05	0.06	31.24	0.53	0.00	0.19	15.04	2.85	0.04	0.03	100.03	74
9DR-12	pl	69	53 44	0.13	28.71	1.10	0.01	0.25	12 46	4.38	0.08	0.04	100.60	61
	pl	70	52.98	0.14	29.18	0.91	0.00	0 18	12.69	4.37	0.06	0 00	100.52	62
10DR-1	pl	136	52.27	0.07	30.10	0.74	0.02	0.23	13.77	3.90	0.07	0.05	101 23	67
	pl	137	52.88	0.09	29.66	0.89	0.00	0.22	13.10	4.06	0.07	0 06	101 04	63
	cpx	138	49.76	2 17	14.12	12.13	0.23	6.39	11.71	3.06	0.30	0.26	100.15	
10DR-6	pl	181	51.07	0.03	30.07	0.66	0.03	0.27	14.19	3.60	0.08	0.00	100.00	70
	pl	180	50.24	0.08	30.90	0.57	0.02	0.24	15.05	2.97	0.05	0.01	100.13	74
10DR-9	pl	177	50.68	0.14	30.66	0.90	0.00	0.29	14.55	3.29	0.07	0.00	100.59	71
	pl	176	51.02	0.16	28.81	1.50	0.04	1.07	14.28	3.42	0.12	0.01	100 43	71
11DR-8	pl	155	49.92	0.10	30.18	0.86	0.00	0.28	14.61	3.35	0.05	0.00	99 36	72
	ol	153	40.16	0.03	0.11	13.36	0.25	46.03	0.31	0 01	0 01	0 00	100.28	
13DR-1	pl	215	52.08	0.20	29.37	1.15	0.00	0.36	13.38	4.13	0.10	0.05	100.83	65
	pl	216	51.72	0.11	29.15	0.82	0.04	0.19	13.31	4.16	0.14	0.02	99.65	66
	pl	210	47.21	0.08	33.41	0.35	0.02	0.21	17.16	1.83	0.02	0 03	100.32	85
	pl	218	46.54	0.03	33.61	0.34	0.01	0.17	17.55	1.79	0.03	0 00	100.06	87
	pl	217	46.81	0.04	32.99	0.33	0.02	0.19	16.79	1.97	0.01	0.00	99.13	84

5 References

Alt, J.C., 1995. Sub-seafloor processes in mid-ocean ridge hydrothermal systems. *In:* Humphris, S.E., Zierenberg, R.A., Mullineaux, L.S., Thomson, R.E. (eds), Seafloor Hydrothermal Systems; Physical, Chemical, Biological and Geological Interactions. American Geophysical Union, Geophysical Monograph 91: 85–114.

Carmichael, I.S.E., Turner, F.J., Verhoogen, F., 1974. Igneous Petrology. McGRaw-Hill, New York.

Clague, D.A., Dalrymple, G.B., 1989. Tectonics, geochronology, and origin of the Hawaiian–Emperor volcanic chain. *In:* Winterer, E.L., Hussong, D.M., Decker, R.W. (eds), The Eastern Pacific Ocean and Hawaii. Geological Society of America, Boulder.

Dalrymple, G.B., Lanphere, M.A., 1969. Potassium Argon Dating. W.H. Freeman Co., San Francisco, 258 pp.

Dalrymple, G.B., Alexander, E.C., Lanphere, M.A., Kraker, G.P., 1981. Irradiation of samples for $^{40}Ar/^{39}Ar$ dating using the Geological Survey TRIGA reactor. U.S. Geological Survey Professional Paper 1176.

Elderfield, H., Suess, E., Mottl, M.J., Wheat, G., 1997. Low-temperature reactions between sea-water and oceanic crust at ridge flanks. Seventh Annual V.M. Goldschmidt Conference, LPI Contribution 921, p. 66–67.

Faure, G., 1986. Principles of Isotope Geology (2nd ed.). Wiley, New York.

Frey, F.A., Garcia, M.O., Roden, M.F., 1994. Geochemical characteristics of Koolau Volcano: implications of intershield geochemical differences among Hawaiian volcanoes. Geochimica et Cosmochimica Acta 58: 1441–1462.

Ghiorso, M.S., Sack, R.O., 1995. Chemical mass transfer in magmatic processes, IV, A revised and internally consistent thermodynamic model for the interpolation and extrapolation of liquid-solid equilibria in magmatic systems at elevated temperatures and pressures. Contributions to Mineralogy and Petrology 119: 197–212.

Hofmann, A.W., 1986. Nb in Hawaiian magmas: constraints on source composition and evolution. Chemical Geology 57: 17–30.

Hofmann, A.W., Jochum, K.P., 1996. Source characteristics derived from very incompatible trace elements in Mauna Loa and Mauna Kea basalts, Hawaii Scientific Drilling Project. Journal of Geophysical Research 101: 11831–11839.

Iskhakov, A.Ya., 1998. Behavior of petrogenic elements during secondary alteration of the ocean floor volcaniclastic rocks. Oceanology 38: 401–403.

Keller, R.A., Fisk, M.R., White, W.M., 2000. Isotopic evidence for late Cretaceous plume–ridge interaction at the Hawaiian hotspot. Nature 405: 673–676.

Koppers, A.A.P., Staudigel, H., Wijbrans, J.R., Pringle, M.S., 1998. The Magellan Seamount trail, implications for Cretaceous hotspot volcanism and absolute Pacific Plate motion. Earth and Planetary Science Letters 163: 53–58.

Lanphere, M.A., Dalrymple, G.B., Clague, D.A., 1980. Rb-Sr systematics of basalts from the Hawaiian–Emperor volcanic chain. Initial Reports of the Deep Sea Drilling Program 55: 695–706.

Lassiter, J.C., DePaolo, D.J., Tatsumoto, M., 1996. Isotopic evolution of Mauna Kea volcano: results from the initial phase of the Hawaii Scientific Drilling Project. Journal of Geophysical Research 101: 11769–11780.

Lonsdale, P., 1988. Geography and history of the Louisville hotspot chain in the southwest Pacific. Journal of Geophysical Research 93: 3078–3104.

Manhes, G., Minster, J.F., Allegre, C.J., 1978. Comparative uranium-thorium-lead and rubidium-strontium study of the Saint Severin amphoterite: consequences for early solar system chronology. Earth and Planetary Science Letters 39: 14–24.

McDonough, W.F., Sun, S.S., Ringwood, A.E., Jagoutz, E., Hofmann, A.W., 1992. Potassium, Rubidium and Cesium in the Earth and Moon and the evolution of the mantle of the Earth. Geochimica et Cosmochimica Acta 56: 1001–1012.

McDougall, I., Harrison, T.M., 1988. Geochronology and Thermochronology by the $^{40}Ar/^{39}Ar$ Method. University Press, Oxford.

Morgan, W.J., 1978. Rodriguez, Darwin, Amsterdam, ..., a second type of hotspot island. Journal of Geophysical Research 83: 5355–5360.

O'Connor, J.M., Stoffers, P., Wijbrans, J.R., 1998. Migration rate of volcanism along the Foundation Chain, SE Pacific. Earth and Planetary Science Letters 164: 41–59.

O'Connor, J.M., Stoffers, P., Wijbrans, J.R., 2001. En Echelon volcanic elongate ridges connecting intraplate Foundation Chain volcanism to the Pacific–Antarctic spreading center. Earth and Planetary Science Letters 189: 93–102.

Pan, Y., Batiza, R., 1998. Major element chemistry of volcanic glasses from the Easter Seamount Chain; constraints on melting conditions in the plume channel. Journal of Geophysical Research 103: 5287–5304.

Pringle, M.S., 1992. Geochronology and petrology of the Musicians Seamounts and the search for hot spot volcanism in the Cretaceous Pacific. PhD Dissertation, University of Hawaii, pp. 235.

Pringle, M.S., 1993. Age progressive volcanism in the Musicians Seamounts; a test of the hotspot hypothesis for the late Cretaceous Pacific. *In:* Pringle, M.S., Sager, W.W., Sliter, W.V., Stein, S. (eds), The Mesozoic Pacific; Geology, Tectonics and Volcanism. American Geophysical Union, Geophysical Monograph 77: 187–215.

Rea, D.K., Naugler, F.P., 1971. Musicians Seamount Province and related crustal structures north of the Hawaiian Ridge. Marine Geology 10: 89–111.

Regelous, M., Hofmann, A.W., Abouchami, W., Galer, S.J.G., 2001. Influence of lithsphere thickness on the composition of Mesozoic–Cenozoic Hawaiian magmatism. Geology *in press*.

Rhodes, J.M., 1996. Geochemical stratigraphy of lava flows sampled by the Hawaii Scientific Drilling Project. Journal of Geophysical Research 101: 11729–11746.

Smith, W.H.F., Sandwell, D.T., 1997. Global seafloor topography from satellite altimetry and ship depth soundings. Science 277: 1956–1962.

Todt, W., Cliff, R.A., Hanser, A., Hofmann, A.W., 1996. Evaluation of a ^{202}Pb-^{205}Pb double spike for high-precision lead isotope analysis. American Geophysical Union, Geophysical Monograph 95: 429–437.

White, W.M., Patchett, J., 1984. Hf-Nd-Sr isotopes and incompatible element abundances in island arcs: implications for magma origins and crust-mantle evolution. Earth and Planetary Science Letters 67: 167–185.

Wijbrans, J.R., Pringle, M.S., Koppers, A.A.P., Scheveers, R., 1985. Argon geochronology of small samples using the Vulkaan argon laser probe. Proc. Kon. Ned. Akad. Wet. 98: 185–218.

Yang, H-J., Frey, F.A., Rhodes, J.M., Garcia, M.O., 1996. Evolution of Mauna Kea volcano: inferences from lava compositions recovered in the Hawaii Scientific Drilling Project. Journal of Geophysical Research 101: 11747–11767.

York, D., 1984. Cooling histories from $^{40}Ar/^{39}Ar$ age spectra: implications for Precambrian plate tectonics. Annual Review of Earth and Planetary Sciences 12: 383–409.

York, D., Hall, C.M., Yanase, Y., Hanes, J.A., Kenyon, W.J., 1981. Laser-probe $^{40}Ar/^{39}Ar$ dating of terrestrial minerals with a continuous laser. Geophysical Research Letters 8: 1136–1136.